THE PROXIMAL PROMOTER OF THE MELANOCORTIN 4 RECEPTOR

HARBORS REGULATORY ELEMENTS RESPONSIBLE FOR BRAIN

PREFERENTIAL EXPRESSION

By

CLIFFORD R. LAMAR II

Thesis

Submitted to the Faculty of the

Graduate School of Vanderbilt University

in partial fulfillment of the requirements

for the degree of

MASTER OF SCIENCE

in

Molecular Physiology and Biophysics

December, 2007

Nashville, Tennessee

Approved:

Professor Richard M. O'Brien, Ph. D.

Professor P. Anthony Weil, Ph. D.

Professor Ronald B. Emeson, Ph. D.

ACKNOWLEDGEMENTS

TABLE OF CONTENTS

LIST OF FIGURES

LIST OF TABLES

CHAPTER I

INTRODUCTION AND BACKGROUND

Introduction

Obesity has become a major health concern in both developed and developing

nations (1). The relative contribution of *Environment* versus *Genetics* on obesity remains

highly debated; however, monogenic obesity has been demonstrated in humans (2, 3),

other mammals (4), and even the fruit fly *Drosophila melanogaster* (5). Many of the

known mutations found to be causative in monogenetic obesity syndromes in mammals

lie in genes involved in a humoral-neuronal circuit that culminates (theoretically) in the

hypothalamus of the brain. The hypothalamus contains many nuclei known to control

feeding behavior and other aspects of energy homeostasis (6), some of which were

discovered by physical lesion studies, especially the ventromedial hypothalamus, prior to

the age of genetics (7). As researchers in this field, we have also benefited from the

"mouse fanciers" who collected odd and interesting strains of mice. Five of these strains

were examples of monogenetic obesity, some of which will be discussed later in this

chapter.

One of the genes currently thought to play a key role in the energy balance

equation that takes place in the hypothalamus is the melanocortin receptor type 4

(MC4R). We now know that the MC4R gene is expressed in many specific nuclei within

the hypothalamus; however, the study of the melanocortin signaling pathways and,

eventually, their role in feeding behavior began with an observation that frog pituitary

extracts had two interesting and seemingly unrelated properties when injected into the bloodstream of other frogs: vasodilation and quickening of the pulse (adrenocorticotrophic activity) and pigmentation deposition in the skin (melanotrophic activity) (8). These observations led to the discoveries of the glucocorticoids released from the adrenals and eumelanin synthesis in melanocytes of the skin. Ultimately, the pre-prohormone from the pituitary extract responsible for both physiological actions was cloned, namely the pro-opiomelanocortin gene (POMC).

The POMC pre-prohormone is cleaved to form several bioactive peptides, including the agonists for the five melanocortin receptors in addition to the mu-opioid receptor (9). One of these fragments, alpha-MSH, is the hormone agonist for MC1R in melanocytes of the skin and MC4R in the CNS. The physiological actions of alpha-MSH upon MC1R and the melanocytes in the skin has been better characterized.

Upon binding of the alpha-MSH ligand, the MC1R activates a cAMP-dependent pathway, which results in eumelanin synthesis and deposition (See Figure 1.1). Genetic studies of mouse strains harboring interesting coat colors led to the cloning and physiological characterization of the agouti signaling protein (agouti), a paracrine hormone normally produced in close proximity to melanocytes (10). The function of this hormone is to act as an endogenous antagonist of the MC1R (11), though some studies claim evidence for agouti acting as a reverse-agonist (12). The physiological consequence in melanocytes in response to agouti signaling is the lowering of cAMP levels, which in turn leads to production of pheomelanin (red to yellow pigment) instead of eumelanin (dark brown to black pigment) (See Figure 1.1).

Figure 1.1
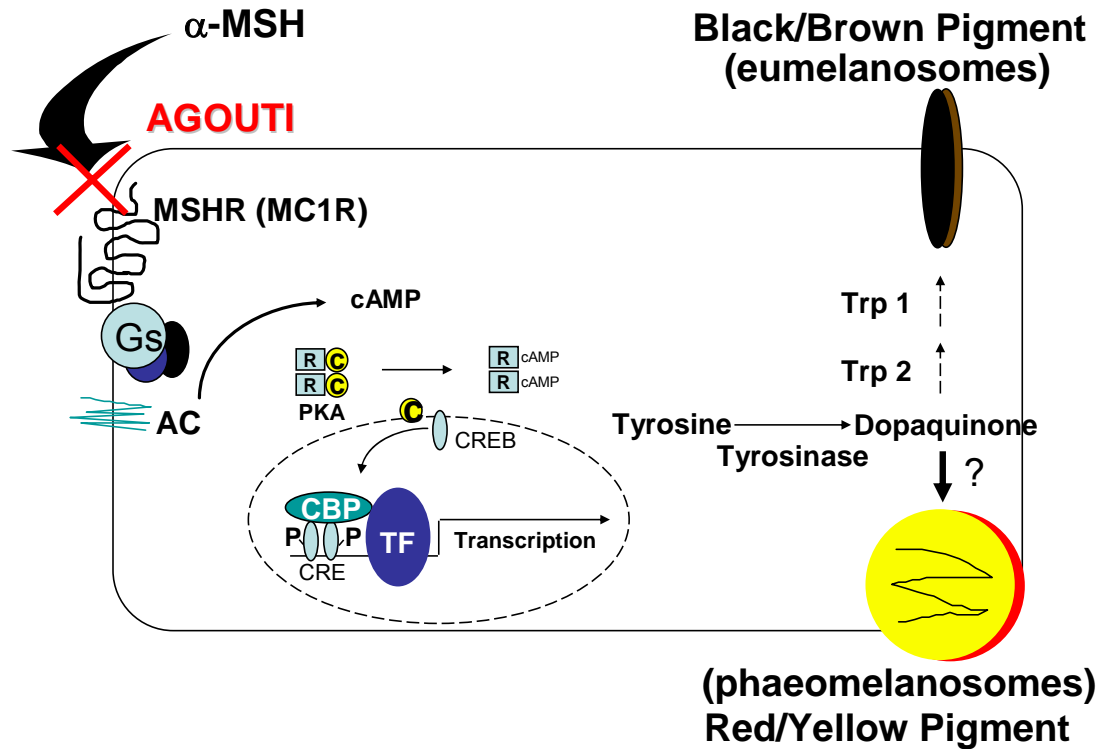
Figure 1.1: Competing Action of Alpha-MSH and Agouti Signaling Protein on Melanocortin Receptor Type 1 in Melanocytes of the Skin. Alpha-MSH is released by the pituitary gland into the bloodstream of fur bearing mammals. Upon reaching its target site in the skin (melanocytes) it binds to and activates the MSH Receptor (MC1R). Activation of MC1R yields an increase in intracellular concentration of cAMP. The increased levels of cAMP activate a PKA dependent signaling cascade that culminates in deposition of eumelanosomes (brown or black pigments). When the paracrine Agouti Signaling Protein (Agouti) is released from nearby cells, it binds to and blocks alpha-MSH binding of MC1R. The result is relatively low levels of intracellular cAMP and the deposition of phaeomelanosomes (yellow or red pigments).

Mice in the wild (or in your kitchen cupboard) have a brownish coat color due to a temporal expression of agouti in the skin during growth of the fur. The resulting eumelanin-pheomelanin-eumelanin banding pattern results in a brownish appearance. Dominant hypermorphic mutations in MC1R (13), as well as recessive mutations in agouti (14), lead to a "black" coat color. The latter mutation example is the genetic cause

of the coat color phenotype familiar to all who have worked with the popular laboratory model animal, the C57bl6 strain of mice. Conversely, dominant overexpressing mutations of agouti result in a yellow coat color phenotype (10). One such strain is the Obese Lethal Yellow (Ay) mouse, named because of the fact that two copies of the mutant allele (harboring a large upstream deletion in the agouti and adjacent gene) are lethal *in utero*. As the name implies, the mice are also obese with melanocortinergic signaling blockade due to the ectopic expression of agouti causing the unique phenotype, albeit initially it was unclear which melanocortin receptor in the CNS was being targeted by agouti.

Cloning of the Central Melanocortin Receptors

At the time of the discovery of the mutational cause of the agouti yellow obesity syndrome, four melanocortin receptors had been cloned in mouse and human. The MC1R, or MSH-Receptor, has been discussed above. The ACTH-R (MC2R) was cloned at the same time by the Cone Laboratory (15). The primary tissue of MC2R expression is the adrenal glands, where it takes a key role in adrenal cortical function. The MC3R and MC4R were cloned shortly thereafter, and were found to have the highest expression in the CNS; therefore, they were collectively termed the "Neural" or "Central" melanocortin receptors (16). The fifth and final melanocortin receptor, MC5R, was cloned and found to be widely expressed in the periphery, but its primary function is in sebaceous glands (17, 18, 19). Table 1.1 lists the five melanocortin receptors, principal sites of expression, and physiological function(s).

Table 1.1

The Melanocortin Receptors

RECEPTOR	PRINCIPAL SITES OF EXPRESSION	FUNCTION(S)
MC1 (MSH-R)	MELANOCYTES	PIGMENTATION
MC2 (ACTH-R)	ADRENAL CORTEX, ADIPOCYTES	STEROIDOGENESIS
MC3	HYPOTHALAMUS, LIMBIC SYSTEM, PLACENTA, GUT	UNKNOWN, Energy Partitioning? Kidney Function?
MC4	HYPOTHALAMUS, LIMBIC SYSTEM, CORTEX, BRAIN STEM	FEEDING, METABOLISM, ERECTILE FUNCTION, Memory?, Axon Guidance? Cachexia?
MC5	EXOCRINE GLANDS	EXOCRINE FUNCTION

Expression Profiles of the Central Melanocortin Receptors

The sites of expression of both MC3R and MC4R led to the hypothesis that one or both of these melanocortin receptors were responsible for the metabolic syndrome of the agouti yellow lethal mouse. Both of these receptors are widely, yet weakly expressed throughout the brain, as determined by *in situ* hybridization studies of mammalian brains: rodent (20), and sheep (21). Such widespread expression suggests a number of autonomic physiological roles for the Central Melanocortin Receptors.[1] Two sites of expression were especially suggestive of a central role in energy homeostasis for MC4R: relatively dense expression of RNA transcripts of the receptor in the hypothalamus

---

[1] Central Melanocortin Receptors have been postulated to be involved in learning and memory formation (22), feeding behavior (23, 24), naturesis (25), erectile function (26), drug addiction and drug seeking behavior (27, 28), axonal guidance (29), and possibly immuno-regulation in dermal papilla cells (30).

(ventromedial, dorsomedial, and lateral hypothalamic nuclei) and in the midbrain portion of the brain stem (ventral tegmental area). Both of these sites had long been known to induce feeding behavior via physical disruption and/or electrical stimulation.

Feeding behavior, *per se*, is best described in context of energy homeostasis. Energy homeostasis is in constant flux, and the body has developed a complex set of sensory neuro-humoral circuits that detect levels of stored and circulating energy molecules. These neuro-humoral circuits culminate in one or both of the classic "feeding centers" of the brain (hypothalamus and brain stem). The hypothalamic feeding center neural-circuitry is better characterized, albeit still poorly understood at the present, despite the hypothesis that the brain stem controlled feeding behavior is probably more ancient and/or primitive (31).

A schematic representation of the hypothalamic neuro-humoral circuitry is depicted in Figure 1.2. Signaling molecules (i.e., hormones or metabolites) from the periphery are able to cross the blood brain barrier at the structure known as the median eminence (ME). Neurons located in the arcuate nucleus (ARC) project dendrite-like appendages into the ME, where their various receptors (and possibly transporter proteins) will detect the presence of the signaling molecule(s). Some of these ARC neurons are tasked with orexigenic (pro-food seeking) control of feeding behavior, while others are tasked with anorexigenic (anti-food seeking) control (32).

The anorexigenic ARC neurons express and process the pre-prohormone POMC into alpha-MSH. These cells also produce Cocaine and Amphetamine Regulated

Transcript (CART).[2] Electrophysiology studies have determined that POMC/CART

neurons have a relatively high basal activity, presumably translating into a constant

release of alpha-MSH and CART at their axonal synapses (34). Upon stimulation by

leptin, or some other humoral signaling molecule, these anorexigenic neurons increase

their firing rate even more. One hypothesis is that these neurons must keep this constant

anorexigenic signaling to stem the tide of the pre-programmed food seeking circuitry of

the CNS. This is an appealing hypothesis because food seeking behavior is key to

survival and inherent in the thriving behavior of newborn animals. However, it should be

noted that MC4R connections in the hypothalamus are not believed to be fully active

until sometime after birth in rodents (35).

The orexigenic ARC neurons produce Agouti Related Protein (AgRP). AgRP

was discovered by *in silico* mining, when two groups made a GenBank search for

sequences homologous to the agouti signaling protein (36, 37). The two proteins share a

conserved cysteine-rich c-terminus primary structure. However, AgRP was found to be

expressed in the CNS, while agouti is normally only expressed in the periphery. Since its

cloning, molecular and biochemical studies have shown that AgRP binds preferentially to

the central melanocortin receptors, thus its actions in the CNS are believed to be similar

to its homologous cousin: blocking alpha-MSH stimulation of melanocortin receptors to

inhibit the intracellular increase in cAMP (38-40).

These orexigenic neurons also produce Neuropeptide Y (NPY, 41). NPY is the

most potent natural orexigenic molecule known to science (42). Like CART, NPY has its

own family of receptors independent of the melanocortins, which may provide alternative

---

[2] As the name suggests, this neuropeptide was discovered as an upregulated transcript following cocaine or amphetamine regimens (33). It may also be one of the physiological reasons that these drugs of abuse generally lead to weight loss in habitual users.

feeding and/or autonomic pathways to diverge from the first order neuro-humoral circuitry of the hypothalamus or brain stem. Interestingly, mice lacking NPY are not lean when given *ad libitum* access to chow; it is only when these animals are challenged with a high fat diet that a lean phenotype presents (43).

Figure 1.2

Figure 1.2

Arcuate Nucleus   Hypothalamus, Higher Neurons

BBB

NPY/AgRP   AgRP
+
MC3Rs   ↑cAMP
−   MC4R
POMC/CART   α-MSH
Ob-R

Behavioral and
Metabolic Changes

Peripheral Signals
Leptin, Insulin, Glucose, etc.

WAT
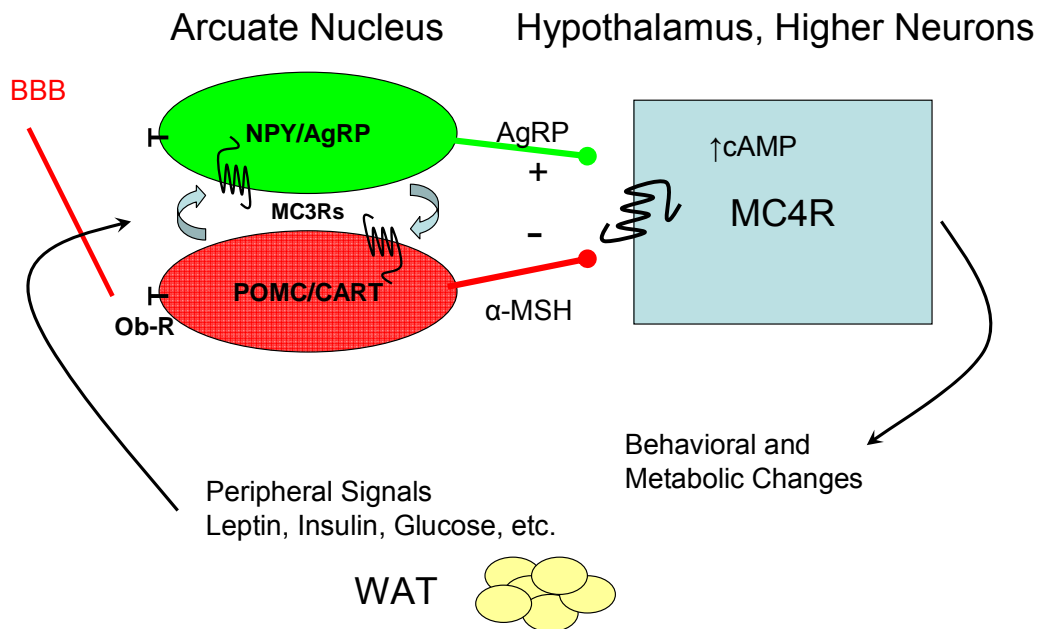
Figure 1.2: Central Melanocortin Circuit. The neuro-humoral circuit begins in the periphery of the body where hormones (e.g., leptin) are produced in response to feeding, metabolism, or energy stores (e.g., leptin). Leptin is exclusively produced by white adipose tissue (WAT) generally in proportion to the amount of lipid stored in these cells. Leptin travels to the brain where it is able to cross the blood brain barrier (BBB) at the median eminence at the base of the hypothalamus. The median eminence is populated with dendrite-like appendages from orectic (Green) neurons and anorectic (Red) neurons located in the Arcuate Nucleus of the hypothalamus. Leptin activates the anorectic neurons, causing them to increase the release of alpha-MSH, while leptin inhibits the release of AgRP from the orectic neurons. The net effect is increased activation of MC4R. The molecular events beyond the activation of MC4R are not well understood, but the behavioral and metabolic changes are well documented.

The number of signaling molecules that interact with the neuro-humoral circuitry rapidly expanded in the past decade. Leptin, shown in Figure 1.2, is the classic example

of this class of molecule. The hormone was found to be the gene disrupted in the Obese (ob/ob) mouse (4); one of the five classic mouse models of obesity collected by mouse fanciers. Leptin is expressed exclusively in white adipose tissue, the body's primary energy storage depot. The proportion of circulating leptin hormone correlates with the adiposity of the subject animal. In addition to leptin, gherelin (44), CCK (45), bombesin-like peptides (46), insulin (47), glucose (48), fatty acids (49), and other molecules have been found to activate ARC neurons and/or affect feeding behavior.

Physiological Functions of MC4R Signaling in the CNS

MC4R Knock-Out mice are also morbidly obese (24). The phenotype is remarkably similar to that of the Agouti Lethal Yellow (Ay) obese mouse (i.e., increased linear growth and morbidly obese). This paper demonstrated that MC4R was the central melanocortin receptor that is predominantly responsible for energy homeostasis in the CNS. The MC4R KO allele is autosomal dominant, but heterozygous MC4R KO mice present intermediate obesity and metabolic phenotypes. Upon the discovery of an autosomal dominant obesity syndrome, the race was on to find a human proband with a mutation in the MC4R gene. Two independent groups found patients with a frame shift mutation in their MC4R gene that presented with increased linear growth and early onset morbid obesity (2, 3).

Mutations in the coding region of the human MC4R gene are now estimated to be associated with nearly 4% of morbid obese human patients (50). These mutations are predominantly inherited in an autosomal dominant pattern, and studies have been conducted to assess the functional activity of some mutants in transient transfected cell

lines (51). Most mutations show greatly reduced functional activity, possibly due to frame shift mutations that destroy the gene's membrane localization signal sequence at the C-terminus (52).

However, the severity of lost activity is reduced in some families whose mutations appear to present with incomplete penetrance (53). The resulting receptor in one of these mutations has been found to have approximately 60% of the wildtype receptor's activity in transient transfection studies (51, 54). Such a relatively small loss of activity that can still lead to morbid obesity in adults is reminiscent of the intermediate phenotype found in heterozygous MC4R KO mice. The studies of this mutation suggest that adults with small losses in receptor activity, or expression, could lead to an increased risk for energy imbalance and the horde of related metabolic diseases.

While many lines of research have determined how MC4R is regulated by its cognate ligands, coupled to adenylate cyclase, and functions *in vivo*, little is known about the mechanisms which control MC4R expression in the CNS. The importance of MC4R activity in energy homeostasis predicts that the expression must be tightly regulated. Therefore, given the weak expression in discrete neural loci and the constant modulation of alpha-MSH and AgRP signaling, I have hypothesized that MC4R expression must be tightly regulated in the feeding centers of the CNS in order to properly monitor energy stores and direct appropriate feeding behavior.

Regulation of MC4R

Little has been learned about the MC4R promoter since the gene was cloned in 1994. The apparent reason for this has been largely due to a concerted focus on the

10

physiological role of the gene *in vivo*. Other reasons include a lack of appropriate model cell lines and, more importantly, the great technical challenge of detecting MC4R transcripts reliably in a system that is capable of monitoring even robust changes in expression. However, some groups have recently begun to lay down a foundation upon which exciting discoveries will be made concerning the MC4R promoter and how it controls temporal and spatial MC4R expression.

Recently, Professor Duman's found that rat MC4R expression in certain brain regions (striatum and hippocampus) increases about 100% in response to a regimen of acute, high dose morphine (27). The group has since shown that a regimen of chronic cocaine will induce nearly 100% increase in MC4R expression in the same neural regions (28). The method of expression monitoring chosen by Duman's group was traditional Northern blots. This method requires a relatively high amount of total RNA to detect MC4R expression in isolated brain regions. The size of the rat brain allows for a greater yield in RNA extraction, which facilitated these studies. Doing the same study using Northern blots in laboratory mice (the most common mammal amenable to genetic studies) would require pooling RNA from several animals to detect even baseline levels of MC4R transcript. This would necessarily increase the likelihood of variance in results, leading to a lower probability of finding statistically significant data.

Another group has recently reported that CART and MC4R are acutely upregulated by increase in dietary calories from fats (55). This group hypothesized that acute or intermediate changes in energy balance would lead to compensatory action in the hypothalamus and other tissues to reach energy homeostasis. In order to find such acute effects, adult rats were fed a high fat diet for 14 days. During the 14 day period, some

11

animals were sacrificed at 12, 24, and 48 hours after switching the diets, while the

remaining animals were all analyzed after 14 days. Interestingly, no change in *leptin*

gene expression or circulating levels was detected over the experimental period. Similar

to the Duman Laboratory studies, this study used laboratory rats and showed by *in situ*

hybridization increases in transcript expression in the hypothalamus. This method is an

improvement over that employed by the Duman group because RNA does not have to be

pooled to detect the minutely expressed levels of endogenous MC4R. However, *in situ*

hybridization studies are still very difficult to reproduce in mice because of the weak

expression of MC4R.

In 2001, Professor Mountjoy's group published a paper describing the basal

activity of the murine MC4R promoter (56). By using RT-PCR, the group showed that

UMR106 (bone), HEK-293 (kidney), and GT1-7 cell lines expressed endogenous MC4R

transcripts, while no transcripts were detected in Neuro-2A cells. The group noted

multiple transcription start sites were evident from 5'-RACE assays, but the primary start

site was located approximately 430 bp upstream of the start of translation in C57BL6

mice. Their results show almost no difference in the luciferase (promoter) activity when

increasing 5'-flanking sequence from -600 to -1500 (relative to start of translation) in

GT1-7 cells. However, a marked increase was observed between the -434 construct (2.0

± 0.1) and the -600 construct (5.2 ± 0.1), which includes a highly conserved region of the

5'-flanking sequence (see Chapter 3).

Mountjoy's group has recently published a paper describing MC4R promoter

beta-galactosidase transgenic mice (57). The group created three independent lines;

however, only one of three transgenic lines showed a pattern of transgene expression that

almost entirely mimicked endogenous MC4R expression in the CNS. The sequence used in these transgenic mice was from -1500:-1 of 5'-flanking sequence without any of the 3'-flanking sequence used in their *in vitro* experiments.

The Vaisse group described the basal promoter activity of the human MC4R promoter (58). This group used luciferase reporter constructs ranging in 5'-flanking sequence from -2900 to -470 (relative to the start of translation), and all constructs shared a 3'-end at 10 bp into the 5'-UTR (i.e., the constructs did not contain the hMC4R 5'-UTR). Basal promoter activity was determined in both neuronal cell lines (GT1-7 and Neuro-2A) and non-neuronal cell lines (HEK-293 and NIH3T3). Luciferase (promoter) activity was weak in all cell lines, relative to the empty pGL3 vector, with the shortest constructs (-470 and -600 constructs). However, the larger constructs reached a peak plateau with the -1200 through -1900 constructs in all but the NIH3T3 cells. The largest construct (-2900) showed some loss in peak activity in all cell lines but Neuro-2A. These data suggest that the crucial promoter sequence of the human MC4R 5'-flanking sequence is between -600 and -1900 bp upstream from the start of translation, but the experiments fail to consider the possible contribution of promoter activity in the 5'-UTR of the human gene.

These foundational papers are important steps in learning about the regulation of MC4R temporal and spatial expression. Determining which promoter regions control the spatial expression pattern of MC4R will help investigators understand which neuronal regions control which aspects of autonomic physiology, or more importantly, which regions could lead to increased risk for diseases of metabolic imbalance.

CHAPTER II

MATERIALS AND METHODS

Materials and Providers

All common laboratory reagents mentioned in the following chapter were

obtained from Sigma, Fisher Scientific, VWR Scientific Products and EMD Chemicals,

unless specifically noted. Restriction and DNA/RNA modifying enzymes were

purchased from Promega and New England Biosciences, except those contained in kits or

noted otherwise. All Real Time PCR reagents were obtained from Invitrogen. All cell

culture reagents, including sterile media, sera, and liposomal transfection agents, were

purchased from Gibco/Invitrogen (Life Technologies, Inc.). Luciferase and Beta-

Galactosidase (Bea-Glo) assay reagents were obtained from Promega. Radioactivity in

the form of alpha-^{32}P dCTP was purchased from Amersham Biosciences.

RNA and Recombinant DNA Methods

General Techniques

All recombinant DNA techniques and methods were performed following the

general procedures as outlined in Molecular Cloning: A Laboratory Manual (Maniatis et

al., 1982). Radiolabeling of all Southern probes was carried out using Ready-To-Go

DNA Labeling Beads (Amersham Biosciences). Any modifications or variations of these

procedures are noted in the text below. All sequence for the genomic MC4R loci are

referenced from the start of translation. All linear vectors were treated with Calf Intestine

Alkaline Phosphatase (Promega) prior to ligation, as per the manufacturer's directions.

All ligations were performed using the Rapid DNA Ligation Kit (Roche) following the

manufacturer's provided protocols.

BACmid Screening and Subcloning of mMC4R

We isolated genomic DNA flanking the MC4R coding region by screening a

mouse BAC library (129/SvEvTACfBr obtained from Roswell Park Cancer Institute), a

generous gift of Dr. David Threadgill (Duke University). A ^{32}P labeled 999 bp mouse

MC4R predicted coding sequence probe was used to screen the library digested with

KpnI or HindIII. Three independent and overlapping BACmid clones were isolated,

restriction mapped, and characterized by Southern blot analysis using probes

corresponding to the coding region or 3'-untranslated regions (UTR) of the mouse MC4R

gene. One positive BACmid was digested with KpnI, resulting in a 13.4 kb fragment

containing 12.7 kb of 5'-flanking sequence and 700bp of coding sequence and a 4.6 kb

fragment containing 299bp of coding sequence and 4.3 kb of 3'-flanking sequence.

These fragments were each cloned into pSP72 (Stratagene) and sequenced (pSP72+14 kb

MC4R and pSP72+4.6 kb MC4R, respectively). The positive BACmid was also digested

with HindIII, and a 4.8 kb fragment containing 3.3 kb of 5'-flanking sequence, the entire

coding sequence, and approximately 500bp of 3'-flanking sequence was cloned into

pSP72 and sequenced (pSP72+4.8 kb mMC4R).

These three subcloned genomic fragments were used as templates and/or restriction digested for generating all of the murine MC4R promoter-reporter fusion constructs and Southern blot probes.

Generation of Promoter-Reporter Fusion Constructs

The proximal murine MC4R (mMC4R) promoter fragments were amplified by PCR with a series of forward primers located at -648bp, -432bp, -344bp, and -186bp paired with a single reverse primer at -5bp using the pSP72+4.8 kb mMC4R as PCR template. Each forward and reverse primer contained an Acc65I site engineered onto its 5'end. These PCR products were cloned into the Acc65I restriction site of the luciferase reporter vector pGL3-Basic (Promega) 5'-multiple cloning site (5'-MCS) and sequenced for verification (designated pGL+648m, +430m, +340m, and +180m, respectively). A 1.6 kb PstI fragment (-1607:-5) was isolated from pSP72+4.8 kb mMC4R and cloned into pBKS+ (pBKS+1.6 kb mMC4R). The 1.6 kb fragment was subsequently freed, subcloned into the Acc65I and XhoI sites of pGL3-Basic, and sequence verified (pGL+1600m). A 2.4 kb Acc65I-PacI fragment was lifted from pSP72+4.8 kb mMC4R and cloned into Acc65I/PacI digested pGL+1600m (pGL+3300m). A 6.4 kb EcoRI fragment from pSP72+14 kb mMC4R was cloned into EcoRI linearized pGL+1600m (pGL+7900m). Finally, the pGL+3300m was restriction digested with EcoRV and PacI, the overhang from PacI was filled with Klenow fragment, and subsequently ligated to create pGL+890m.

Sequencing of the clones revealed an unstable CA di-nucleotide repeat located approximately 1500bp upstream of the mMC4R starting codon. All of the constructs

containing this repeat were verified to contain between ten and fifteen CA di-nucleotide repeats following each large scale plasmid prep.

The human MC4R (hMC4R) gene was cloned via PCR using primers based on sequence data obtained from the Ensembl genome website (http://www.ensembl.org). Forward cloning primers for the human MC4R were located at -2030bp, -1770bp, -1554bp, -895bp, -744bp, -594bp, -419bp, -233bp, and -133bp relative to the start of translation. A single reverse cloning primer with 5'-end at -1, also relative to the start of translation, was paired with each of the forward cloning primers, such that the constructs would contain the entire 5'-UTR. Each forward primer had an Acc65I site engineered onto their 5'-ends, while the reverse primer had an XhoI site engineered onto its 5'-end. The PCR products were restriction digested with Acc65I and XhoI, cloned into linear pGL3-Basic, and sequence verified (designated pGL+2030h, +1770h, +1550h, +900h, +740h, +600h, +420h, +230h and +130h, respectively).

The human DNA material used for cloning the MC4R 5'-flanking was a generous gift from Dr. James Sutcliffe (Vanderbilt University). Sequencing of each construct revealed a 100% match between the donor's DNA sequence and that obtained from the Ensembl genome website, *supra*.

Sequencing and In Silico Analysis

Sequencing PCR reactions were performed using Big Dye Terminator (Applied Biosystems) chemistry following the manufacturer's instructions. The reactions were resolved on sequencers in the DNA Sequencing Core laboratory at Vanderbilt University

17

Medical Center and the Heflin Center for Human Genetics at the University of Alabama at Birmingham.

The MC4R locus sequence from multiple species available in the public databases and that from the 129 strain mouse BACmid was submitted for VISTA sequence conservation analysis following the guidelines provided on the VISTA website (http://genome.lbl.gov/vista/index.shtml). The threshold for "significant" conservation was left at the default level of 75%, as provided by the VISTA site. Putative cis-element sites were identified and confirmed by at least two of the following software packages: rVISTA (http://genome.lbl.gov/vista/index.shtml), MacVector 7.1 (Accelrys), GenomatixSuite (Genomatix Software GmbH), or AliBaba2.1 (http://www.gene-regulation.com).

Polymerase Chain Reaction and Analysis

PCR was performed using standard protocols for a variety of polymerases. Cloning PCR was performed using murine or human genomic DNA as template (~100-200ng per 25μL reaction) and *Pfu* polymerase (Stratagene) for high fidelity cloning. General PCR (genotyping, construct screening, RT-PCR, etc.) was performed using 0.01-10ng of plasmid/BACmid DNA or 50-100ng genomic DNA and *Taq* polymerase provided in AccuPrime SuperMix II (Invitrogen). PCR reactions (with the exception of Real Time PCR) were performed on DNA Engine Dyad Peltier Thermal Cyclers (MJ Research/Bio-Rad). Genotyping PCR and Real Time PCR conditions and protocols are discussed further below.

PCR reactions were analyzed by running on 1.0-2.0% agarose matrix gels to separate DNA bands by size. Molecular weight markers of standard size were run to determine if reactions yielded the predicted size products.

Total RNA Extraction and DNase I Treatment

Total RNA was prepared following the manufacturer's suggested protocol for cell culture dishes or tissue mass using TRIzol reagent (Invitrogen) for cell lines and non-brain tissue samples, respectively (see below for tissue harvesting protocol).

For cell culture preparations of total RNA, the growth medium was aspirated and the cell dish was washed twice with warmed phosphate buffered saline (Gibco). Eight milliliters of reagent was pipetted onto the cells and incubated at room temperature for approximately one minute. Then, the cell lysate was passed through a pipet four to five times to aid lysis, and the cell lysate was placed in a 15mL conical tube with cap. After a five minute room temperature incubation, 1.6mL of chloroform was added to the tube and vigorously shaken for 15 seconds. The lysate:chloroform mixture was allowed to incubate at room temperature for 2-3 minutes prior to a low speed spin in a tabletop centrifuge for 15 minutes to separate the phases. Upon centrifugation, the clear top (aqueous) phase was removed (approximately 3-3.5mL) and placed in a fresh tube with cap. Careful attention was paid not to disturb the white interphase, which contains DNA that would contaminate the sample preparation. The RNA was precipitated by adding an equal volume of ice cold Molecular Biology Grade isopropyl alcohol (Sigma) and mixed thoroughly. During a ten minute room temperature incubation, the sample was placed

into 7-8 1.5mL microfuge tubes. The microfuge tubes were spun at maximum speed for ten minutes in a microfuge to pellet the RNA.

For tissue samples (~50-150mg), the harvested tissues were physically homogenized in the presence of 0.5mL of TRIzol reagent in a 1.5mL microfuge tube using a plastic capped pestle. If more than one tissue was being homogenized, the pestle was cleaned thoroughly with Kimwipes and autoclaved double distilled water, and they were rinsed with RNase-Away (Invitrogen) between each sample preparation. The tissue lysates for kidney and liver samples were spun at 1500 rpm for five minutes to remove insoluble debris before continuing with the protocol. The tissue lysate would then be added to an additional 1.5mL of TRIzol reagent, and the above described protocol for cell culture RNA preparations would then followed, albeit with smaller volumes and fewer microfuge tubes for the RNA precipitation step.

All samples were analyzed for concentration and purity, and subsequently treated to remove any residual genomic DNA contaminants with RNase-Free DNase I (Promega) following the manufacturer's directions. Following DNase treatment, the enzyme was heat inactivated and removed via phenol:chloroform extraction. The precipitated DNase treated RNA was then resuspended in DEPC-treated water.

Due to the small mass of the brain tissue samples (ranging from 5mg to 20mg), these samples were prepared using the Absolutely RNA RT-PCR Miniprep Kit (Stratagene) following the manufacturer's suggested protocol by sample mass. Samples were physically homogenized in the prepared lysis buffer using the pestles and cleaning regimen as previously described above. The brain tissue lysates were spun through a column to remove insoluble materials and then through a second column designed to

20

collect RNA preferentially. The kit includes a DNase treatment step, which was performed while the sample was incubated on the second column. Following DNase treatment and column washes, the RNA was eluted from the second column with two consecutive 30μL elution buffer rinses.

DNase treated samples (cell culture, peripheral, and brain region samples) were analyzed for concentration and purity prior to cDNA synthesis reactions. All RNA was stored ultrafrozen at -80C.

cDNA Synthesis from RNA

Two micrograms of DNase I treated RNA from cell culture and tissue samples or 400ng of DNase treated RNA from brain tissue samples were used in cDNA synthesis reactions using SuperScript III reverse transcriptase (Invitrogen) following the manufacturer's provided protocol with the following modifications. Sample reactions were performed in 20μL volume reactions. A dNTP-master mix of shared components was prepared containing 0.5μL of provided oligo dT (50μM), 0.5μL of provided random hexamers (50ng/μL), and 1.0μL of dNTP mix (10mM) per reaction to reduce variability between sample reactions. Each sample had two dNTP-master mix tubes for an RT reaction and a -RT reaction control. The 4.0μL dNTP-master mix, sample DNased total RNA (400ng), and DEPC-treated water to 10μL were added to a PCR reaction tube.

The first mixture was incubated at 65C for five minutes, then it was placed on ice for at least one minute before opening the tubes. During the first incubation, an RT-master mix and a –RT-master mix were prepared containing 2.0μL of provided 10X RT Buffer, 4.0μL $MgCl_2$ (25mM), 2.0μL DTT (0.1mM), 1.0μL RNaseOUT (RNase

Inhibitor), and either 1.0μL of SuperScript III Reverse Transcriptase or 1.0μL of DEPC-treated water per reaction, again to reduce inter-reaction variability in these micro volume reactions. The master mixes were added to the respective PCR reaction tubes so that each sample had an RT reaction and a sister -RT control reaction. The cDNA reactions (and control -RT tubes) were incubated at room temperature for ten minutes prior to a 50 minute incubation at 42C. Following the RT reaction, the RT enzyme was heat inactivated at 70C for 15 minutes, and the RNA was destroyed by the addition of 1.0μL of RNase H and a subsequent incubation at 37C for 20 minutes. Samples were stored at -20C until further analysis (PCR, Real Time PCR, etc.) was performed.

Real Time Multiplex Quantitative PCR and Analysis

Triplicate Real Time PCR reactions for brain and peripheral tissue samples from control and transgenic mice were performed using a Chromo4 equipped Real Time PCR 96-well 4-color multiplex thermal cycler (MJResearch). Primers for experimental gene (MC4R, EGFP, or Beta-Galactosidase) were FAM labeled, and control (beta-actin) were JOE labeled. Both an experimental and control primer pair were included in all reactions, allowing for multiplexing with an internal control (beta-actin) in the reactions.

The Real Time PCR reactions were performed using the Platinum Quantitative PCR SuperMix-UDG System (Invitrogen), including loading reference dye, reaction components, and water. Briefly, 2μL of brain tissue cDNA reaction (~40ng of total RNA template) or 3μL of peripheral tissue cDNA reaction (~300ng of total RNA template) was used in each Real Time PCR triplicate reaction. Only one Real Time PCR reaction was performed for each -RT control reaction. To minimize variability between sample

reactions, a master mix containing all reaction components except the template was prepared. The master mix contained 25μL Platinum Quantitative SuperMix-UDG, 17 or 18 μL of nuclease free water (peripheral and brain tissues, respectively), 1.0μL each of ROX reference dye, and the primer pairs for the experimental gene and beta-actin internal control per 50μL reaction. The requisite amount of master mix was added to each well of an opaque 96 well plate (Bio-Rad) on ice, and then the template was vortexed and aliquotted into each reaction tube.

A dilution series of murine MC4R plasmid (EGFP plasmid or LacZ plasmid) of known amplicon copies/volume was used for plotting a standard curve and quantifying amplifiable template from the cDNA reactions as a standard.[3] The Chromo4 equipped thermal cycler took optical readings during each cycle to monitor the reaction in real time. The data was analyzed by the Opticon 2 software in context of the standards provided in the user interface. The ROX reference dye was monitored to ensure loading volume of reaction master mix was consistent. The internal control PCR reaction (beta-actin) was used to normalize the data from each tissue. The results are expressed in terms of cDNA amplicons per nanogram of total RNA template.

SNP Discovery

For the single nucleotide polymorphism discovery, we provided Professor Philippe Froguel's laboratory with the approximate sequence location of the *CR-8* conserved region in the human MC4R locus (centered within a ~250 bp window of sequence). That lab then designed PCR primers (Forward 5'-CAG TCT CTT ATC CGG CTT GC; Reverse 5'-CCA TTG GGA GAC GAA TCT GT) flanking the 250 bp

---

[3] Each plasmid has two amplifiable DNA "amplicons", one for the plus strand and one for the minus strand.

sequence given to screen, amplified the region from a cohort of 162 subjects with early

onset morbid obesity, and sequenced the clones. Sequence data was compared to the

human sequence data available on the *Ensembl* website, *supra*. Over 350 normal weight

control chromosome pairs were then screened in the same manner.

Site-Directed DNA Mutagenesis

Site-directed mutagenesis was performed using the Quick Change II Kit

(Stratagene). Primers harboring a G residue to A residue mutation were synthesized and

purified by HPLC (Invitrogen). Plus strand primer: (090) 5'-GGA TTG GTC AGA AGG

AAG CA<u>A</u> AGG AGG AGC C-3', Minus strand primer: (091) 5'-GGC TCC TCC T<u>T</u>T

GCT TCC TTC TGA CCA ATC C-3' (underlined base is the point of mutagenesis).

Mutagenesis was carried out on mMC4R promoter-luciferase reporter constructs

pGL+640m and pGL+890m and on human constructs pGL+600h and pGL+900h to

generate pMut+640m, pMut+890m, pMut+600h, and pMut+900h, respectively.

<u>Cell Culture</u>

Propagation

Cell lines maintained in a humidified 5% CO_2 incubator. GT1-1, GT1-7, HEK-

293, and HeLa cells were maintained in DMEM (high glucose) medium supplemented

with 1% glutaMAX, 10% heat inactivated fetal bovine serum, and 100U/mL penicillin-

streptomycin. Neuro-2A cells were maintained in 1:1 DMEM/F12 (low glucose, 15mM

HEPES buffer, and pyridoxine hydrochloride) medium supplemented with 1%

glutaMAX, 10% heat inactivated fetal bovine serum, and 100U/mL penicillin-streptomycin. CAD cells were maintained in 1:1 DMEM/Ham's F12 medium supplemented with 1% glutaMAX, 8% heat inactivated fetal bovine serum, and 100U/mL penicillin-streptomycin. SH-sY5Y cells were maintained on 1:1 Earle's MEM/Ham's F12 medium supplemented with 1% glutaMAX, 10% heat inactivated fetal bovine serum, 0.1mM non-essential amino acids (NEAA), and 100U/mL penicillin-streptomycin.

Cell passages were performed using Enzyme Free Dissociation Buffer (Invitrogen). Briefly, cells in 10cm plates (Sarstedt) were washed twice with 5.0mL warmed PBS (37C). Five milliliters of warmed Dissociation Buffer was added to the plate and rocked back and forth for 60-90 seconds at room temperature. After aspiration of the buffer, the plate was rapped 2-3 times on the palm of the hand. After a 2-3 minute room temperature incubation, the plate was rapped again and 5-6mL of appropriate growth medium was added to the plate. The cells were passed through a pipet to aid in dissociation and counted before replating in growth medium.

Transient Transfection and Harvest

All constructs were prepared in triplicate large scale preps using the Endotoxin Free Plasmid Maxi Kit (Qiagen). The endotoxin free plasmid preps ensured lower cell toxicity and greater reproducibility of transfection results between plasmid preps. Each plasmid prep was transfected three times. All transfections were performed in triplicate in the 24-well plates.

Lipofectamine 2000 was used to perform transient transfections in all cell lines. The manufacturer's suggested protocol was optimized for the GT1 cell lines and the

Neuro-2A cell line by varying the amount of total and experimental DNA mass in 24-well plates (Sarstedt). As per the manufacturer's instructions, cells were passaged, counted, and plated in 0.5mL of growth medium without antibiotics per well in the optimized density for a 90-95% confluency on the date of transfection. The optimal confluency of GT1 cell lines was about 95%, while the Neuro-2A cell line's optimal confluency was between 90-95%. All other cell lines were transfected according to GT1 optimized conditions.

For the Neuro-2A cells, however, and additional step was included to induce the cells to enter a quasi-differentiated state, complete with axon-like appendages connecting cells up to 15 cell lengths apart. 24 hours prior to transfection, the medium for Neuro-2A cells was replaced with DMEM (low glucose) supplemented with 1% glutaMAX and 1% N2A-Supplement (N2A experimental medium).

The optimal amount of DNA to transfect for the GT1 cell lines was found to be 600ng total DNA per well. To account for the greatly different mass of the experimental plasmids from large to small promoter-reporter constructs, the total mass of the largest construct transfected was 600ng, while the mass of the smaller constructs would be proportional based on size so that an equal amount of experimental plasmid would be introduced for each construct. Any mass less than 600ng for the smaller constructs would be made up by adding an inert plasmid (e.g., pBKS) up to 600ng total. For Neuro-2A cells, the optimal total mass of DNA per well was found to be 500ng. To normalize the transfection results, an internal control plasmid, phRL-SV40 (Promega), was co-transfected in each experiment. The robust activity of the *Renilla* luciferase reporter gene

and strong promoter allowed for only a negligible addition of 1.0ng of phRL-SV40 control plasmid per well.

The DNA/Lipofectamine 2000 reagent transfection solution was prepared according to manufacturer's suggested protocol for 100μL volume per well. This solution was allowed to bathe the cells for 24 hours before harvesting. Twenty-four hours after transfection, the cells were washed 2x with PBS (warmed to 37C), and cell lysates were harvested by freeze fracture in the presence of 200μL of Passive Lysis Buffer (PLB, Promega). After the PLB was completely frozen in all 24 wells, the plates were removed from the dry ice to the bench to allow to thaw. Upon thawing, the cell lysates were passed through a micro-pipet 3-4 times and transferred to a fresh microfuge tube with cap. The lysates were cleared of cellular debris by spinning briefly in a microfuge, and supernatants were transferred to a fresh tube. Lysates were analyzed immediately (see below for reporter assays), but remaining lysate supernatant was kept at -80C for up to six months with negligible loss in relative activity of experimental firefly luciferase to internal control *Renilla* luciferase.

Transgenic Animals

Generation of Transgenic Animals at Vanderbilt University

The murine MC4R 4.8kb HindIII fragment containing 3.3kb of 5'-flanking, the entire coding sequence, and 450bp of 3'-flanking sequence was cloned into the XhoI site in pIRES-tauGFP-LNL, generously provided by Dr. P. Mombaerts (The Rockefeller University). A 7.8kb XhoI to SalI restriction fragment was gel purified and prepared for

pronuclear micro-injection using the GeneClean kit (BIO-101). The construct fragment was further cleaned using an S&S Elutip (Schleicher & Schuell) following manufacturer's directions. Single cell embryos from hybrid (B6D2 F1) donor females were micro-injected by the Vanderbilt-Ingramm Cancer Center Transgenic Core Facility using approved protocols by the IACUC at Vanderbilt University. Tail clippings from 30 potential founders were collected approximately 21 days after birth, and these were used to extract genomic DNA for genotyping. Four founder animals with germline transmission were backcrossed and maintained on C57BL6NTac strain mice from Taconic Farms.

Generation of Transgenic Animals at UAB

The 3300MC4Luc3 transgenic construct (Construct B) was generated by PCR amplifying the 3'-region of murine MC4R from +975 to +1645, cloned into the BamHI restriction site in the 3'-MCS of the previously described pGL+3300m and sequence verified. The 3300MC4Luc3 transgene was liberated by an Acc65I and SalI restriction double digest. The 3300MC4LacZ3 (Construct A) was similarly generated by removing the luciferase reporter cassette from the 3300MC4Luc3 construct and replacing it with purified restriction cut nuclear localization signal tagged-LacZ reporter cassette from pnls-lacZ (a generous gift of Dr. R. O'Brien, Vanderbilt University). The 3300MC4Luc construct (Construct C) was liberated from pGL+3300m by Acc65I and BamHI double digest, the 890MC4Luc construct (Construct D) was liberated from pGL+890m by Acc65I and SalI double digest, and the 430MC4Luc construct (Construct E) was liberated from pGL+432m by Acc65I and SalI double digests. All transgenic constructs

were gel purified using QiaEX II gel purification beads (Qiagen) and resuspended in nuclease free water (Invitrogen). Single cell fertilized embryos from donor female C57BL6NTac (Taconic Farms) were injected with purified linear DNA for 3300MC4Luc, 890MC4Luc and 430MC4Luc constructs and transferred to pseudopregnant recipient females for gestation (UAB Transgenic Core). The purified linear 3300MC4Luc3 construct was microinjected into fertilized single cell embryos (F2) collected from hybrid C57bl6 x SLJ (Taconic Farms) females (UAB Transgenic Core).

The minimal TK promoter -109:+54 was isolated from pT109-luc by restriction digest with Acc65I and XmaI. The isolated minimal TK promoter fragment was ligated into the Acc65I/XmaI sites of pGL3-Basic 5' multiple cloning site and sequence verified (pTKLuc). The 5' murine MC4R sequence fragment from -614:-495 was PCR amplified and cloned into the Acc65I site upstream of the minimal TK promoter plasmid and verified by sequencing (pTKLuc+-614:-495m, Construct H). Taking advantage of ClaI restriction sites at -560 in the murine MC4R flanking sequence and at +2018 in pGL3-Basic (just 3' of BamHI in downstream MCS), the MC4R-TK heterologous promoter transgenic constructs were isolated by ClaI digestion and gel purified for microinjection. For comparison *in vivo*, an empty TKLuc transgene (Construct G) was isolated from pTKLuc by Acc65I/BamHI double digest and gel purified for microinjection. Linear, purified DNA constructs were microinjected into F2 hybrid (C57BL6 x SLJ) single cell embryos and transferred to surrogate mothers for gestation. At three weeks of age, mice were weaned and tail clippings were collected. Genomic DNA extracted from tail clippings were then analyzed by PCR and Southern Blotting for genotyping. Twelve positive transgenic founders were identified by PCR and Southern Blot.

All luciferase transgenic mice were maintained on C57BL6NTac background strain mice obtained from Taconic Farms.

Housing and Care of Animals

All housing and care of animals were performed according to current IACUC protocols and standards. All animal protocols for experiments were approved by IACUC.

Genomic DNA Isolation

Genomic DNA was extracted from tail clippings (1-3cm in length, depending on age of the animal) of the potential founder animals and offspring. Tail biopsies were digested in Proteinase K buffer 8-24 hours at 55C. Following digestion, the tail solution was phenol:chloroform extracted with an equal volume of 1:1:24 phenol:chloroform:isoamyl alcohol. The DNA in the supernatant (following 10 minute maximum speed microfuge spin) was ethanol precipitated with 2X volume of ice cold 100% ethanol. The pelleted DNA was resuspended in TE buffer (10mM Tris, pH 8.0, 1mM EDTA) for a concentration of about 1.0mg/µL. Genomic DNA was stored at 4C.

Southern Analysis and Genotyping

Genomic DNA Southern analysis and genotyping were performed according to standard protocols by Maniatis, *supra*. However, certain modifications were of the standard Southern protocol were executed. Briefly, genomic DNA (15mg) was digested for 12-24 hours with restriction enzyme(s) at the requisite temperature. Digested DNA was loaded onto a 12cm x 13cm 1.0% agarose gel with ethidium bromide, and it was

30

allowed to run for 8-12 hours at 30 volts (a molecular weight standard was included in the left most lane). Following electrophoresis, the gel was wrapped in cellophane and photographed under UV light (a fluorescent ruler was placed along the left side of the gel. Good restriction enzyme digests show a relatively even "smear" of DNA in each lane, usually with a characteristic bright band(s) of intensity of ethidium bromide, which represents one or more RFLP. Only good digests were blotted for analysis.

The blotting apparatus was constructed to allow 0.4M NaOH solution wick up thick filter paper (Fisher Scientific) and through the gel and cellulose blotting paper (Zeta-Probe GT, Bio-Rad). The blotting paper was marked with a pencil to note which side was facing the gel. The blotting paper was also marked with a pencil on the left side corresponding to the molecular weight standards for 1.0 kb to 12 kb. Blotting was allowed to continue for 10-15 hours. Following blotting, the papers were rinsed for five minutes in 1X SSC Buffer, blotted dry gently with a KimWipe, placed between two pieces of dry filter paper, and baked at 80C for 45 minutes.

Blots were pre-hybed in hybridization buffer at 65C. During pre-hybridization, Southern probes were radiolabeled using the Ready-to-Go Labeling Beads, which utilize a Klenow fragment. A 0.7 kb fragment of the EGFP transgene coding sequence was used as a probe template for the MC4R-ITG transgenic mice. A 1.0kb fragment from the firefly luciferase transgene coding sequence was used as a probe template for all luciferase transgenic mice. A 1.8kb fragment from the beta-galactosidase transgene coding sequence was used as a probe template for the LacZ transgenic mice. Southern probes were analyzed for incorporation of radioactivity by scintillation counting. Probe was added to fresh hybridization buffer at 1,000,000 cps/mL. Hybridization was allowed

to run overnight. Following hybridization, blots were washed four times with Wash Buffer, for one hour each at 65C. Washed blots were sealed in plastic bags devoid of air, and placed on blanked phosphor screens for imaging capture. Image capture was allowed to proceed 12 hours for initial image, then allowed to remain on re-blanked phosphor screen for a second image for up to one week.

Southern blot images were analyzed for hybridization of probe to predicted or known restriction digest fragment sizes. The fragment sizes were calculated from known genomic sequences available through GenBank or *Ensembl*. To determine relative transgene copy number per haploid genome, a calculation available on the University of Virginia Health System Gene Targeting and Transgenic Facility's website was used (http://www.healthsystem.virginia.edu/internet/transgenic-mouse/). A series (1-20 copies per haploid genome) of standardized linear plasmid containing the transgene was added to 15mg of wildtype C57BL6 genomic DNA and restriction digested with experimental samples. The relative intensity of the standards was compared to the intensity of the experimental animal lanes on a single blot.

Transgenes introduced via microinjection often insert in tandem copies in a single site of the genome. In some cases, the transgene was determined to have incorporated into more than one site in the founder animal's genome. These independently segregating transgene integration sites could be tracked by Southern blotting, as each site had its own characteristic banding pattern. Offspring of founders with independently segregating transgene integration sites were monitored with Southern blot genotyping to separate the integration sites into individual lines of transgenic mice.

PCR Genotyping and Analysis

Once relative copy number and integration site analysis was complete for each

line of transgenic mice, PCR genotyping was the standard method for genotyping

offspring. PCR primer pairs ranging in distance of 150-300bp for each transgene coding

sequence was optimized for 10μL reactions using AccuPrime Super Mix, *supra*. 50-

100ng of tail biopsy genomic DNA was used per reaction. PCR reactions were run on

1.2% agarose electrophoresis gels at 120V for 35 minutes. Following electrophoresis,

gels were photographed under UV light and analyzed for the presence or absence of the

transgene sequence. Positive (usually the founder of the line being genotyped) and

negative control (wildtype C57BL6) were included in every PCR run.

Tissue Harvesting and Extract Preparations for Reporter Assays

Adult mice (>12 weeks) were given a lethal IP dose of Avertin (tribromoethanol,

roughly 2-3mL) before dissection, following IACUC approved protocols. To the extent

possible, tissues were removed and placed in crushed dry ice in the following order: (1)

each mouse was decapitated, brain was removed and five regions (bi-lobe –

hypothalamus, hippocampus, striatum [caudate putamen], cortex, and brain stem

midbrain containing the ventral tegmental area])[4] were dissected using the aid of a brain

---

[4] Precise locations of dissecting cuts for the brain regions – For the Hypothalamus, Hippocampus, and Cortex regions, a 2-3mm coronal section was taken in a whole brain positioned in a brain mold with wetted razor blades making incisions at approximately Interaural +1.5mm/ Bregma -2.0mm (caudal) and Interaural +4.0mm/ Bregma +0.5mm (rostral). The Hypothalamus was then excised with three cuts releasing a roughly square tissue (just above the third ventricle and on either side to exclude the lower cortex). The Cortex was cut from either side of the same section so that about 1.0mm X 3.0mm section including outer and Piriform Cortex was included. The Hippocampus was simply freed by cutting away the remainder of the brain to release this neuronal organ. For the Striatum, a 1-2mm coronal section was taken by making incisions at approximately Interaural +4.5mm/ Bregma +1.0mm (caudal) and Interaural +5.5mm/ Bregma +2.0mm (rostral). The Striatum (caudate putamen) was cut free from both hemispheres with wetted blades. The Brain Stem region was taken by making incisions at approximately Interaural -2.0mm/ Bregma -

mold (Brain Tree Scientific), (2) the ear, (3) the tail, (4) the rear paw sans toes, (5) skin from the scalp, back, and abdomen (when applicable), (6) liver, (7) the lower one half of one kidney (to avoid ovaries in females, and adrenal glands in both sexes), (8) soleus skeletal muscle (predominantly slow twitch fibers) and forelimb extensor skeletal muscle (predominantly fast twitch fibers), (9) duodenum of small intestine, stomach, and other portions of digestive track, except esophagus (when applicable), (10) testes (when applicable), (11) lower apex of heart, and (12) top right lobe of lung, and (13) esophagus (when applicable).

Brain tissues were generally between 5-25mg per sample. Peripheral tissues ranged from 35-250mg. Upon dissection, tissues were immediately placed in a fresh tube and flash frozen in a dry ice:ethanol bath and stored at -80C. Tissues to be analyzed for RNA were prepared as described above. Tissues for reporter assay analysis were thawed on ice and physically homogenized with a plastic tipped pestle in the presence of 200μL (brain and small peripheral tissues) or 300μL (most peripheral tissues) of Reporter Lysis Buffer (Promega). After physical homogenization, samples were flash frozen again in crushed dry ice to aid lysis. Samples were then microfuged at 1500 rpm for five minutes to pellet insoluble cellular debris, and approximately 60% of the supernatant was transferred to a fresh microfuge tube to avoid disturbing the pelleted debris. The supernatant was analyzed immediately, and the remainder was stored at -80C for up to three months.

6.0mm (caudal) and Interaural –3.5mm/ Bregma -7.5mm (rostral). For Cerebellum, a 2mm cube was cut with wetted blades.

Reporter Assays for Cell Culture and Transgenic Animals

In Vitro Cell Culture (Dual Luciferase Assay)

All *in vitro* luciferase assay reagents were purchased from Promega. To take advantage of the *Renilla* luciferase internal control, the Dual Luciferase Assay System was employed for reporter assays of transient transfection experiments following the manufacturer's directions. Briefly, twenty microliters of cleared lysate was analyzed for firefly and *Renilla* luciferase activities using the provided reagents in a MonoLight 3010 photometer (Pharmingen) for 10 sec, each. For each construct, firefly luciferase activity was normalized to the *Renilla* luciferase activity and compared to the basal activity of the empty vector, pGL3-Basic (Promega). The reported values are thus relative to the empty vector, which was set equal to 1.0 RLU (relative light unit). Both firefly and *Renilla* luciferase raw activity assays were collected within the linear range of the instrument, or serial dilutions of the samples were analyzed.

In Vitro Transgenic Animal Tissue Extracts (Firefly Luciferase Assay)

Luciferase assays were performed by adding 20μL of cleared sample lysate to 100μL of Luciferase Assay Buffer (Promega) in an opaque 96 well plate with clear bottom window (Bio-Rad). The reactions were mixed by pipeting 3-4 times and assayed for luminescence in a Wallac plate reader for two 10 sec readings. Six samples were read at a time, with one blank per 24 samples. Raw data are reported as average counts per second (cps). The luciferase activity was normalized to total sample protein assayed by using the Coomassie-Plus Bradford Assay Kit (Pierce Endogen). For comparison across

mouse lines and constructs, the normalized data is expressed relative to brain stem

sample activity (average brain stem is set equal to 1.0 arbitrary units).

In Vitro Transgenic Animal Tissue Extracts (Beta-Glo Assay)

Beta-galactosidase assays were performed by adding 20μL of cleared sample

lysate to 100μL of Beta-Glo Reagent (Promega) in an opaque 96 well plate with clear

bottom window. The Beta-Glo System is a luciferase based reporter assay. The beta-

galactosidase activity in the samples is measured indirectly by the amount of luciferin

reagent that is enzymatically cleaved from the 6-O-β-galactopyranosyl-luciferin molecule

in the Beta-Glo Reagent. The reactions were mixed by pipeting 3-4 times and assayed

for luminescence in a Wallac plate reader for two 10 sec readings. Due to the steady state

reaction of the Beta-Glo System, up to 96 samples were read at a time after a 60 minute

room temperature incubation. The Beta-Glo reaction was found to yield consistent

readings from 45-120 minutes after mixing reagent with sample lysate (data not shown).

One blank sample was included per 24 samples. Raw data are reported as average counts

per second (cps).

Total Protein Assay for Animal Tissue Extracts

To compare the *in vitro* luciferase activity data from mouse to mouse, tissue

sample lysates were analyzed for total protein concentration following the microplate

sample protocol included in the Coomassie Plus - The Better Bradford Assay" Kit (Pierce

Endogen) following the provided procedure. Briefly, protein concentration standards

ranging from 25μg/mL to 2,000μg/mL of albumin was prepared fresh for each run in

Reporter Lysis Buffer. Duplicates (10μL each) of standards, blanks, and samples were loaded into an opaque 96 well plate with clear window bottoms. 300μL of Coomassie Plus Reagent (warmed to room temperature) was added to each well via a multi-channel pipet. An adhesive strip was placed over the top of the plate, and the plate was shaken for 30 seconds. Following a twelve minute room temperature incubation, the plate was read on a plate reader equipped with a spectrophotometer read at 595nm wavelength. The readings for the blanks were subtracted from all other samples, and the standards were plotted on an Excel spreadsheet. Each sample was then fit to the resulting curve to determine the total protein concentration in the sample.

Beta-Galactosidase Staining

Animal Preparation

For whole brain and sagittal brain section staining, mice were given a lethal dose of Avertin by intraperitoneal and prepared for perfusion. The thoracic cavity was opened and an 18-gauge needle was inserted into the left ventricle of the heart. The right atrium was cut open, and 50mL of normal saline was perfused into the animal using its vasculature. Then, about 60mL of fresh 4% paraformaldehyde in borate buffer (pH 9.5, kept at 4C) was perfused to fix the tissues. The brain was promptly removed and stored in PBS buffer containing 10% sucrose at 4C until blocked and/or stained.

For whole fetus or embryo staining, the timed pregnant females were given a lethal dose of Avertin by intraperitoneal injection. The abdominal cavity was opened to expose the uterine horn and the embryos/fetuses. The embryos or fetuses were removed

and carefully dissected away from their protective sacs. The animals were washed twice

in PBS and placed in fixative solution (1% formaldehyde, 0.2% gluteraldehyde, 2mM

$MgCl_2$, 5mM EGTA [pH 8.0], 0.02% Nonidet P40 ([NP40], all in PBS) overnight at 4C.

After fixation, the animals were washed five times in PBS + 0.1% Tween-20 (PBT) for

15 minutes each. The fixed animals were stored in PBS at 4C for less than 24 hours

before staining.

CNS Tissue Staining

The LacZ staining procedure was modified from the method described in Mercer

et al in the journal *Neuron* (59). Briefly, after fixation the whole brains were thinly sliced

in a brain mold to ~1mm sagittal sections. These sections were washed twice in the PBT

solution, *supra*, then placed in 10mL of staining solution (5mM potassium ferricyanide,

5mM ferrocyanide, 2mM $MgCl_2$, 0.01% sodium deoxycholate, 0.02% NP-40, 1.0mg/mL

X-Gal, all in PBS) in a 50mL conical tube with cap. The tube was wrapped in aluminum

foil to shield the tissue and staining solution from light. The wrapped tube was placed on

its side in a 37C incubator equipped with a rotor set to low speed. Depending on the

level of beta-galactosidase activity, the reaction was allowed to continue for 1-3 hours.

Following staining, the sections were post fixed for 24 hours in 10% formalin, and stored

at 4C.

Whole Embryo and Fetus Staining

For whole embryo and fetus staining, after fixation the embryos were placed in

staining solution in 24 well plates and the fetuses were placed in 15mL conical tubes with

caps. One half milliliter or 5mL of staining solution, *supra*, was placed in the wells and tubes, respectively. The plates or tubes were wrapped with aluminum foil to protect the tissues and staining solution from light, and they were placed on a rotor table at room temperature set to low speed. Depending on the level of beta-galactosidase activity, staining was allowed to continue for 2-12 hours.

Following staining, animals were washed twice in PBS. The blue stain would intensify if allowed to set at 4C in PBS for ore than 12 hours. Stained animals were stored indefinitely at 4C in 70% ethanol.

Bioluminescence Imaging

D-Luciferin Preparation

Purified firefly D-luciferin potassium salt was purchased from Xenogen. Luciferin was reconstituted for animal injections into sterile pharmaceutical grade saline (Sigma) to a concentration of 25mg/mL. The reconstituted luciferin was filtered using a 0.2 micron PTFE filter disc. The luciferin:saline solution was drawn into sterile insulin syringes (100μL per syringe, or 2.5mg per dose). The luciferin syringes were stored in sealed black opaque plastic bags at -20C. Just prior to use, the necessary number of syringes were thawed to room temperature.

High Casein Diet for Bioluminescent Imaging

Normal mouse chow contains a large proportion of plant material. Plant material will create phosphorescence in the gut of the animal as it is digested, so an alternative

chow was needed. For these experiments, it was necessary to feed the mice a casein-based diet (Formula 89222, Harlan Teklad), as the background signal was reduced by a factor of 200, as compared with that from normal mouse chow with plant material that showed greater phosphorescence. Mice to be imaged were given fresh cages with the Formula 89222 chow at least 48 hours before to imaging to be certain that all prior ingested plant material was passed by the animals prior to image capture.

Animal Preparation

Natural and artificial light is absorbed by animals and remitted as phosphorescence. The fur of C57BL6 mice is capable of absorbing light and giving off phosphorescence, which would greatly increase background or cause false positives in the light capture imaging apparatus. Removal of the fur was necessary to reduce background. Animals were anesthetized under 5% isoflurane from a vaporizer, and kept under anesthetic with 2% isoflurane. Animals were depilated with clippers from the eyes to the base of the tail and the paws.

To further reduce background, all fur remaining in the shorn areas was removed by Nair (Church & Dwight Co., Inc.). Animals were then thoroughly rinsed with warmed water (37C) and dried. While animals were recovering from the anesthetic, either a heating pad was placed under the cage or an incandescent light was placed above the cage to maintain the animals' body temperature. Fur removal was performed at least 24 hours prior to (first) image capture.

In Vivo Imaging and Analysis

After a minimum 24 hour recovery period, mice were injected with 2.5mg firefly

D-luciferin by intraperitoneal injection. The luciferin requires about 10 minutes to reach

saturating and stable levels for 30-60 minutes in all tissues, and it readily crosses the

blood-brain barrier (60). Substrate was allowed to circulate for 15 minutes prior to first

image capture. Bioluminescence imaging was carried out with a highly sensitive, liquid

nitrogen cooled charge-coupled device (CCD) camera with anesthetized (1-2%

isoflurane) animals in a light-tight heated (37° C) specimen chamber (IVIS-100,

Xenogen). Depending on the sample signal, light capture was allowed to continue from

1-600 seconds with a binning of 8 (8 x 8 digital pixels binned together for software

analysis). The binning allows for "tuning" of the light capture, and 8 x 8 binning is

sufficient for determining luciferase activity through a variety of internal tissues,

including the thin murine skull.

The image capture and subsequent analysis was performed using the Living

Image Software available with the IVIS-100 bioluminescence instrument (Xenogen).

The intensity of the light emitted from the animals is represented by a pseudocolor scale

of intensity per digital pixel area (red being the most intense and blue/violet being the

least intense). The software makes sure that no pixel is saturated. Thus, independently

imaging of two animals with vastly different levels of ubiquitous luciferase activity can

result in identical images. However, the scale of the pseudocolor can be user

manipulated to show the disparity of the true differences, as if the animals were imaged

together.

The bioluminescent images were overlayed on black and white digital photographs of the animals in the light-tight box. Thus, the user is able to determine the location of the light source within the animal. Of course, the further distance (or thicker the tissue) the luciferase generated photon must travel the more likely photon scatter is to occur. Photon scatter can cause a strong signal from a precise location to appear to have a halo of weaker intensity light emission, while weak signals could be reduced to near background levels.

In addition to using bioluminescent images as a screening device for transgenic animals, the Living Image Software package also can give light emission results per unit of area over per second. This feature allows the user to quantify the level of luciferase activity in a given animal or portion of that animal's body under varying experimental conditions.

CHAPTER III

IN SILICO SEQUENCE ANALYSIS AND TRANSIENT TRANSFECTIONS OF
MC4R PROMOTER-LUCIFERASE FUSION CONSTRUCTS

Note: Base pairs are numbered from the MC4R start of translation.

Results

In Silico Sequence Analysis

We cloned the murine MC4R and flanking sequences from a 129 strain BAC

library. The murine MC4R sequence was compared to that of the human MC4R locus

available on the *Ensembl* database for homology using the VISTA webtool

(http://genome.lbl.gov/vista/index.shtml). The homology plot (shown in Figure 3.1)

revealed twelve distinct regions of the proximal 3.5 kb of 5'-flanking sequence with

~75% sequence conservation. The boundaries of the twelve conserved regions are listed

in Table 3.1, along with putative cis-elements reproducibly identified by more than one

transcription factor binding site prediction software tool.

The most striking conserved region (designated *CR-8*) is 32bp in length, 100%

conserved between human and mice, and located approximately 100bp upstream of the

putative major start of transcription in both species. *CR-8* is also highly conserved in

other mammalian species, such as rat, pig, dog, and the old world primate macaque, but

not in non-mammalian chordates chicken or fugu rubripes (data not shown).

Interestingly, the central nervous system is not the only tissue of predominant expression

of MC4R in chicken and fish (61, 62). The predicted cis-elements within *CR-8* (Sp1 and

CCAAT motifs), along with the distance to the putative major start of transcription,

suggest that this element could be involved in basal transcription. Using the rVISTA

Figure 3.1
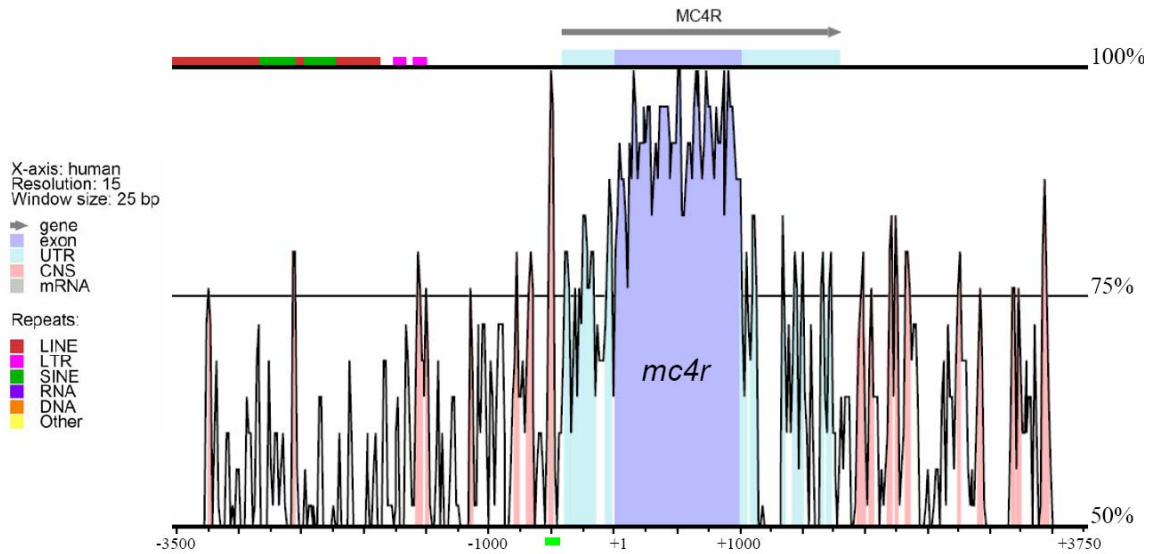
Figure 3.1: VISTA Homology Plot: Mouse and Human Genomic Loci. Human sequence is on the X-axis, and the percent homology (from 50-100%) in 25 bp sliding blocks is graphed. The most prominent feature is the homology of the coding sequence of the two species (dark blue, +1:+999). Several highly conserved regions are also present in the immediate 5'- and 3'-UTRs (light blue). All regions of at least 75% homology are shaded pink (default setting for significant sequence homology in the VISTA program). *CR-8* is marked with a green bar below the X-axis. Above the 100% homology line are the length of the MC4R mRNA (UTR and coding sequence), as well as conserved locations of various DNA repeat motifs.

(regulatory VISTA) program, these two putative cis-elements were determined to be

conserved between human and rodent species (See Table 3.1).

Also, located approximately 12 kb upstream of the *mc4r* gene, there are multiple

regions of significant sequence homology focused around an expressed sequence tag

(EST, accession BG168153) isolated from both rodent and human kidney tissue.

Northern blot and *in situ* hybridization analyses were both negative for brain expression
of this EST (data not shown).

Table 3.1

Conserved Region	Location and Size Human (Mouse)*	Putative Conserved Cis-Elements**
CR-1	-3246 (-3203) to -3220 (-3177) =27bp at 77.8%	Oct-1
CR-2	-2567 (-2303) to -2548 (-2284) =20bp at 90.0%	*None*
CR-3	-1591 (-1523) to -1542 (-1475) =50bp at 76.0%	Ap-1, GATA-1, Sp1, SRF
CR-4	-1510 (-1444) to -1486 (-1420) =25bp at 76.0%	*None*
CR-5	-1163 (-1114) to -1139 (-1088) =27bp at 77.8%	C/EBP beta, NF-1,HNF-1
CR-6	-792 (-787) to -768 (-764) =25bp at 80.0%	Oct-1, E2A
CR-7	-703 (-691) to -645 (-634) =59bp at 76.3%	NF-kappaB,
CR-8	-521 (-535) to -490 (-504) =32bp at 100.0%	CCAAT box, GATA-1, Sp1, & AP-1
CR-9	-401 (-411) to -352 (-364) =50bp at 78.0%	HSF-1, Sp1
CR-10	-327 (-332) to -303 (-308) =25bp at 76.0%	NF-AT, Oct-1
CR-11	-292 (-299) to -151 (-152) =142bp at 71.8%	Oct-1, Sp1, GR
CR-12	-70 (-73) to -22 (-26) =49bp at 77.6%	NF-kappaB, RXR/RAR
Exon	+1 (+1) to +999 (+999) =999bp at 88.7%	MC4R Coding Sequence

* As determined by VISTA web tool, http://genome.lbl.gov/vista/index.shtml
** As determined by at least two of the following: rVISTA web tool, MacVector 7.1, GenomatixSuite, and AliBaba2.1 (www.gene-regulation.com)

Endogenous Expression of MC4R in Cell Lines

A panel of cell lines, neuronal (GT1-1, GT1-7, Neuro-2A, CAD, and SH-SY5Y)
and non-neuronal (HEK-293 and HeLa), were selected to characterize the murine MC4R
promoter activity *in vitro*. Previous publications have reported endogenous MC4R
transcript expression in Neuro-2A (29), GT1-1 and GT1-7 (63), and HEK-293 (56). I
chose neuronal catacholaminergic CAD, human neuroblastoma SH-sY5Y cell lines, and
HeLa cells as examples of cell lines with no report of endogenous MC4R expression.

The GT1 cell lines were a logical choice to focus *in vitro* promoter analysis
because the cell lines were derived from an induced tumor cell line located in the Medial
Pre-Optic Nucleus of the hypothalamus, a region with endogenous MC4R expression in

rodents. We confirmed the expression of endogenous MC4R transcript in the hypothalamic gonadotropin releasing hormone (GnRH) producing GT1-1 and GT1-7 cells; however, we found all other cell lines contained no detectable level of MC4R by reverse transcriptase (RT) coupled to Real Time PCR (RT-Real Time PCR, data not shown). Similar to the report by Khong et al (63), we found that the GT1-1 cell line express approximately twice the level of MC4R transcript as GT1-7 cell line (data not shown).

Murine MC4R Promoter Results

The murine MC4R promoter-reporter constructs that were used in transfection analyses are shown in the left-hand panel of Figure 3.2. A series of deletion fragments were cloned into the 5'-MCS of the pGL3-Basic luciferase vector by either restriction fragment subcloning or PCR, or a combination of the two. The fragments are progressively shorter with 5'-end ranging from -7.9 kb at the largest to -180bp at the smallest for the murine constructs. All murine constructs have a 3'-end at the PstI site, at -5bp relative to the ATG start codon. The constructs have been given the following designations: pGL+7900m, pGL+3300m, pGL+1600m, pGL+890m, pGL+648m, pGL+432m, pGL+340m, and pGL+180m.

Endogenous MC4R Expressing Cell Lines

All *in vitro* firefly luciferase activity results were normalized to a co-transfected internal control expression vector carrying the *Renilla* luciferase gene (phRL-SV40), and the results are presented as relative light units (RLU relative to the luciferase activity

from transfections of the promoter-less pGL3-Basic vector). In the hypothalamic GT1-1

cell line, the largest promoter construct yielded modest promoter activity (Figure 3.2,

pGL+7900m, 8.8 ± 1.6 relative to pGL3-Basic = 1.0). Deleting from 7.9 kb to 3.3 kb of

Figure 3.2
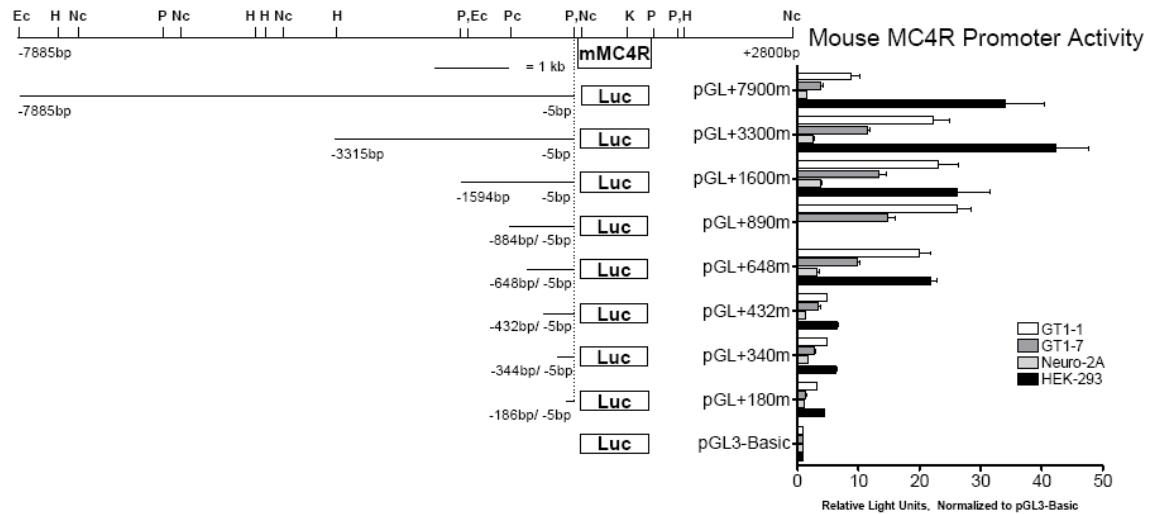
Figure 3.2: Murine MC4R Promoter-Luciferase Reporter Constructs and *In Vitro* Results. The left-hand panel shows a schematic representation of the murine MC4R locus and the promoter-luciferase reporter constructs used in the experiments. The dashed line represents the PstI site at -5 bp from the start of translation that is the 3'-end of the MC4R sequence used in all murine MC4R-promoter reporter constructs. The right-hand panel is a graph representation of the luciferase activity from transient transfected cells lines. The data is the average of at least three transfections from three independent plasmid preps. Error bars represent S.E.M. Ec = EcoRI; H = HindIII; Nc = NcoI; P = PstI; Pc = PacI; K = KpnI.

5'-flanking sequence shows an increase in activity (pGL+3300m, 22.2 ± 2.8) that peaks

with the pGL+890m construct (26.2 ± 2.2). A small decrease in activity is seen upon

deletion of the sequence from -890 to -648 (pGL+648m, 19.9 ± 1.9). However, a marked

decrease in luciferase activity is seen when deleting the sequence from -648 to near the

putative major start of transcription (pGL+432m, 4.8 ± 0.1), which contains the entire 5'-

UTR sequence. This deleted sequence included the *CR-8* conserved region.

47

Further deletions yielded little decrease in promoter activity in the GT1-1 cell line. The same relative pattern of luciferase activity is present in transiently transfected GT1-7 cells, albeit at approximately 50% of the luciferase activity relative to the promoter activity seen in the GT1-1 cells (Figure 3.2, pGL+7900m, 3.8 ± 1.2; pGL+3300m, 11.4 ± 1.7; and pGL+648m, 9.9 ± 1.2).

Non-Expressing Cell Lines

A similar pattern of luciferase activity for the murine MC4R promoter constructs was also found in the murine neuroblastoma cell line Neuro-2A and the human embryonic kidney cell line HEK-293 (see Figure 3.2). Note that the luciferase activity did not markedly drop between the two largest constructs, as it did for the GT1 cells lines and the Neuro-2A cells. HeLa, SH-SY5Y and CAD cells also produced modest to low luciferase activity, despite not expressing detectable levels of transcript (data not shown). The luciferase activity in these cell lines tracked similarly to that of HEK-293 results.

Distal Conserved Regions

Since the relative basal promoter activity decreased from a maximum in the GT1 cell lines with the pGL3+890m to less than half of the level of the pGL3+648m with the longest construct (pGL3+7900m), it was possible that negative promoter elements could be located in the sequence between -890 to -7.9 kb. To further characterize the more distal conserved regions found through the VISTA homology plots, I PCR cloned the conserved regions (with 300-500 flanking base pairs both upstream and downstream for sequence context) in the murine MC4R genomic locus located from -2.5 kb to -12.5 kb.

These PCR fragments harboring individual conserved regions (at least 75% homologous to human MC4R genomic locus) were cloned upstream of the murine MC4R sequence in the pGL+648m luciferase construct. The PCR fragments were also cloned upstream of the TK minimal promoter in the pGL3-TK plasmid (Promega).

These heterologous promoter constructs were then transiently transfected into GT1-1, GT1-7, Neuro-2A, and HEK-293 cell lines. However, no significant difference in relative promoter activity was seen with the heterologous constructs and their base line constructs (pGL3+648m and pGL3-TK, respectively) (data not shown).

Human MC4R Promoter Results

Each human 5'-flanking fragment was cloned by PCR from genomic DNA generously provided by Dr. Sutcliffe (Vanderbilt University). For the human constructs, the fragments range from -2030bp at the largest to -130bp at the smallest. All human constructs have a 3'-end at -1 position, relative to the first codon. The human constructs have been given the following designations: pGL+2030h, pGL+1770h, pGL+1550h, pGL+900h, pGL+740h, pGL+600h, pGL+420h, pGL+230h, and pGL+130h. A schematic representation of the human MC4R promoter-reporter constructs are shown in the left panel of Figure 3.3.

Endogenous MC4R Expressing Cell Lines

I transiently transfected the human promoter constructs into the same panel of cell lines used for the murine constructs. As with the results for the murine constructs, sequence within the putative 5'-UTR of the human promoter also had weak promoter

activity in GT1-1 cells (Figure 3.3, pGL+130h, 0.8 ± 0.04; pGL+230h, 1.2 ± 0.1;

pGL+420h, 1.9 ± 0.1, relative to pGL3-Basic = 1.0). A marked increase in luciferase

activity was observed with the pGL+600h construct (5.4 ± 0.2), which includes the 32bp

conserved region *CR-8*. The luciferase activity of the human constructs slightly

increased from the level of the pGL+600h construct to a plateau starting with pGL+740h

construct (pGL+740h, 6.4 ± 0.4). A small increase in activity is seen with the

pGL+1550h construct that is not sustained in larger constructs (pGL+900, 6.4 ± 0.3;

pGL+1550h, 8.6 ± 0.3; pGL+1770h, 7.1 ± 0.3; pGL+2030h, 7.1 ± 0.6).

Figure 3.3
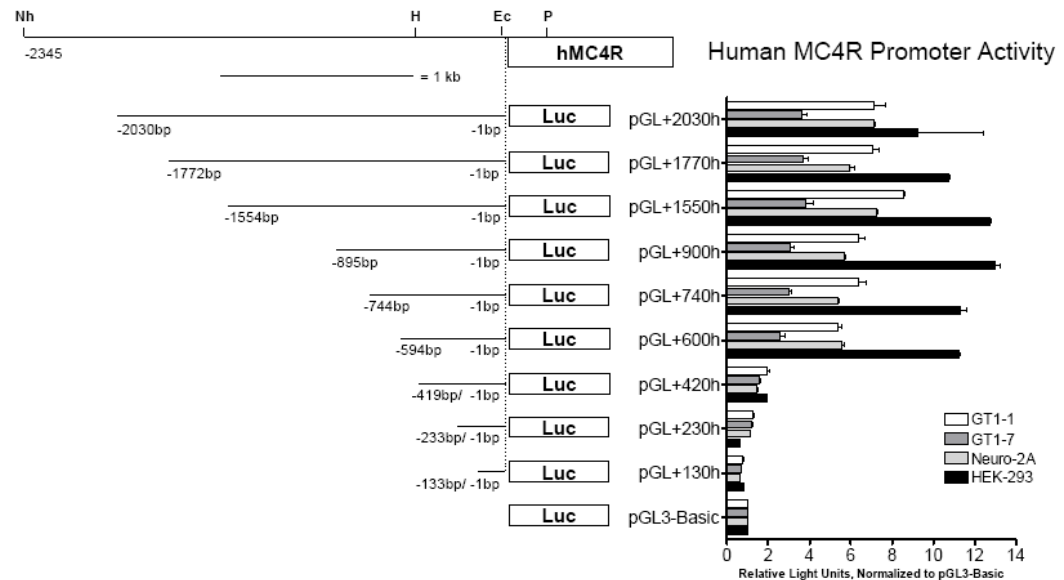
Figure 3.3: Human MC4R Promoter-Luciferase Reporter Constructs and *In Vitro* Results. The left-hand panel shows a schematic representation of the human MC4R locus and the promoter-luciferase reporter constructs used in the experiments. The dashed line represents the start of translation that is the 3'-end of the MC4R sequence used in all human MC4R-promoter reporter constructs. The right-hand panel is a graph representation of the luciferase activity from transient transfected cells lines. The data is the average of at least three transfections from three independent plasmid preps. Error bars represent S.E.M. Nh = NheI; H = HindIII; Ec = EcoRI; P = PstI.

50

The relative pattern of promoter activity for the human constructs was identical in the GT1-7 cells. As observed with the murine promoter constructs, a similar decrease of roughly one half in the activity levels of the human constructs was noted in GT1-7 cells compared to the activity seen in GT1-1 cells for constructs pGL+600h and larger (Figure 3.3, pGL+600h, 2.6 ± 0.6; pGL+900h, 3.1 ± 0.4; pGL+2030h, 3.6 ± 0.6).

Non-expressing Cell Lines

Luciferase activity from the human constructs was also observed in each of the other cell lines (Neuro-2A and HEK-293 cells, Figure 3.3; CAD, SH-SY5Y, and HeLa cells, data not shown), regardless of cell type or tissue of origin.

Identification of Human Single Nucleotide Polymorphism in Proximal MC4R Promoter Conserved Region

Discovery of Human SNP

To identify mutations that could adversely affect transcription of the MC4R gene in humans and therefore be telling of a risk for energy imbalance, we focused on the ~250bp region surrounding the highly conserved *CR-8* region. The *CR-8* region and flanking sequence was PCR amplified and sequenced in 162 obese patients with a phenotype that closely mimics that of known MC4R coding mutation subjects, which is hallmarked by severe early onset morbid obesity and increased linear growth. One G to A single nucleotide polymorphism (SNP) was identified in a single obese subject at residue -502 (SNP-502). The location and context of the SNP within the *CR-8* conserved

region is shown in Figure 3.4. No mutations/polymorphisms were observed in over 700 control chromosomes within the *CR-8* and flanking sequences.

Figure 3.4


```
                    CTF/NF1 Site                SNP
-522  5'- GGA TTGGTC AGA AGGAAGCA(G/A)AGGAGGAGCCA  -3'  -491
            Inverted CCAAT box                   Sp1
              AP-1 Half Site
```
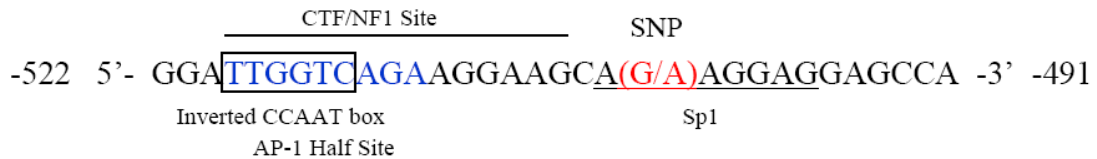
Figure 3.4: Human SNP in the *CR-8* Conserved Region of an Early Onset Obesity Subject. The sequence is 100% conserved between rodents and human MC4R loci. The sequence shown here is numbered from the human start of translation. The "G" residue in the putative Sp1 site is present in all species in which the *CR-8* is conserved. The "A" residue was found in one proband presenting with early onset morbid obesity and increased height, which are hallmark phenotypes of MC4R deficiency. Other putative conserved cis-elements are depicted. The G-502A SNP is in red. The AP-1 half site is in blue.

Site-Directed Mutagenesis of MC4R Promoter-Luciferase Fusion Constructs

The proband with the SNP was unavailable for further genetic studies, so we set about studying the SNP's effects on basal transcription *in vitro*. In order to recreate the SNP, I used site-directed mutagenesis to substitute the guanine residue at -502 of the human and mouse promoter in the normal human promoter-luciferase construct pGL+900h and normal mouse promoter-luciferase construct pGL+890m with an adenine residue observed in the proband. The normal human and mouse constructs (henceforth referred to as hWT and mWT, respectively) and the mutated human and mouse constructs (henceforth referred to as hMut and mMut, respectively) were transiently transfected into the GT1-7 cell line.

The mMut construct showed a small but significant decrease in relative basal promoter activity compared to the mWT construct in the GT1-7 cell line (mWT 1.0 ±

0.05; mMut 0.94 ± 0.04; $p < 0.05$, Paired 2-Tailed t-Test). However, in the native

context of the human MC4R genomic locus the hMut construct showed a larger decrease

Figure 3.5
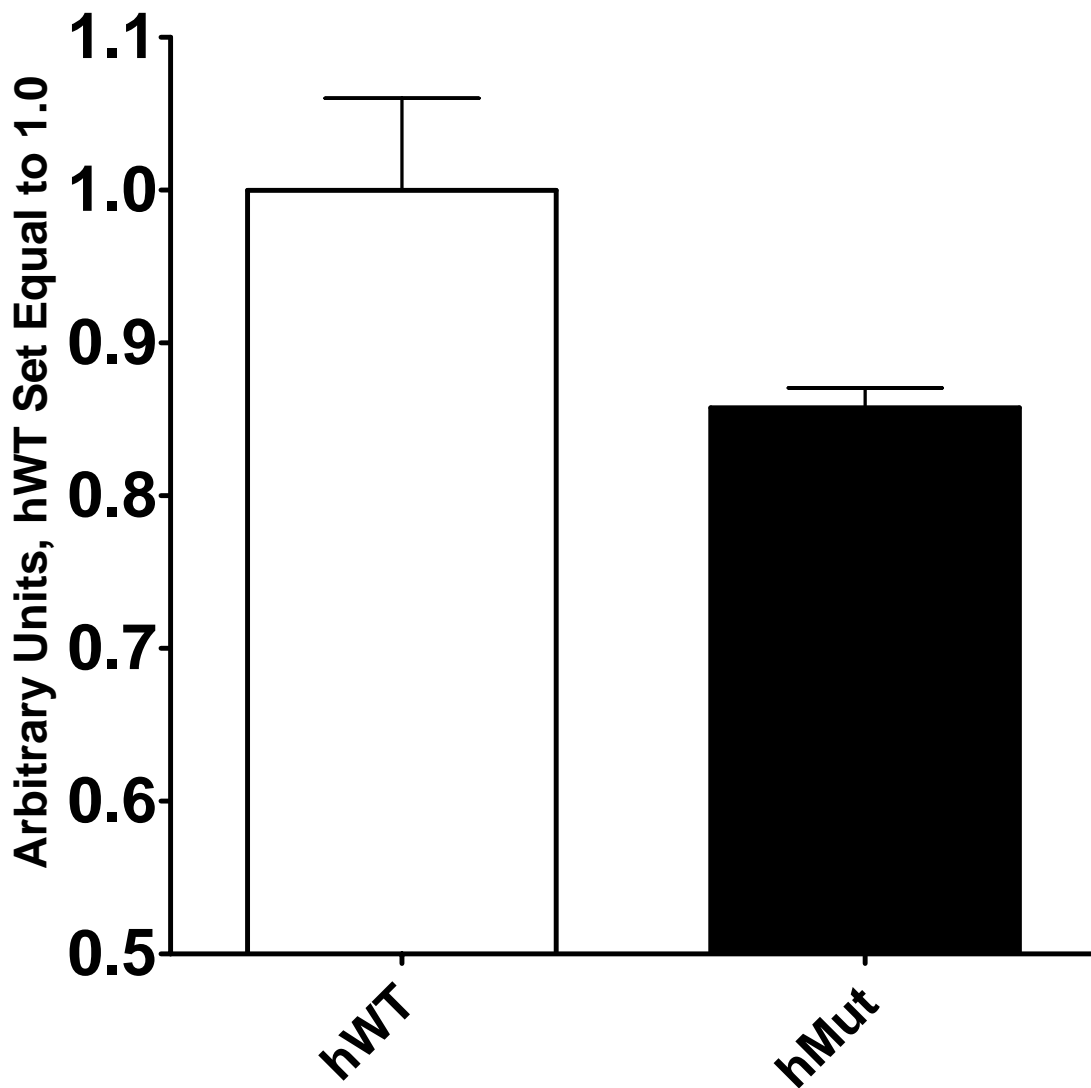
Figure 3.5: Transient Transfection of Human SNP Promoter-Luciferase Construct. GT1-7 cell line cultures were transient transfected, as described above, with the empty pGL3-Basic vector, hWT, and hMut plasmids. The results are shown as average RLU relative to the hWT construct (set to 1.0). The results are an average from three transient transfections from two independent plasmid preps. Error bars are S.E.M. *p*=0.10 by two tailed Paired t-Test. Data analysis performed by GraphPad Prism Software.

in relative basal promoter activity, but the change was not statistically significant (See Figure 3.5). The decrease in luciferase activity was just under 90% of the hWT construct basal activity (mWT 1.0 ± 0.08; mMut 0.86 ± 0.02).

Discussion

The data from the murine and human MC4R promoter-luciferase reporter constructs together suggest that positive promoter elements reside in the proximal 5'-flanking sequence of the MC4R gene, specifically between positions -430 and -600 in both species and between positions -650 and -900 in the murine sequence context. The previously noted 100% conserved *CR-8* region resides within the former, and the highly conserved *CR-6* and *CR-7* regions reside within the latter. Interestingly, weak promoter activity was observed within the putative 5'-UTR of both species. This may be due to cis-elements or alternative transcription start sites within the 5'-UTR. The *in silico* predicted cis-elements of the *CR-8* region (CCAAT box and Sp1 family) are consistent with a region that is important for basal promoter activity of TATA-less promoters, such as MC4R.

The expression patterns seen in the various cell lines, both neuronal and non-neuronal in origin, was interesting in that my data refutes the conclusions drawn in the Dumont et al (56) paper that the MC4R promoter imparts cell specific expression *in vitro*. However, the reporter constructs in those experiments also contained a significant amount of 3'-flanking sequence which could have been responsible for purported tissue-specific expression in the cell lines chosen. Given the results and conclusions drawn from the Lubrano-Berthelier et al study of the human MC4R promoter along with my

results presented herein, it is quite clear that the 5'-flanking sequence is typical of many weak expressing TATA-less promoters in which promoter activity "leakage" is possible absent some strong negative enhancer or insulator sequence tag in stable transfection studies. The heterologous construct data not detailed herein show that no such negative enhancer resides within the 14,000 bp upstream of the *mc4r* translational start site.

The *in vitro* and *in silico* results was highly suggestive of the highly conserved *CR-8* region could be crucial for proper *in vivo* expression of the gene. Our collaborators screened a cohort of morbidly obese patients and found one SNP (G-502A) in the middle of the *CR-8* region. My *in vitro* characterization data is suggestive of causation of this patient's obesity, but we were unable to pursue that line of investigation further due to lack of consent from the patient. The SNP remains an open question that will be pursued in other screens as new cohorts are formed.

Altogether, the data from the *in vitro* studies (particularly the lack of tissue specificity *in vitro*) led me to direct my studies to making transgenic animals to characterize the proximal flanking sequences *in vivo*.

CHAPTER IV

EXPRESSION OF TAU-EGFP TRANSGENE IN 3.3KBMC4ITG TRANSGENIC
MICE

Results

Due to the limitations of the cell culture models, I generated transgenic mice to

study the promoter *in vivo*. Based on the tissue culture results, I decided to focus on the

proximal 3.3 kb of 5'-flanking sequence that included the 12 highly conserved regions. I

created a transgenic construct using a 4.8 kb HindIII murine MC4R fragment cloned

upstream of an Internal Ribosome Entry Site-bovine tau-EGFP (MC4ITG) reporter

cassette to generate a bicistronic transgene (See Figure 4.1). The construct, therefore,

also includes approximately 500 bp of 3'-UTR in the MC4ITG construct.

FIGURE 4.1
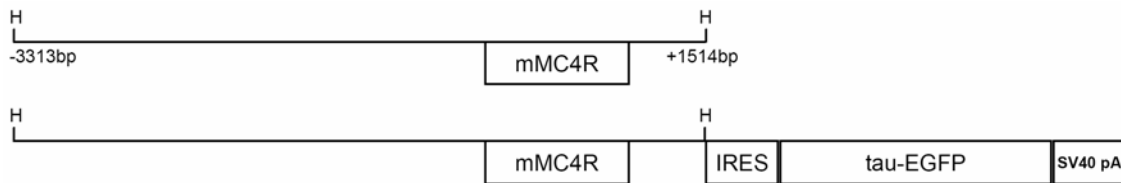
Figure 4.1: MC4R-ITG Transgenic Construct. Schematic of MC4ITG transgene with murine MC4R
HindIII 4.8kb restriction fragment. The bicistronic transgene contains 3313bp upstream and 1514bp
downstream of the start of translation, including the entire coding sequence. An Internal Ribosome Entry
Site (IRES) allows for an independent translation product for the bovine tau-EGFP fusion gene. An
immediate early SV40 polyadenylation site follows the tau-EGFP reporter. H = HindIII; IRES = Internal
Ribosome Entry Site; pA = poly-adenylation signal sequence.

Transgene Expression Validation in Cell Culture

Before using the construct to generate transgenic mice, I first validated the construct by transient transfections into Neuro-2A and GT1-1 cell lines. The bovine tau portion of the transgene binds to microtubules present in the axons and dendrites of neurons, which renders the EGFP reporter to be capable of demarking positive expressing cell bodies and their appendages. Figure 4.2 shows a successful validation experiment in which Neuro-2A cells are expressing the tau-EGFP transgene. The tau-EGFP is clearly deposited in both the cell body and the appendages of the "differentiated" cell.

Endogenous MC4R Expression in C57BL6 Mouse Strain

Five transgenic founders were identified by PCR screening and Southern blot analysis for the EGFP coding sequence, of which four passed the transgene to offspring (Lines MC4ITG#1, MC4ITG#6, MC4ITG#13, and MC4ITG#15). These four lines were maintained and used to analyze tau-EGFP reporter expression.

Using non-transgenic C57BL6 as controls, endogenous murine MC4R transcript was found to be present in all brain regions sampled (See Figure 4.3). In order to detect this weakly expressed endogenous gene, I had to optimize a highly sensitive RT-PCR reaction using Real Time PCR Multiplexing technology. The highest level of endogenous MC4R transcript in quantity of amplifiable cDNA was found to be in the hypothalamus (163 ± 40 amplicons/ng total RNA) and the lowest in the cerebellum (11.1 ± 5.6 amplicons/ng total RNA). I did not expect to find endogenous transcript in the cerebellum of adult mice, as all previous reports claim this adult tissue to be negative for MC4R expression.

Figure 4.2
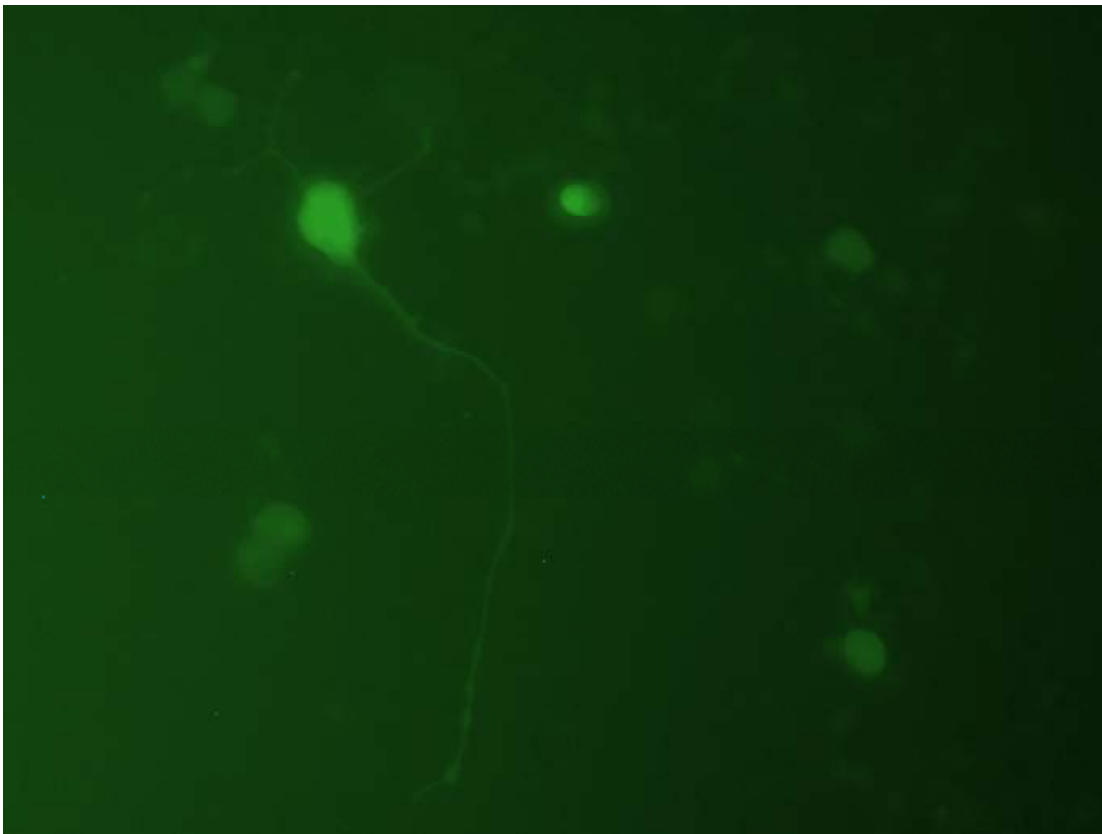
Figure 4.2: Photomicrograph of Neuro-2A Expressing Tau-EGFP Reporter Gene. Neuro-2A cells were passaged in a 10cm dish and given N2A Experimental medium. The cells were allowed to culture into the pseudo-differentiated state for 24 hours prior to transient transfection. Cells were transient transfected with Lipofectamine 2000 using 10μg of MC4ITG construct. The cells were screened for EGFP expression using a GFP filter and mercury lamp 12 hours post transfection. Cell image was captured using NIH Image software. The photomicrograph shows several Neuro-2A cells positive for EGFP expression. The objective is focused on a plane that shows the tau-EGFP reporter gene properly localizing in the microtubule filled appendages of the cell in the center left of the field.

The kidney was the only peripheral tissue to have a detectable level of endogenous MC4R transcript (6.6 ± 2.7 copies/ng total RNA), but still lower than that observed in the cerebellum. All other peripheral tissues were not significantly higher than the reaction lacking RT enzyme or no-template (water) control reactions (data not shown).

Figure 4.3
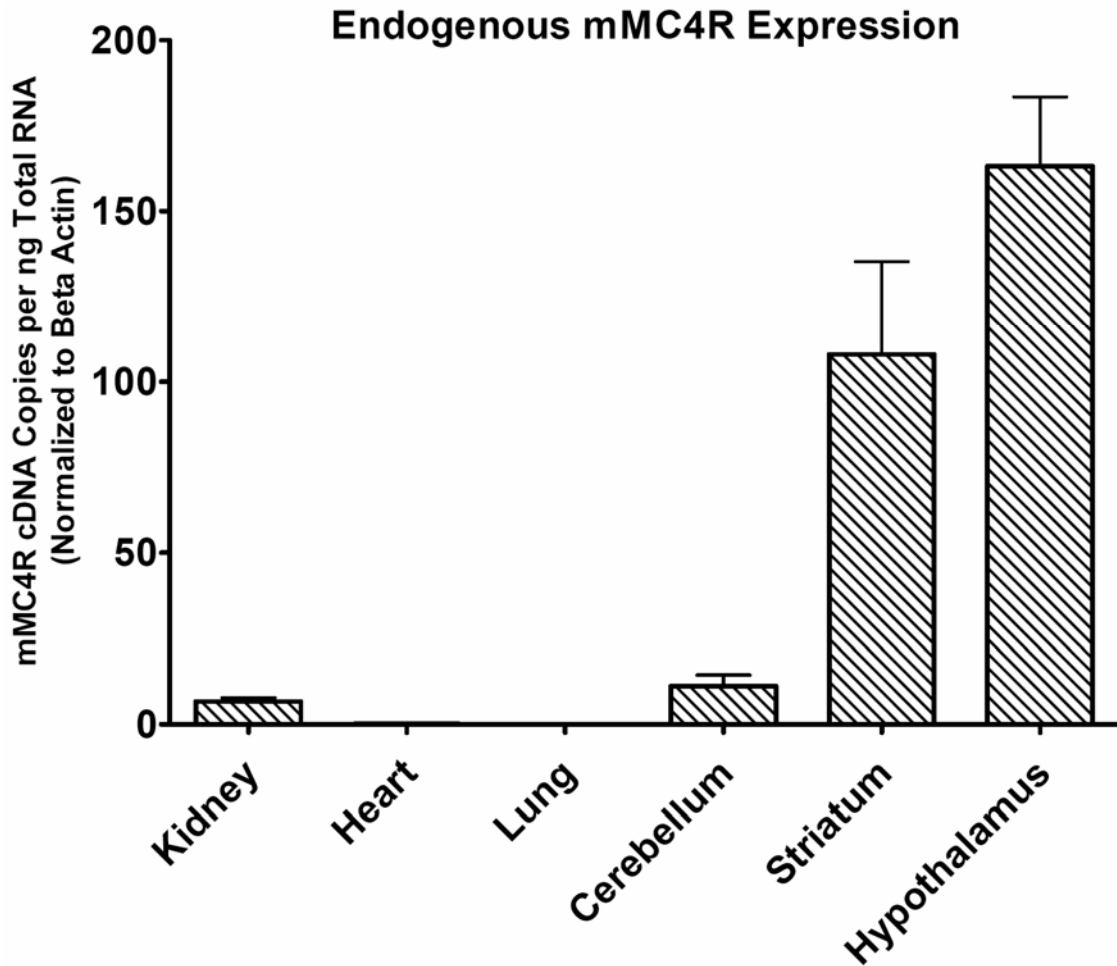
Figure 4.3: Endogenous MC4R Expression in C57bl6 Mice. Endogenous MC4R expression pattern, as determined by Reverse Transcriptase Real Time PCR (RT-Real Time PCR) of non-transgenic MC4ITG littermates. Endogenous MC4R transcript was detected in five of five isolated brain regions (hypothalamus, striatum, cerebellum, piriform cortex, and brain stem). The kidney was the only peripheral tissue found to have endogenous MC4R transcript levels above background. Data represents mean from at least three wildtype C57bl6 male tissue RNA preps. Error bars represent S.E.M.

Expression Pattern of tau-EGFP Reporter mRNA in the CNS of Transgenic Mice

I then performed RT-Real Time PCR on the four MC4ITG transgenic lines for tau-EGFP mRNA expression to compare to that of the endogenous MC4R pattern of expression (See Figure 4.4). The relative pattern of tau-EGFP transcript expression between the various brain regions was found to be similar to that of endogenous MC4R

59

transcript in three of four lines, where highest transcript levels were observed in

hypothalamus and lowest in cerebellum.

Figure 4.4
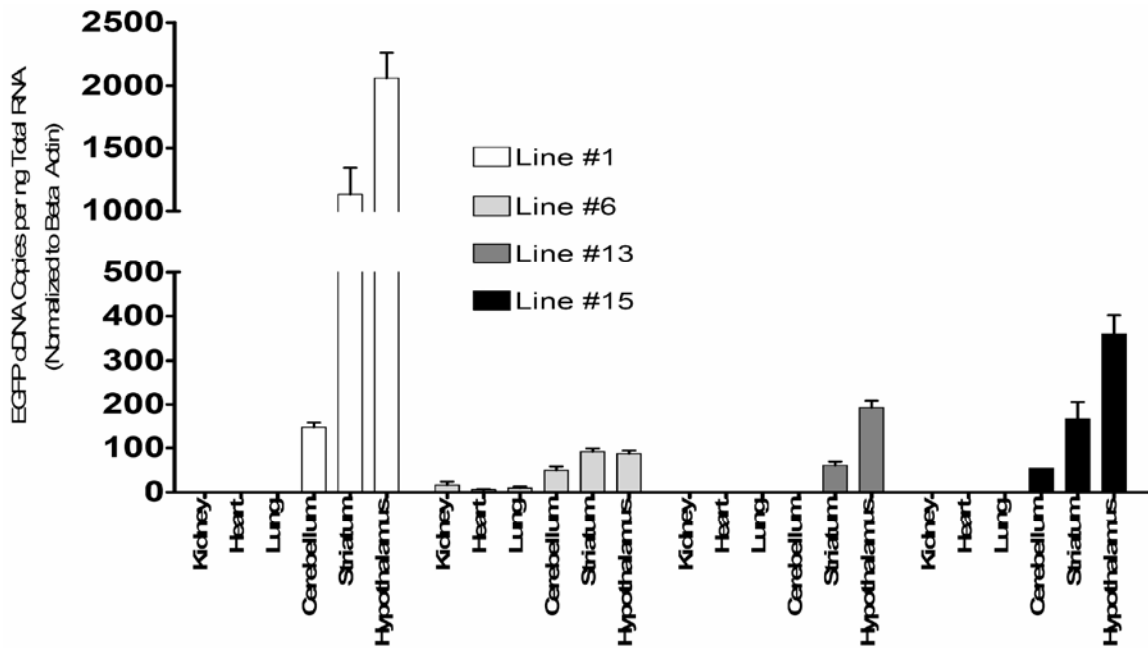
Figure 4.4: Tau-EGFP Expression in MC4ITG Transgenic Mice. RT-Real Time PCR detection of EGFP transcript in four independent MC4ITG transgenic lines. All four lines were found to have highest expression in the hypothalamus and striatum, two regions chosen for analysis based on their relatively high expression of endogenous MC4R as determined by published *in situ* hybridization experiments. EGFP transcript was also detected in piriform cortex and brain stem tissue samples in lower levels than striatum abut greater than cerebellum in all MC4ITG lines. Line #6 was the only MC4ITG line having detectable levels of EGFP transcript in the kidney, but low levels of EGFP transcript was also detected in the heart, lung and soleus muscle of the hind limb. No sexual dimorphic expression of MC4R or EGFP was observed in the MC4ITG lines. Data is mean from at least three transgenic mice for each tissue RNA prep. No sexual dimorphism of reporter expression was found. Error bars represent S.E.M.

Line MC4ITG#6 also had detectable expression of the transgene in kidney (16.7 ±

7.8 amplicons/ng total RNA), heart (5.4 ± 4.1 amplicons/ng total RNA), and lung (9.7 ±

6.8 amplicons/ng total RNA), although expression was highest in the CNS

(hypothalamus, 87.3 ± 16.1 amplicons/ng total RNA; striatum, 91.8 ± 16.6 amplicons/ng

total RNA).

Discussion

Unfortunately, the tau-EGFP reporter was not detectable by visual analysis under a fluorescent microscope; however, I was able to detect expression of the transgene throughout the CNS by RT-Real Time PCR. The modest promoter activity of the MC4ITG transgenic mice forced me to consider more sensitive and less expensive reporter gene systems for future experiments.

Another (anticipated) weakness in the MC4ITG transgenic construct was the bicistronic nature of the transgene, which precluded analysis of endogenous MC4R levels in the transgenic animals. Only one line (MC4ITG Line #1) had transcript levels of MC4R that were significantly higher than those seen in the non-transgenic animals in each of the brain regions analyzed. In experiments not detailed herein, a partial, yet significant, rescue of the MC4R-KO obesity phenotype was found when crossing to either MC4ITG Line #1 or Line #15.

The results presented in this chapter show that the MC4ITG transgene is expressed preferentially in the CNS. Furthermore, the quantitative ratio pattern of expression is similar to that of the endogenous MC4R transcript within distinct regions of the CNS in three of four independent lines.

EXPRESSION OF *E. COLI* BETA-GALACTOSIDASE IN 3300MC4LACZ3 MICE

Results

Generation of MC4-LacZ Trangenic Mice

Due to the limitations of the MC4ITG transgenic mice, I decided to use a different in vivo approach with alternative reporter transgenes. The classic mouse transgenic reporter is the beta-galactosidase gene from the *E. coli* lacZ operon. The advantages of using this reporter gene are the technical developments in detection garnered by its wide-spread use. Dr. Richard O'Brien (Vanderbilt University) kindly provided a nuclear-localized beta-galactosidase reporter cassette.

A schematic of the LacZ transgene construct (Construct A) is shown in Figure 5.1. For comparison of the included MC4R sequence, the MC4ITG construct and a relevant VISTA homology plot are included. The LacZ construct contains all of the 5' sequence included in the MC4ITG construct, but it lacks the MC4R coding sequence. The 3'-sequence included in the LacZ construct is about 250bp more than what was included in the MC4ITG construct; however, no putative conserved transcription factor binding sites were located in this downstream sequence.

Initially, three founders were positively identified by PCR and Southern blot screening at UAB. Of these, only two transmitted the transgene to progeny (Lines A2 and A3). Southern blot analysis showed that Line A2 harbored a single copy of the

transgene, while Line A3 carried more than 20 tandem copies of the transgene. Line A1

never threw positive pups, and this male founder was sacrificed for data collection.

However, no detectable expression was found by either Beta-Glo *in vitro* assays or RT-

Real Time PCR. A fourth and final founder (A4) was generated once it was discovered

that the Line A1 founder was not expressing the transgene. Yet, this female founder died

during a breached delivery, and no data was recoverable.

Figure 5.1
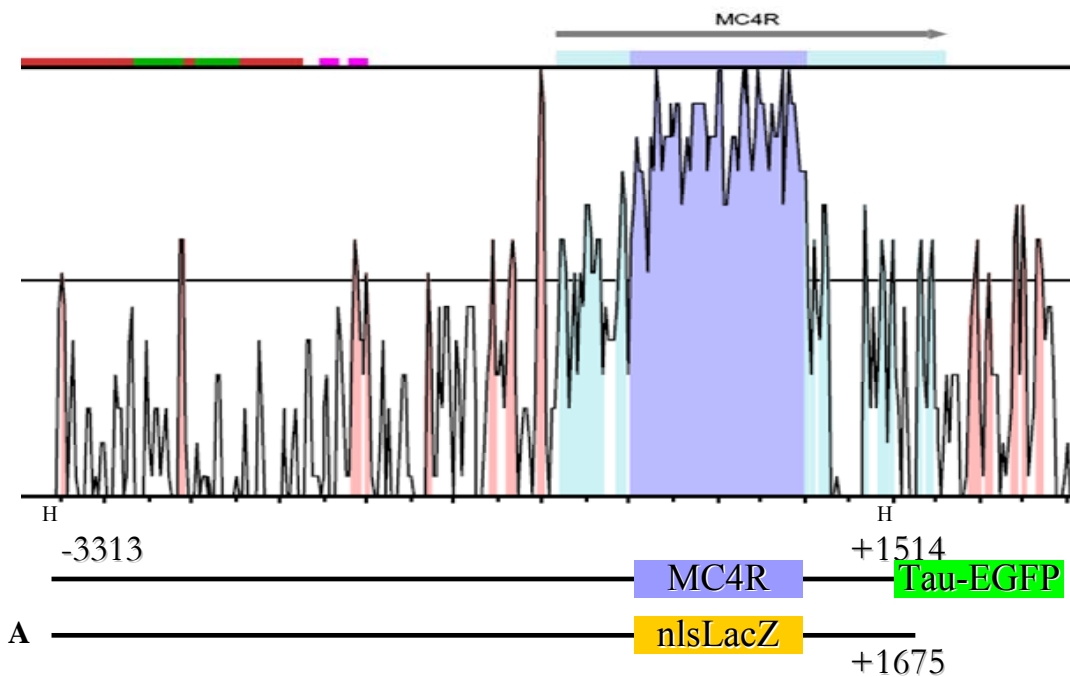
Figure 5.1: Nuclear Localized LacZ Transgene Construct. The figure shows a schematic representation of the MC4R promoter- nuclear localized LacZ transgenic construct. For comparison, a schematic drawing of the MC4ITG transgenic construct and a VISTA plot of the relevant human and mouse sequence are included above the MC4R-LacZ construct.

Previous studies had shown that MC4R is expressed in the CNS of developing

mouse embryos no earlier than day 14 (e14) past implantation (64, 65). The gestational

period of a mouse is typically 21 days, but the embryo has all major organs formed by

e15 (technically a fetus at this point). I chose to harvest and stain whole embryos at e15-

16. At this stage, the brain has taken form and the hypothalamus has been expressing

MC4R for at least one day. Also, the embryos are capable of staining with X-Gal without

a Proteinase K digestion step in the protocol, which could also degrade the transgene that

is expected to be produced in low quantities.

Line A2 and A3 males were caged with wildtype females until a copulation plug

was found so that the pregnancies could be timed. After 15 days, the pregnant dams were

euthanized and the embryos were harvested and stained. Line A3 embryos showed no

visible staining after 24 hours at 37C in staining solution, at which time the non-specific

staining in the abdominal cavity of both transgenic and wildtype animals became deep

blue. Due to the very weak expression of the endogenous MC4R gene, it was not

unexpected to have a seemingly negative result.

Line A2 embryos, however, expressed enough LacZ transgene *in utero* to stain

within a very short time at room temperature (less than one hour to show blue staining in

the cortex of the CNS). Staining was allowed to continue for two hours at room

temperature. The pattern of expression visible through the transparent skin of the e15

embryos is shown in Figure 5.2. These photographs show relatively high transgene

expression in the CNS (given the short staining time and extent of staining), down the

midline of the back, olfactory nerves, snout/jaw, ears, paws, eyes, tail, and the fast twitch

muscles in the limbs. Extra-CNS expression in the fetal animals was not expected at the

time of the experiments.

Figure 5.2
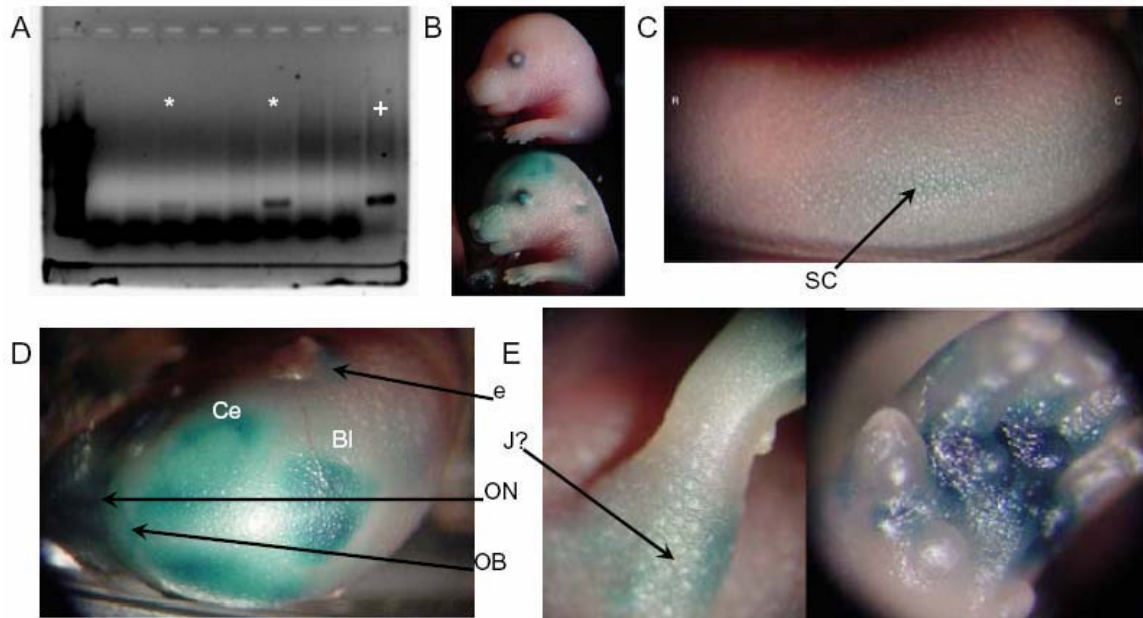
Figure 5.2: X-Gal Staining of Line A2 Whole Embryos. Dam euthanized and killed before harvest of ~e15.5 embryos. (A) Genomic DNA prepared from placenta for PCR genotyping. Embryos 'C' and 'F' are positive for the LacZ transgene (marked *, positive control marked +), and these were the only embryos with specific staining. (B) View of head and forelimb of embryos 'A' (top, negative) and 'C' (bottom, positive). Specific staining is apparent below the skin near the forelimb joint, paw, ear, nose, eye, olfactory bulb and cerebrum. (C) Specific staining at the midline of the back (likely the spinal chord). (D) Closer view of staining around the head. The olfactory nerves, olfactory bulb, cerebrum, and cerebellum are densely stained. Lighter staining is observed around the ear and at the spinal chord. (E) Closer view of staining under the skin near the forelimb joint (left) and the paw (right). Note: embryos stained in the dark for 10.5 hours at room temperature while gently shaking. At end of staining, only the back midline, paws, olfactory nerves, cerebellum, and cerebrum were noticeably stained. The staining at the olfactory bulb, limbs, and eyes became apparent only after intensification in PBS. SC – spinal chord (midline); Ce – cerebrum; Bl – cerebellum; e – ear; ON – olfactory nerve; OB – olfactory bulb; J? – fast twitch skeletal muscle in forelimb.

Beta-Galactosidase Activity in Adult Transgenic Mice

I next wanted to determine whether the adult transgenic animals expressed the

reporter transgene. To test for CNS expression, adults were perfused and the whole

brains were removed for X-Gal staining. Wildtype brains showed no staining whatsoever

in the time periods utilized for staining either transgenic line (see Figure 5.3). Similar to the results in the fetal staining experiments, the Line A2 adult brains needed less than one hour to stain deep blue in the cortex and the supraoptic nucleus (the location of the hypothalamus, see Figure 5.3). The Line A3 adult brains required substantially longer to stain (data not shown). These brains were sliced using the aid of a brain mold into 1mm sections. However, the interiors of the adult brains from both lines were completely devoid of staining. This suggested that the X-Gal reagent was not penetrating the whole brains, so I next made 1-2mm sections of perfused brains which were then allowed to stain directly in the reagent.

The brain sections from Line A3 adult animals showed modest staining throughout the CNS, primarily in the hypothalamus, hippocampus, and striatum, but the highest level of staining was in the cortex (data not shown). In fact, reporter activity in the hypothalamus and striatum was only evident after prolonged staining (> 5 hours). The brain sections from Line A2 adult mice, however, showed staining throughout the CNS (cerebellum, cortex, and hypothalamus staining shown in Figure 5.3). The highest level of staining appeared to be in the cortex in this transgenic line. Attempts to make slices for slides were unsuccessful, apparently due to insufficient fixing of the tissues (note: post fixing was not performed in order to preserve reporter activity). Despite the fact that the staining patterns were not 100% reproduced between the two LacZ transgenic lines, the widespread reporter activity throughout the CNS was promising that at least part of the MC4R promoter responsible for CNS preferential expression was within the flanking sequence used for the transgene, which would be consistent with the MC4ITG transgenic mice (see previous chapter).

Since the Line A2 fetus showed deep blue staining in unexpected peripheral tissues, I next wanted to test for expression of the transgene in adult animals using an *in vitro* method that would allow for comparison between CNS and peripheral tissue

Figure 5.3
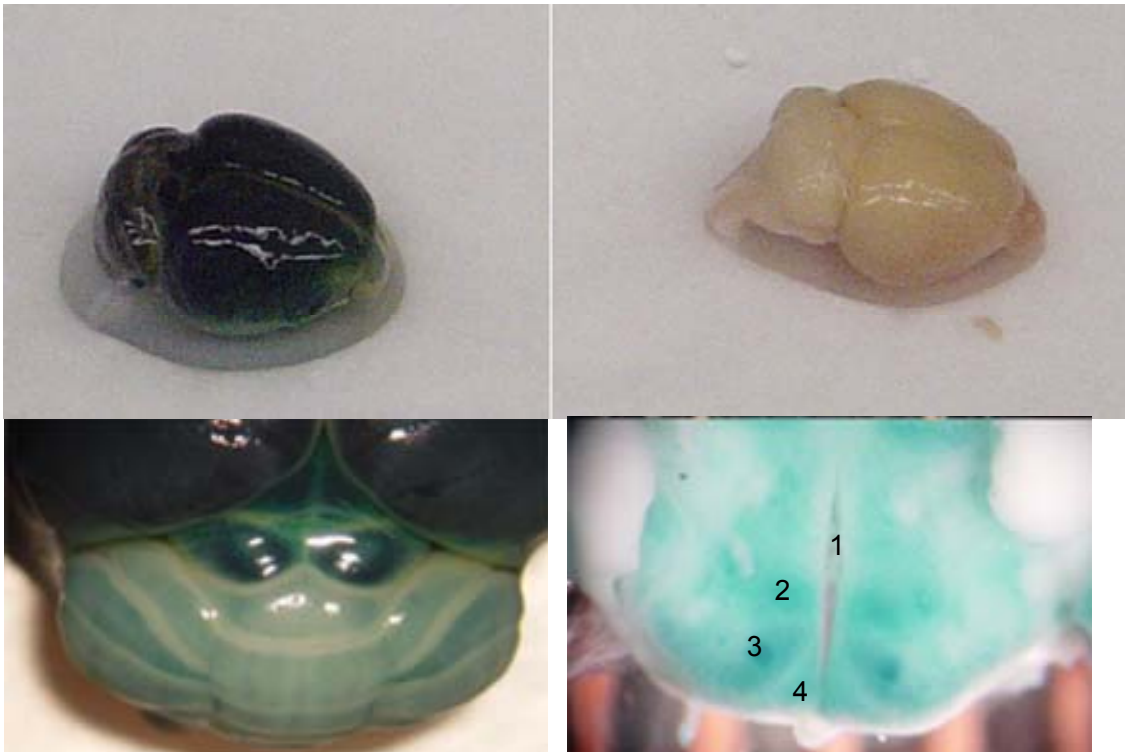
Figure 5.3: X-Gal Staining in Adult Line A2 Brain Tissue. The top panels show an over-stained whole brain from a transgenic (right) and wildtype (left) littermate. The bottom left panel shows a detailed close up of the caudal section (including the cerebellum and cortex) of the same over-stained transgenic brain in the top left panel. Note the contrast in staining between the cortex (deep blue) and the cerebellum (light blue), suggesting the transgene correctly directs weekend expression of the reporter in the cerebellum. The bottom right panel shows a detailed image of the hypothalamus of a 1.0mm coronal section stained with X-Gal. 1 = Third Ventricle; 2 = Dorsomedial Hypothalamic Nucleus; 3 = Ventromedial Hypothalamic Nucleus; 4 = Arcuate Nucleus.

expression. The method chosen was the Promega Beta-Glo Assay system, which utilizes an indirect means of detecting LacZ reporter activity with a highly sensitive luciferase assay (the LacZ reporter gene frees the luciferin reagent which is then free to react with

the firefly luciferase included in the reagent). The hope was that even small levels of expression in tissues would be detected reproducibly due to the high sensitivity of the assay. No published reports were available in the literature for a method of using the assay from tissues harvested from transgenic animals, so I had to develop a method independently (See Chapter II).

Tissue samples from the CNS (same regions used for the MC4ITG transcript assays) and a panel of peripheral tissues (liver, kidney, paw, tail, ear, skin, heart, lungs, digestive tract, skeletal muscle, and spleen) from Lines A2 and A3 adult transgenic mice and wildtype littermates were harvested. Wildtype and transgenic samples from each tissue were analyzed simultaneously so that the wildtype results could be subtracted from the transgenic tissue results as background. This was necessary because every tissue has some level of background beta-galactosidase activity present. The background levels were found to be the lowest in the brain, while the kidney, liver, and digestive tract tissues had background levels that dwarfed all bona fide transgene reporter activity.

The results for the Beta-Glo assays for Lines A2 and A3 are shown in Figures 5.4 and 5.5, respectively. The *in vitro* results closely approximated the relative staining levels seen in the adult brain slices for both lines. For example, the striatum samples had roughly twice the reporter activity *in vitro* as the hypothalamus and the cortex samples. Although the staining did not appear to be twice the level as these other two CNS regions, it was certainly more densely stained than both. Also, Line A3 mice clearly have the highest reporter activity in the cortex under both assays.

Due to the high levels of background in the peripheral tissues, no tissue reproducibly had higher levels of Beta-Glo activity in transgenic over wildtype mice.

Nonetheless, the means from several peripheral tissues were higher than the background levels. None of these means are statistically significant from the wildtype background activity for these tissues. This was an interesting result, especially for Line A2, because the fetal staining assays clearly showed X-Gal staining many times higher than background levels in peripheral tissues ranging from the paw to skeletal muscle that was comparable to the level seen in the cortex of the same animals. None of these tissues were determined to have expression in the adult *in vitro* assays in either transgenic line. Another interesting result was that the relatively low level of expression of the reporter transgene in the cerebellum of Line A2 adults (staining and *in vitro* assays) did not match what was observed in the staining of the fetal cerebellum tissue (see discussion).

Comparing between the lines, the Beta-Glo assay results also reproduced the relatively higher expression of the transgene in Line A2. Figures 5.4 and 5.5 show that the highest expression (reporter activity) in Line A2 CNS was more than ten times higher than the highest level of expression (reporter activity) in Line A3 CNS. The data also confirmed the lack of reproducibility between both LacZ transgenic lines in relative expression pattern between CNS regions, which was seen with the MC4ITG transgenic mice. However, like the data from the MC4ITG mice, the data from Lines A2 and A3 show that the flanking sequence in the transgene is sufficient to direct CNS preferential expression of the beta-galactosidase reporter *in vivo*, albeit in adult animals because as the Line A2 fetal staining assays show, the transgene is also sufficient to temporally direct extra-CNS expression in the fetus *in vivo*. This extra-CNS expression is then lost between birth and adulthood, suggesting temporal expression control within the flanking

sequence within the transgene that mimics the endogenous temporal MC4R expression

pattern.

Figure 5.4
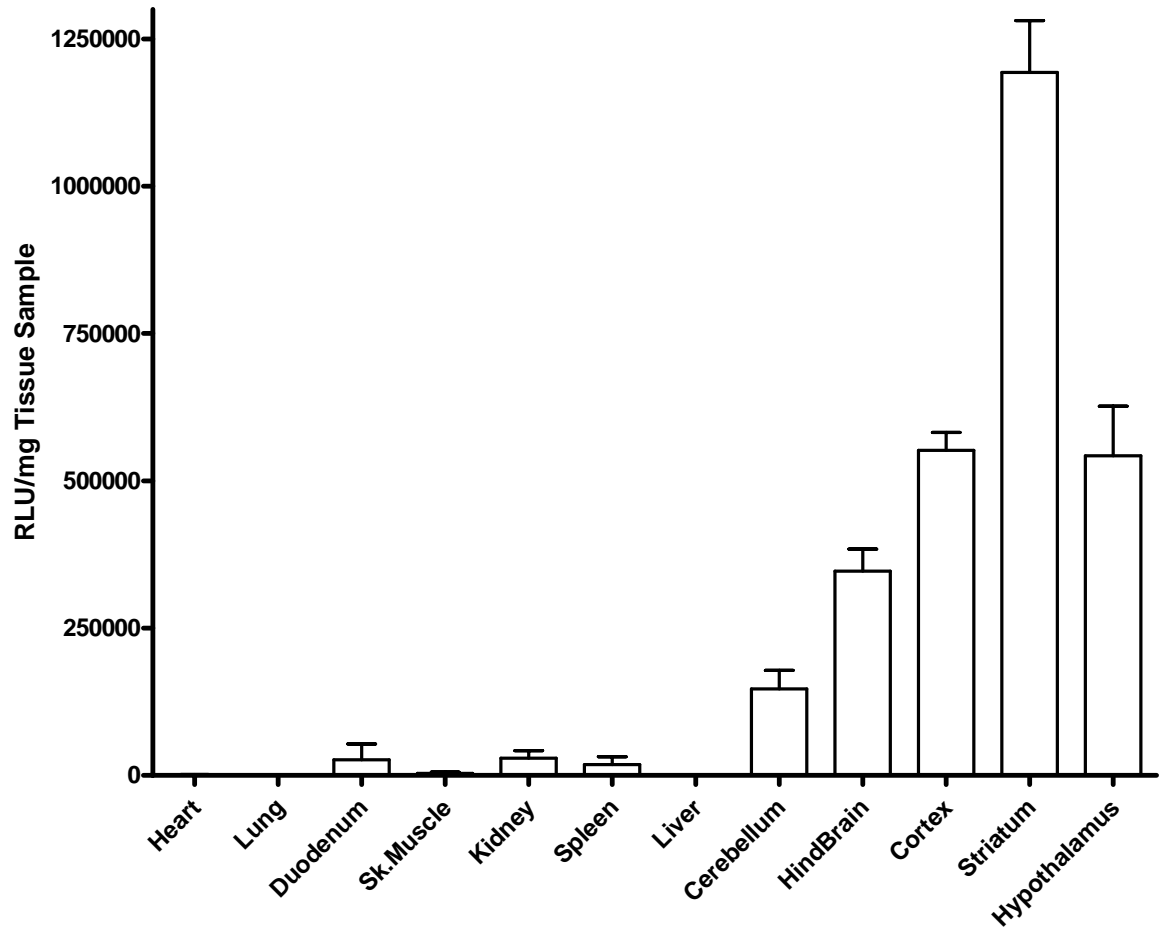
Figure 5.4: Quantitative Beta-Galactosidase Activity for Line A2. Tissues harvested and homogenized in Promega Reporter Lysis Buffer. Assay performed using Promega BetaGlo reagent. Reactions are allowed to reach a steady state (multiple reads). The data is reported in Relative Light Units (indirect beta-galactosidase activity), which has been normalized to the sample mass homogenized. Results are means of duplicate samples from at least three transgenic animals with non-transgenic BetaGlo activity subtracted out. Error bars represent S.E.M.

Figure 5.5
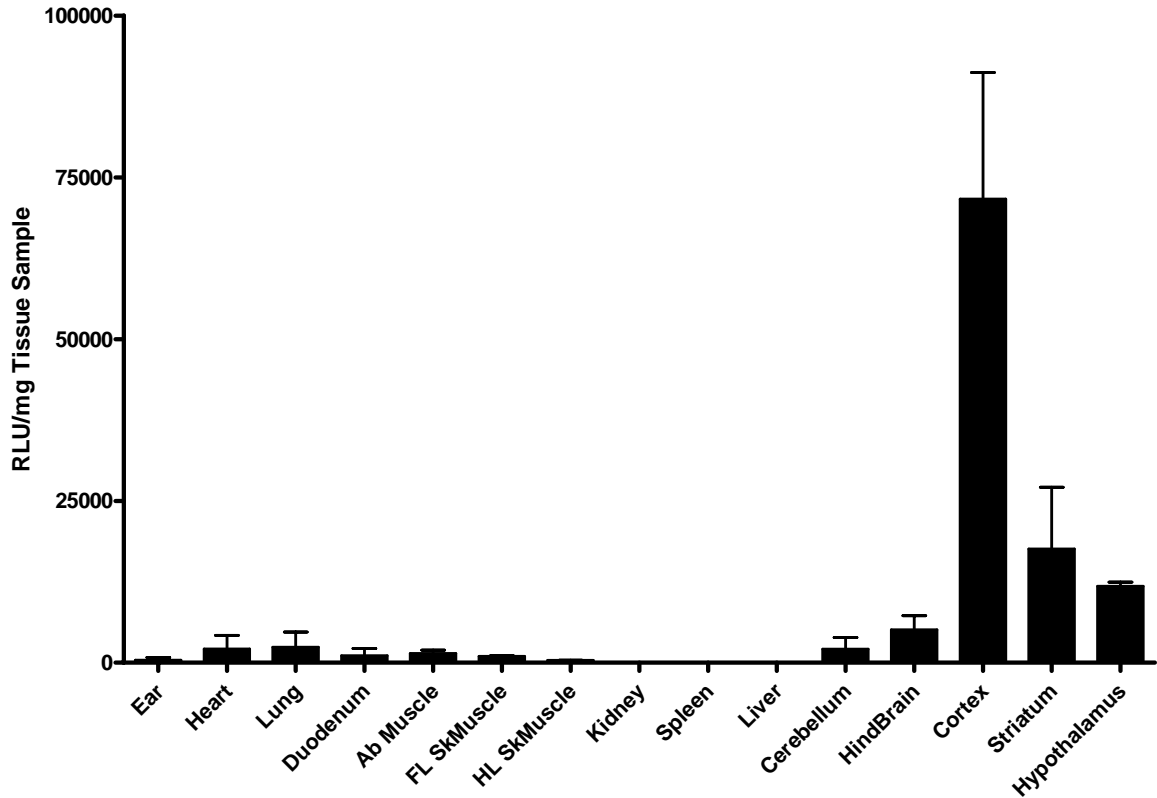
Figure 5.5: Quantitative Beta-Galactosidase Activity for Line A3. Tissues harvested and homogenized in Promega Reporter Lysis Buffer. Assay performed using Promega BetaGlo reagent. Reactions are allowed to reach a steady state (multiple reads). The data is reported in Relative Light Units (indirect beta-galactosidase activity), which has been normalized to the sample mass homogenized. Results are means of duplicate samples from at least three transgenic animals with non-transgenic BetaGlo activity subtracted out. Error bars represent S.E.M.

Beta-Galactosidase mRNA Expression Analysis

I next wanted to test whether the pattern of the reporter transcript would be consistent with that seen with the MC4ITG mice or the Beta-Glo activity assays performed. Due to budget constraints, only Line A2 was analyzed in these pilot experiments. The results in Figure 5.6 show that the transcript levels for the striatum are not consistent with the *in vitro* Beta-Glo activity assays; however, the relative ratios of expression for the other four CNS regions was consistent with the *in vitro* data. The cortex region had the highest level of reporter transcript in these assays, which was a

71

departure from the results seen for the MC4ITG transgenic mice; however, the ratio of transcript expression in the other four brain regions tested did roughly mimic that which was observed in the MC4ITG transgenic mice (Compare Figure 4.4 with Figure 5.6). Importantly, no transgene expression was detected in any of the peripheral tissues tested, including the kidney.

Figure 5.6
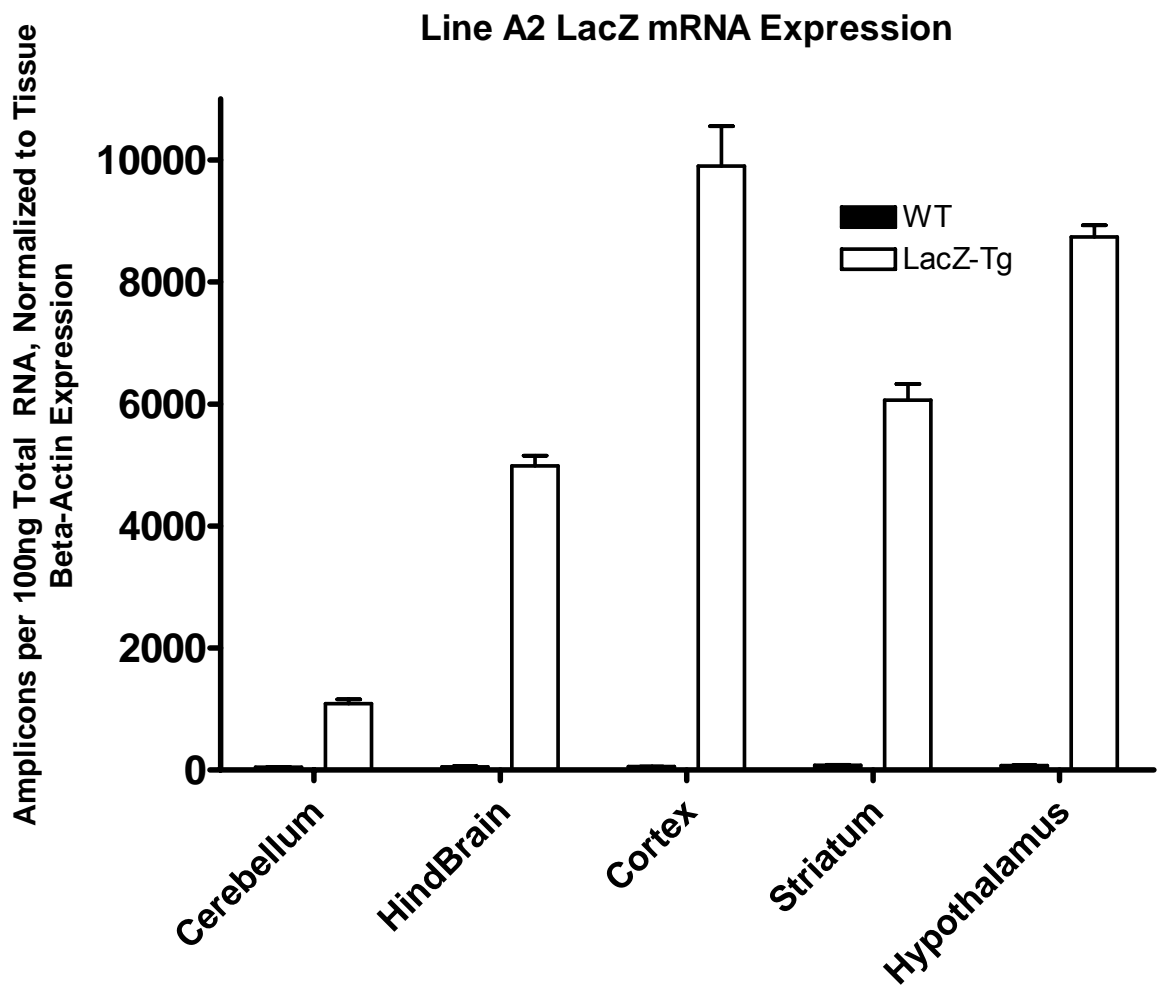
Figure 5.6: Beta-Galactosidase Transgene Transcript Expression in the CNS of Line A2 Mice. RT-Real Time PCR results for LacZ transcript normalized to beta-actin expression. The data is expressed in terms of amplicons per 100ng total RNA used in the cDNA synthesis reaction prior to Real Time PCR. No expression was detected in any peripheral tissue analyzed. Results are the means from three individual animals for both transgenic and wildtype littermates. Error bars represent S.E.M.

<u>Discussion</u>

Even though the pattern was not reproducible in the CNS between both lines that threw transgenic pups, the data does show that the nls-LacZ reporter transgene was restricted to the CNS in adult tissues. The Beta-Glo *in vitro* assay data shows that the expression was limited to the CNS, as the levels of beta-galactosidase activity in the peripheral tissues analyzed were not significantly different in transgenic and wildtype littermates. Moreover, the complete lack of reporter transcript in peripheral tissues of adult animals via RT-Real Time PCR assays confirmed this conclusion. Also, this data was consistent with the results fro three of four MC4ITG transgenic lines that showed reporter expression restricted to the CNS.

Another interesting result from the nls-LacZ transgenic mice was the unexpected finding of reporter activity in fetal staining experiments. At the time of my results, no one had done a detailed study of endogenous MC4R expression in animals prior to birth. Even though the fetal staining showed extensive, organ-specific expression of the reporter, this extra-CNS expression was lost in the adult transgenic animals. Also, the expression of the reporter in the cerebellum greatly decreased from *in utero* to adult animals. This apparent promoter control of temporal expression is consistent with recent data from a study detailing endogenous MC4R expression in the fetal rat (66). In summary, the data from the MC4ITG and nls-LacZ transgenic mice show that the proximal 3.3 kb of 5'-flanking (and possibly 600 bp of proximal 3'-flanking) sequence is sufficient for CNS preferential expression *in vivo*.

CHAPTER VI

EXPRESSION OF FIREFLY LUCIFERASE IN 3300MC4LUC3, 3300MC4LUC,
890MC4LUC, AND 430MC4LUC MICE

Results

Bioluminescent Imaging of Transgenic Founders and Offspring

In addition to the LacZ transgenic construct, four transgenic constructs utilizing

the firefly luciferase gene were prepared following the MC4ITG transgenics (See Figure

6.1A). The luciferase reporter gene allows for highly sensitive *in vitro* assays in

transgenic promoter characterization studies (67, 68). Additionally, founders and

progeny can be screened for luciferase expression by *in vivo* bioluminescence imaging.

Bioluminescence imaging can also be used to monitor changes in gene expression in

living animals. This is because the firefly luciferase enzymatically produces photons,

which are emitted in a broad spectrum (530-640nm) with a peak at 562nm (69, 70). Due

to the optical properties of mammalian tissue, light of this spectrum and peak emission

can pass through and be detected on highly sensitive CCD cameras, including bones (60,

71). Thus, there are many advantages to using luciferase as a promoter-reporter

transgene.

The four luciferase transgenic constructs were chosen based mostly on the *in vitro*

results (see Chapter 3) and the results of the MC4ITG mice generated at Vanderbilt. Of

paramount importance in this decision was the ability to compare the results of these

transgenic mice (and Construct A) with the MC4ITG mice, which had three of four lines

show CNS specific expression (see Chapter 4). Also important was the need to narrow down regions of the murine MC4R 5'-flanking sequence (*i.e.*, the promoter) that are responsible, if at all, for MC4R's CNS preferential expression pattern. This was to be accomplished by comparing the results of luciferase expression in transgenic mice of shorter and shorter length of flanking sequence (see Figure 6.1). Initial results from two-week old founders of Construct B that died unexpectedly were promising because two of two transgenic animals expressed luciferase in the CNS without any detectable signal in the liver, kidney, or heart – all of the peripheral tissues analyzed (data not shown). Thereafter, the constructs were put in queue starting with the largest (B) to the smallest (E) for generation at UAB. Founders and breeding success are discussed along with results below. Representative *in vivo* bioluminescence images are shown in Figure 6.1B. Due to better reproducibility of expression patterns between independent lines, I chose to use luciferase as the reporter gene for the remainder of the studies.

Luciferase Transgene Activity Assay in Transgenic Mice

Sixteen transgenic founders for 3300MC4Luc3 (construct B) were initially identified by PCR and Southern blot genotyping. *In vivo* bioluminescence imaging confirmed luciferase reporter gene activity in 15 of the founder animals, of which four representative lines (B5, B6, B11, and B18) were chosen for further analysis. *In vivo* bioluminescence images are shown in panels B and C of Figure 6.1 for the 3300MC4Luc3 construct lines B6 and B18, respectively. Three of the four representative 3300MC4Luc3 construct lines show the highest detectable level of luciferase activity at

the caudal area of the head in the dorsal bioluminescent images. *In vitro* luciferase assays

performed on tissue extracts

Figure 6.1

Panel A
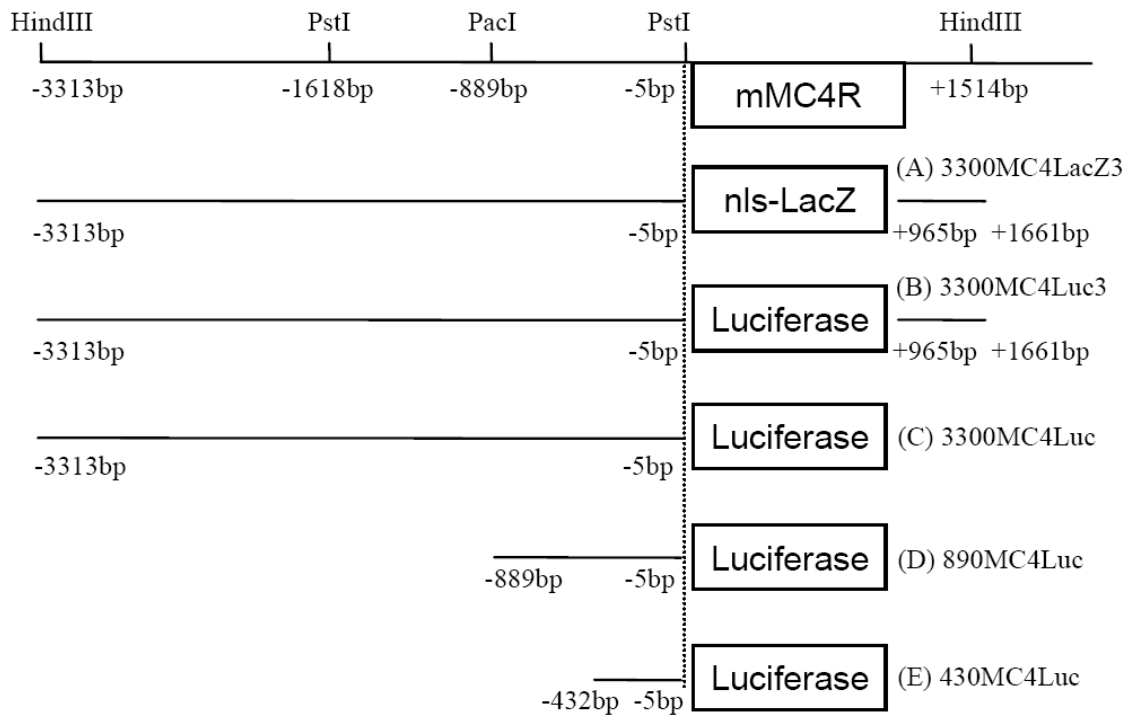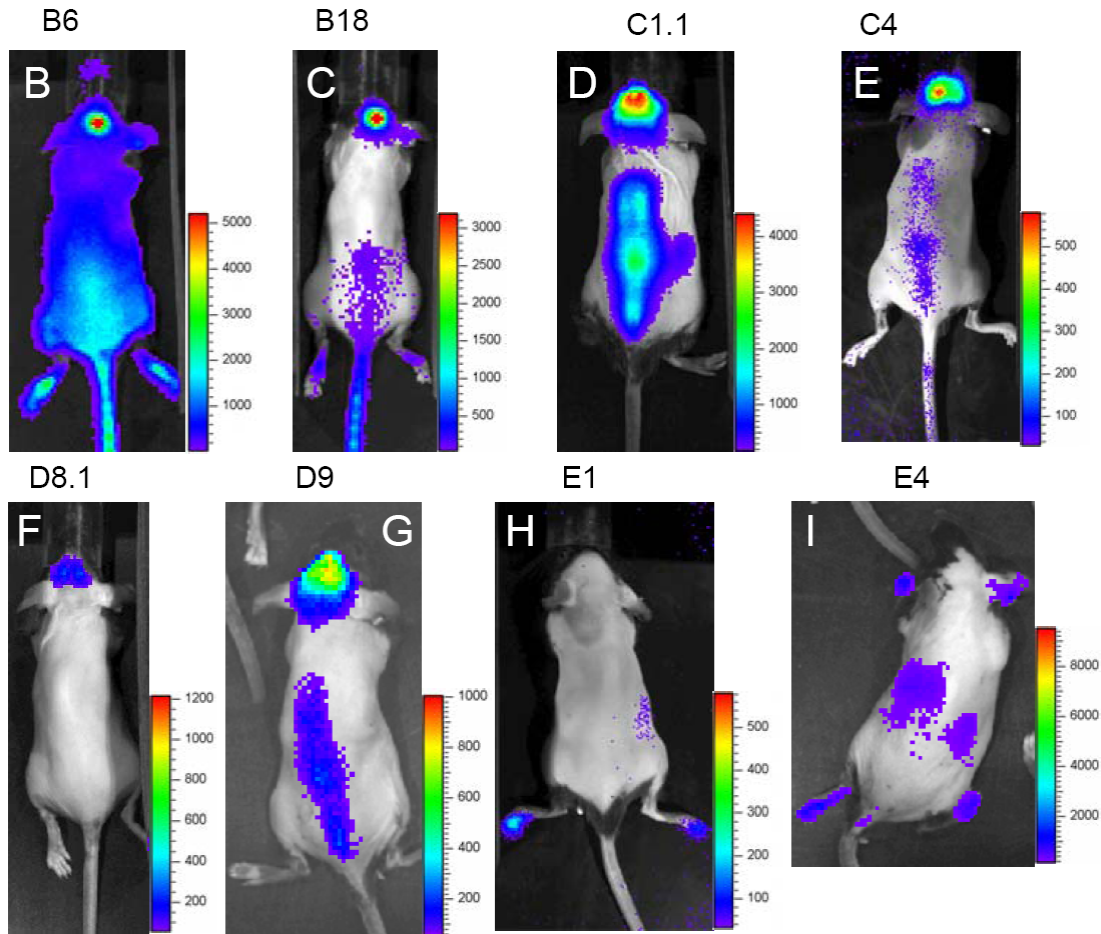
Figure 6.1: Luciferase Transgenic Constructs and *In Vivo* Bioluminescence Imaging. (A) A schematic representation of each Luciferase Transgenic construct (B-E) is shown in this panel. For comparison, a schematic drawing of the murine MC4R locus is placed at the top of the transgenic constructs, along with restriction sites for reference. Of particular importance is to note that all constructs share the same 3'-end for the 5'-flanking sequence, but the 5'-end of this varies from -432 bp to -3313 bp. Constructs B and C share the same 5'-flanking sequence, but B also shares the 3'-flanking sequence included in the LacZ Transgene Construct (Construct A). NOTE: Due to the software's programming, the *in vivo* bioluminescence images are best compared by intensity rater than actual photon emission levels. Therefore, this data is best used as a preliminary comparison between lines and for direction of which tissues to analyze using the *in vitro* methodologies discussed in Chapter 2. (B) *In vivo* bioluminescence imaging of line B6. Note the ubiquitous pattern of expression (determined to be in the skin, ears, and paws) with the highest intensity of expression coming from the head (determined to be the CNS). (C) *In vivo* bioluminescence imaging of line B18. Note the pattern is remarkably similar to B6, except for the expression in the skin. (D) *In vivo* bioluminescence imaging of line C1.1. Note the staining down the midline of the back (undetermined origin, but somewhat similar to the patterns seen in B18, C4, and D9 lines). (E) *In vivo* bioluminescence imaging of line C4. Note that the pattern is almost identical to C1.1, only the actual expression levels are lower. (F) *In vivo* bioluminescence imaging of line D8.1. The only expression detected by the imaging software is emitted from the head of this line. (G) *In vivo* bioluminescence imaging of line D9. Very similar pattern of expression to that seen in C1.1 and C4 with an actual level of light emission that is between the two. (H) *In vivo* bioluminescence imaging of line E1. Note that only the paws and the right flank of the animal appears to be expressing the transgene; however, *in vitro* data actually shows that the highest level of transgene expression is in the CNS. (I) *In vivo* bioluminescence imaging of line E4.

demonstrated that this site of expression is the brain stem (Table 6.1, B5 = 0.4 photon counts per second/microgram total protein ± 0.1; B6 = 21.1 ± 4.3; B11 = 119 ± 37; B18 = 21.8 ± 9.6). The *in vivo* dorsal image of line B6 mice also show expression throughout the body, which was found to be from luciferase expression in the skin. Low level (less than 100 photons per 8 x 8 pixel in a five minute light capture image) skin expression of the luciferase reporter was observed in four of the 15 transgenic lines for the 3300MC4Luc3 "B" construct. Most 3300MC4Luc3 transgenic lines exhibit ectopic luciferase activity in the ears, snout, paws, and tail (see discussion). Luciferase reporter expression was found to be present in numerous peripheral tissues in the 3300MC4Luc3 mice; however, reporter expression outside of the CNS was not consistent from line to line (See Table 6.1).

Seven 3300MC4Luc (construct C) transgenic founders were identified by initial PCR genotype screening and Southern blot analysis. Three of the founders (C1, C4, and C5) were selected for further analysis. Of these, the C4 transgenic founder failed to pass on the transgene to F1 offspring. Southern analysis of F1 offspring from the line C1 founder revealed four transgene integration sites which segregated independently. Offspring from three of the independent C1 integration sites were maintained as separate lines (C1.1, C1.2, and C1.3), of which line C1.1 recapitulated the *in vivo* bioluminescence pattern of luciferase activity that was observed in the founder animal.

In vivo bioluminescence imaging of line C1.1 F1 and C4 founder are shown in panels D and E of Figure 6.1, respectively. These images show a similar pattern of luciferase activity in the CNS and the dorsal midline of the back. *In vitro* luciferase assays of tissue samples from these two lines revealed that each had a similar pattern of

Table 6.1

HindIII — Pst — PacI — PstI — HindIII

-3313bp   -1618bp   -889bp   -5bp   [mMC4R]   +1509

Luciferase

(B) 3300MC4Luc3

Line	Tg Copy #	Transmitting	Expression: Hypothalamus	Striatum	Cortex	BrainStem	Cerebellum	Liver	Kidney	Heart	Lung	SkMuscle	Ear	Paw
B5	5-10	Yes	0.5 ± 0.2	<0.1	0.2 ± 0.2	0.4 ± 0.1	0.3 ± 0.2	<0.1	10.1 ± 7.7	0.6 ± 0.2	122 ± 53	<0.1	1.9 ± 0.3	9.5 ± 3.6
B6	>>20	Yes	3.6 ± 0.9	1.8 ± 0.6	8.6 ± 0.8	21.1 ± 4.3	1.7 ± 0.6	<0.1	<0.1	0.3 ± 0.1	<0.1	0.8 ± 0.8	2.2 ± 1.5	8.4 ± 5.5
B11	>20	Yes	17.8 ± 5.8	6.6 ± 3.7	12.2 ± 4.2	119 ± 37	8.4 ± 4.0	<0.1	0.2 ± 0.1	0.1 ± 0.1	0.1 ± 0.1	1.8 ± 1.0	<0.1	3.4 ± 3.1
B18	>>20	Yes	2.6 ± 0.3	4.5 ± 1.9	8.8 ± 3.2	21.8 ± 9.6	<0.1	<0.1	<0.1	<0.1	<0.1	0.1 ± 0	<0.1	<0.1

Luciferase

(C) 3300MC4Luc

Line	Tg Copy #	Transmitting	Expression: Hypothalamus	Striatum	Cortex	BrainStem	Cerebellum	Liver	Kidney	Heart	Lung	SkMuscle	Ear	Paw
C1.1	1	Yes	9.0 ± 4.9	11.2 ± 0.2	7.3 ± 2.9	14.0 ± 5.1	1.0 ± 0.2	<0.1	<0.1	<0.1	<0.1	<0.1	0.3 ± 0.1	<0.1
C1.2		Yes	<0.1	<0.1	<0.1	<0.1	<0.1	<0.1	<0.1	<0.1	<0.1	<0.1	<0.1	<0.1
C1.3		Yes	<0.1	<0.1	<0.1	<0.1	<0.1	<0.1	<0.1	<0.1	<0.1	<0.1	<0.1	<0.1
C4	1	No	5.4	7.0	4.4	8.0	0.4	<0.1	<0.1	<0.1	<0.1	<0.1	0.2	NA
C5	5-10	Yes	0.2 ± 0.1	<0.1	0.2 ± 0	0.4 ± 0.2	<0.1	<0.1	<0.1	<0.1	<0.1	0.2 ± 0.1	1.5 ± 0.6	15.7 ± 3.1

Luciferase

(D) 890MC4Luc

Line	Tg Copy #	Transmitting	Expression: Hypothalamus	Striatum	Cortex	BrainStem	Cerebellum	Liver	Kidney	Heart	Lung	SkMuscle	Ear	Paw
D5	1	Yes	3.2 ± 0.4	3.1 ± 0.5	2.3 ± 0.5	4.6 ± 0.5	1.1 ± 0.4	<0.1	<0.1	<0.1	<0.1	<0.1	0.2 ± 0.1	<0.1
D8.1	5-10	Yes	0.4 ± 0.1	3.1 ± 0.9	14.8 ± 4	4.2 ± 3.4	0.2 ± 0.1	<0.1	<0.1	<0.1	<0.1	<0.1	0.3 ± 0.1	<0.1
D8.2	5-10	Yes	<0.1	<0.1	<0.1	<0.1	<0.1	<0.1	<0.1	<0.1	<0.1	<0.1	57.8 ± 2	27.5 ± 9
D9	5-10	Yes	22.3 ± 4.2	11.7 ± 7.1	25.8 ± 14	24.5 ± 8.4	11.0 ± 2.1	<0.1	<0.1	<0.1	<0.1	<0.1	0.1 ± 0.1	<0.1

Luciferase

(E) 430MC4Luc

Line	Tg Copy #	Transmitting	Expression: Hypothalamus	Striatum	Cortex	BrainStem	Cerebellum	Liver	Kidney	Heart	Lung	SkMuscle	Ear	Paw
E1	2	Yes	3.1 ± 0.3	0.3 ± 0.1	<0.1	0.2 ± 0.2	<0.1	<0.1	<0.1	<0.1	<0.1	<0.1	0.3 ± 0.1	0.3 ± 0.2
E3	2	No	0.4	0.2	0.5	0.5	0.2	<0.1	<0.1	<0.1	<0.1	<0.1	<0.1	<0.1
E4	4	Yes	0.5 ± 0.1	0.5 ± 0.2	0.6 ± 0.1	1.1 ± 0.3	0.1 ± 0.1	<0.1	0.2 ± 0.1	2.3 ± 0.4	0.5 ± 0.1	0.2 ± 0.1	3.8 ± 1.5	3.8 ± 1.0

Luciferase Activity in counts per second/ug of total protein for each tissue above

NA = Not Analyzed

luciferase activity within the CNS. The expression in the CNS of line C5 (Table 6.1) also had a similar pattern as the C1.1 and C4 lines, albeit at much lower levels of activity. Similar to the 3300MC4Luc3 expression patterns in the CNS, the highest reporter activity in the CNS was found to be in the brain stem in these three "C" construct lines (Table 6.1, C1.1 = 14.0 ± 5.1; C4 = 8.0; C5 = 0.4 ± 0.2). The data suggest that the 3'-flanking sequence present in the 3300MC4Luc3 construct have little or no effect on brain expression of MC4R, but the data does support a hypothesis that extra CNS expression sites could be controlled from this sequence.

In vivo bioluminescence imaging of line C1.2 mice initially suggested that this line was non-expressing, and imaging of line C1.3 showed very low levels of expression in the tail, paws and snout – areas of presumed ectopic expression (see discussion). Expression in the brain, as determined by *in vitro* luciferase assays, was inconsistent for line C1.2 and negative for lines C1.3; however, *ex vivo* imaging of 1mm coronal brain slices (sectioned on brain mold, BrainTree Scientific) bathed in Promega Luciferase Assay Reagent (Promega) demonstrated weak luciferase activity throughout the brain in line C1.2 mice (data not shown).

Six transgenic founders for 890MC4Luc (construct D) were identified from genotyping PCR screens and *in vivo* bioluminescence imaging. Of these, three representative lines (D5, D8, and D9) were chosen for further analysis. Dorsal view *in vivo* bioluminescence images of D8.1 and D9 F1 offspring are shown in panels F and G of Figure 6.1, respectively. The founder of line D8 was found to pass on two independently segregating transgenic alleles when analyzed by Southern blot, and both genomic integrations were maintained as individual lines (D8.1 and D8.2).

Three of the four maintained 890MC4Luc lines clearly show CNS preferential expression (See Table 6.1) defined as greater than five fold expression in the CNS over that observed in peripheral sites of expression. Interestingly, by deleting the MC4R 5'-flanking sequence from -3313:-890 (numbered from the start of translation) increased CNS specificity of the luciferase reporter transgene. However, the expression pattern within the individual brain regions is less consistent between each 890MC4Luc transgenic line where expression is relatively higher in the cortex compared to the brain stem in these mice (Table 6.1, D5 Piriform Cortex = 2.3 ± 0.5, Brain Stem = 4.6 ± 0.5; D8.1 Piriform Cortex = 14.8 ± 4, Brain Stem = 4.2 ± 3.4; D9 Piriform Cortex = 25.8 ± 14, Brain Stem = 24.5 ± 8.4).

Three luciferase expressing transgenic founders for 430MC4Luc (construct E) were identified by PCR genotyping and *in vivo* bioluminescent imaging. The E3 transgenic founder did not produce any F1 offspring, but lines E1 and E4 were successfully maintained for further analysis. The initial *in vivo* bioluminescent imaging suggested no expression in the CNS from any of the 430MC4Luc lines. Line E1 transgenic mice appeared to express luciferase in the paws and ears (Figure 6.1H), while the *in vivo* bioluminescence imaging of line E4 transgenic mice suggested reporter gene expression in an area consistent with the kidneys in a dorsal view (Figure 6.1I) and the heart in a ventral view (data not shown). However, subsequent *in vitro* luciferase assays from isolated brain regions showed reporter expression in the CNS of all three 430MC4Luc lines.

With the exception of the luciferase expression in the paws, line E1 transgenic mice have an interesting luciferase expression pattern within the CNS that is limited to

the hypothalamus, striatum, and dorsal brain stem (Table 6.1, Hypothalamus = 3.1 ± 0.3, Brain Stem = 0.2 ± 0.2). When normalized to total protein, the expression in the hypothalamus is ~10 fold greater than in the paws. The false *in vivo* imaging results is likely due to the relative ease of luciferase generated photons to reach the detector from the paws, while the luciferase generated photons from the hypothalamus at the base of the brain is sufficiently scattered in its path to the detector due to the amount and type of tissue it must pass through (particularly the bone tissue of the skull).

Line E4 mice also show luciferase activity in the CNS, but the expression in the heart was found to be highest in this line (Table 6.1, Heart = 2.3 ± 0.4; Hypothalamus = 0.5 ± 0.1). The line E3 founder shows a similar pattern of expression in the CNS as line E4 (Table 6.1, E3 Hypothalamus = 0.4; E3 Piriform Cortex = 0.5; E3 Cerebellum = 0.2; E4 Hypothalamus = 0.5 ± 0.1; E4 Piriform Cortex = 0.6 ± 0.1; E4 Cerebellum = 0.1 ± 0.1); however, there was no detectable expression in the peripheral tissues of the line E3 founder.

With the exception of the relatively high expression in the hypothalamus of line E1 transgenic mice, the 430MC4Luc construct has consistently low levels of expression throughout the CNS. Only line E4 transgenic mice had peripheral expression in tissues other than ears, tail, and paws (see discussion), suggesting that a brain selective element(s) reside within the 5'-UTR of the MC4R gene, albeit much weaker in promoter activity than the regions found in the sequence upstream of the putative major start of transcription.

<u>Discussion</u>

The results for the *in vivo* imaging of the 3300MC4Luc3 luciferase transgenic mice were at first troubling because of the prominent light emission from the snout, ears, tails, and paws from many of the founders. This construct contained the same MC4R flanking sequences as the 3300MC4LacZ3 construct, and it was very similar to the sequence used in the MC4ITG transgenic construct. I went back to the MC4ITG and LacZ transgenic mice to perform RT-Real Time PCR on ear and foot pad tissues, with negative results in all six lines.

A careful review of the literature, however, revealed that the likely culprit of this reproducible non-specific expression was the pGL3-Basic vector. In all luciferase transgenic studies that used the pGL3-Basic vector as a donor for the firefly luciferase reporter the mice showed this characteristic pattern of non-specific expression in the snout, ears, tails, and paws in *in vivo* light-capture imaging. This pattern of expression was clearly present no matter what the promoter utilized to drive expression was: PPAR response element (72); serum amyloid protein and major urinary protein promoters (73), and human prostate-specific antigen promoter (74). However, even when the data from these sites of non-specific expression are included in comparisons with all other tissue results from the *in vitro* luciferase assays, the CNS expression is clearly preferential in all but a small number of MC4-Luc transgenic lines (e.g., Line E4, which only includes the putative 5'-UTR).

The *in vitro* data from the 3300MC4Luc3 and 3300MC4Luc transgenic constructs, though consistent with the data from 3300MC4LacZ3 and MC4ITG transgenic mice as being CNS preferentially expressed, are different in the fact that the

highest level of normalized luciferase activity in the CNS is almost always the brainstem region. However, it should be noted that the MC4ITG data was exclusively RT-Real Time PCR. Also, the RT-Real Time PCR data from the 3300MC4LacZ3 line A2 was inconsistent the *in vitro* Beta-Glo data, and ore consistent with the MC4ITG pattern of results.

The data, taken together up to this point suggests that the 3300 bp flanking sequence is sufficient for CNS preferential expression. Also, the data from the 890MC4Luc mice suggest that the *CR-6-8* regions may be sufficient by themselves for CNS preferential expression. Interestingly, the 430MC4Luc data also suggest that the 5'-UTR may harbor elements sufficient for preferential expression in the hypothalamus and brainstem (both evolutionarily conserved autonomic feeding centers in the CNS). Since the most promising region in the proximal sequence was the highly conserved *CR-8* region, I decided to further focus on the *CR-8* region by generating a heterologous transgenic construct, to determine whether this region of the promoter was capable of directing CNS preferential expression of a non-specific viral minimal promoter.

CHAPTER VII

EXPRESSION OF FIREFLY LUCIFERASE IN TKLUC, -560:-495MC4-TKLUC, AND
-560:-450MC4-TKLUC MICE

Results

        Data from the *in vitro* promoter analysis (see Chapter III), *in vivo* transgenic

promoter analysis (see Chapters IV-VI), and the novel human SNP (see Chapter III)

directed me towards characterizing the *CR-8* region further using the *in vivo* approach.

To do so, I created heterologous promoter transgenic constructs – constructs that contain

promoter elements from more than one source. These constructs (Construct G – TKLuc

and Construct H – MC4-TKLuc) include a core minimal promoter from the Herpes

Simplex Virus Type 1 thymidine kinase (*tk*) gene (see Figure 7.1A). The minimal *tk*

gene promoter is sufficient for positive promoter activity in a variety of cell lines in *in*

vitro assays, and it is often used for a positive control in such experiments or as a

heterologous promoter system to study an enhancer in isolation of its cognate promoter

(75). However, the virus itself is specialized for infecting dorsal root ganglia of the

peripheral nervous system *in vivo* where it sets up a lifelong latency with periodic and

poorly understood reactivation (76). Therefore, the expected expression pattern for the

luciferase reporter in the TKLuc transgenic mice was ubiquitous with a strong possibility

for tissue specific expression following the promoters of "trapped" genes – more or less

acting as random heterologous promoters for the integrated TKLuc cassette. Also, males

were expected to have relatively higher levels of expression in testes, given the known

85

preferential expression in the male gonads of transgenic mice using the minimal *tk* gene promoter (77).

The MC4-TKLuc constructs contain only the highly conserved 32bp *CR-8* region with very little flanking sequence on either side (<100bp, see Figure 7.1A). This heterologous promoter arrangement should act as if the TKLuc construct has "trapped" the *CR-8* region of MC4R. If the highly conserved *CR-8* region is sufficient for CNS preferential expression, then one would expect the resulting luciferase activity to be highest throughout the CNS, given the broad *in vivo* expression pattern of the transfactors that would bind to putative cis-elements contained in this region (see Table 3.1 and Figure 3.4). The known preferential expression in the testes will serve as a good "internal control" in these experiments. However, if the highly conserved *CR-8* region is not sufficient for CNS preferential expression, one then might expect to see something similar to the expected TKLuc pattern: a ubiquitous expression pattern with a relatively strong chance of "trapping" another enhancer. The results are clear, the highly conserved *CR-8* region is sufficient to drive the expression of the heterologous promoter preferentially in the CNS. Moreover, the highly conserved *CR-8* region was sufficient to block testes expression in the heterologous constructs, while it was expressed in the testes of all but one male founders and two of three lines maintained from female founders.

Bioluminescent Imaging of Transgenic Founders and Offspring
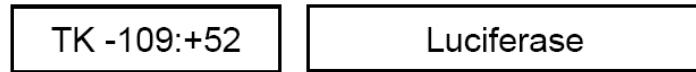
Six positive transgenic founders were identified by initial PCR screens and southern blot analysis. These founders were subsequently screened for expression of the luciferase reporter gene by *in vivo* bioluminescence analysis, of which three were

Figure 7.1

Panel A

(G) TKLuc

| TK -109:+52 | Luciferase |

(H) MC4-TKLuc

mMC4R -560bp: -496bp

| TK -109:+52 | Luciferase |
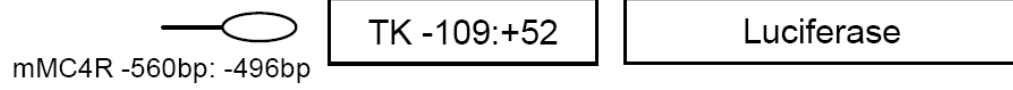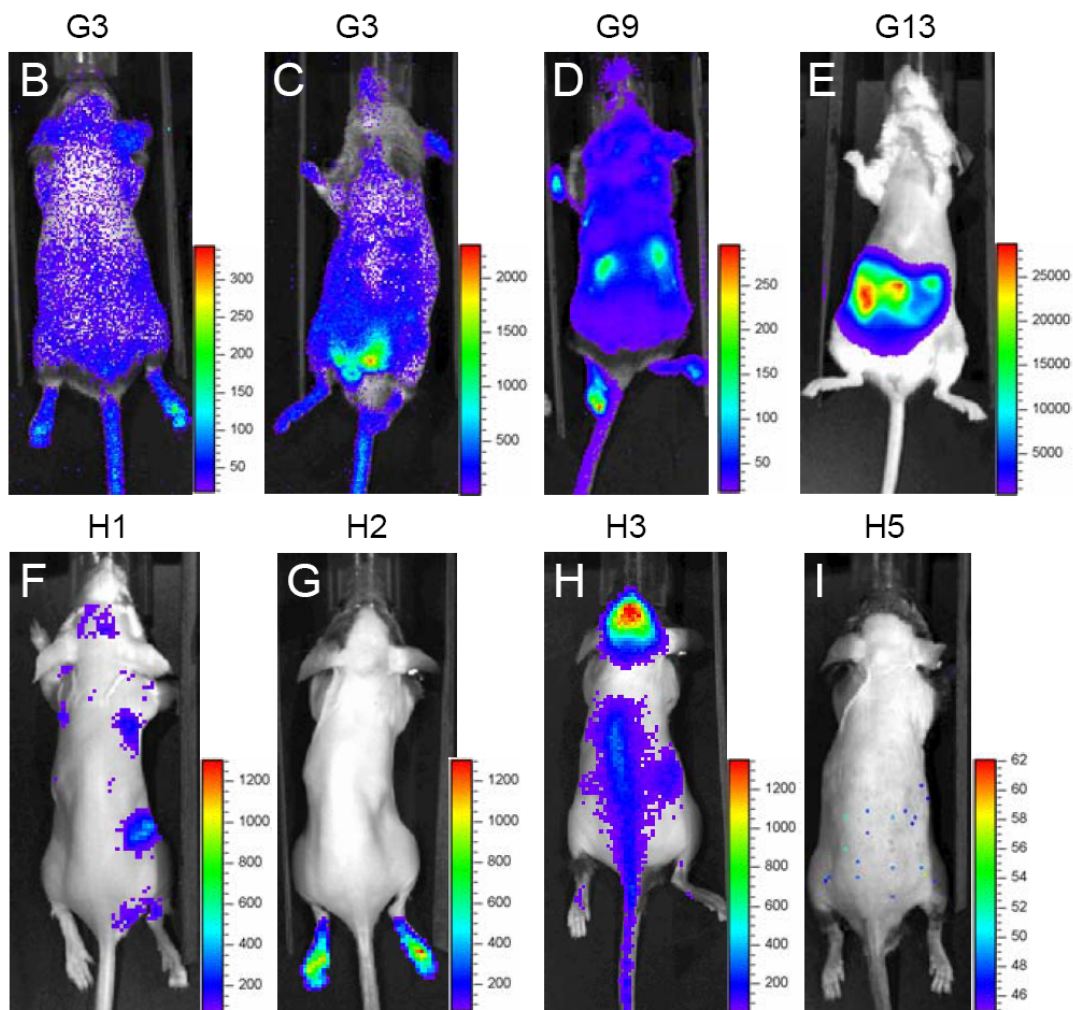
Figure 7.1: Heterologous MC4R-TK Luciferase Constructs and In Vivo Bioluminescence Imaging. (A) A schematic representation of the TK heterologous transgenic constructs (G-H) is shown in this panel. For comparison, a schematic drawing of the murine MC4R locus is placed at the top of the transgenic constructs, along with restriction sites for reference (the sequence included in the D construct is that which is shown for reference, as it is the shortest construct that includes the *CR-8* region). Also shown for reference is the position of the highly conserved *CR-8* region in the murine MC4R locus and the transgene (transparent oval). NOTE: Due to the software's programming, the *in vivo* bioluminescence images are best compared by intensity rater than actual photon emission levels. Therefore, this data is best used as a preliminary comparison between lines and for direction of which tissues to analyze using the *in vitro* methodologies discussed in Chapter 2. (B) *In vivo* bioluminescence imaging of line G3. This image shows the dorsal side of the animal. Note the expression in the ears and paws of this animal. (C) *In vivo* bioluminescence imaging of line G3. This iage shows the ventral side of the same animal imaged in Panel B. (D) *In vivo* bioluminescence imaging of line G9. (E) *In vivo* bioluminescence imaging of line G13 (ventral). Note that the expression appears to be exclusive to the entrails of the animal. (F) *In vivo* bioluminescence imaging of line H1. Note the "patchy" expression pattern. (G) *In vivo* bioluminescence imaging of line H2. (H) *In vivo* bioluminescence imaging of line H3. Note that this expression pattern is remarkably similar to that seen for Lines C1.1, C4, and D9 that also contain the highly conserved *CR-8* region. (I) *In vivo* bioluminescence imaging of line H5. Note that this image appears to be completely null; however, *in vitro* analysis showed that the only detectable expression was in the CNS.

positively identified as expressing detectable levels of the transgene by the imaging

technique (see Figure 7.1B-I). Panels B and C in Figure 7.1 show a male founder for

Line G3 of the TKLuc construct. As shown in the ventral imaging position in Panel C,

this line, as does all but two TKLuc construct lines total, expresses the luciferase reporter

gene in the testes. This result confirmed the expected testes-positive expression pattern

for the TKLuc transgenic lines. Also note the expression in the paws, tails, and ears in

Panels B-D. This was also seen in the MC4R promoter luciferase mice, and it appears to

be due to sequence associated with the pGL3-luciferase vector from Promega (see

discussion). The image of Line G9 in Panel D shows what appears to be a ubiquitous

expression pattern, with some internal tissues expressing relatively higher levels. Panel E

shows the ventral image of a female F1 animal from Line G13. This represents what

appears to be a "trapped" enhancer mouse, where the enhancer directs expression in the

small intestine. This animal was sacrificed and the entire digestive tract was removed

and imaged beside the animal *ex vivo* to show that the expression pattern observed was

exclusively coming from the small intestine (data not shown). Another interesting

observation taken from the *in vivo* imaging was the relatively low expression observed

for the TKLuc mice, compared to that seen in the MC4R-promoter luciferase mice

(compare intensity bars in the images in Figure 6.1 with Figure 7.1).

 The three known expressing founders were immediately selected to be maintained

for further analysis (H1, H2, and H3). Before analysis on the other three founders (H4,

H5, or H6) was performed, each was paired for breeding in case an interesting expression

pattern was detected using the *in vitro* assays. However, none of these founders produced any offspring.

Of the three MC4-TKLuc mice that had observable expression in the *in vivo* imaging screening, only one, Line H3, appeared to be promising for CNS preferential expression. Indeed, the *in vivo* images of Line H3 mice look markedly similar to *in vivo* images of Line D9 mice, the shortest MC4R promoter-luciferase construct that also contained the highly conserved *CR-8* region (compare Figure 6.1G with Figure 7.1H). The *in vivo* imaging of Line H1 mice showed a spotty pattern that can be seen in Figure 7.1F. The spotty pattern varied in intensity between individual animals; however, all such images showed luciferase activity in the head and what appeared to be the spleen of these animals (note: the spleen was subsequently found to be negative by *in vitro* analysis, data not shown). The most likely cause of the varied intensity of expression would be multiple integration sites, as Southern blots showed that this line harbored nearly 50 copies of the transgene, but no independent integration site was observed on Southern blots. Such results do not rule out the possibility of multiple integration sites on the same chromosome, which would also explain why there was no independent segregation.

Luciferase Transgene Activity Assay in Transgenic Mice

Wildtype and transgenic offspring were sacrificed, and tissues were harvested based upon the pattern of expression seen in the *in vivo* imaging. The results from the *in vitro* luciferase assays are shown in Table 7.1. Of the six TKLuc lines analyzed, only one line, G3 showed a clear preferential expression in the CNS, but the highest expression

was in the cerebellum (see Table 7.1: 3.5 cps/µg). No MC4 transgenic construct showed preferential luciferase activity in the cerebellum, by either RT-Real Time PCR or *in vitro* assay. The G13 line, the clear "enhancer trap" line, showed a higher mean *in vitro* luciferase activity level in the CNS, but the variance of luciferase activity in the CNS regions of this line was extreme (see Table 7.1: Hypothalamus 10.9 ± 12.2, Cortex 12.7 ± 12.9). The variance in the small intestine (duodenum results shown) was much less in Line G13 (see Table 7.1: Small Intestine 11.8 ± 3.8). All other lines show clear preferential expression in peripheral tissues – G9: Heart at 14.5 ± 9.4; G10: Ear at 0.9 and Paw at 0.7; G11: Ear at 0.2 (note that Line G5's preferential tissue expression is in the testes 0.4 ± 0.3, skin 0.5 ± 0.3, and tail 0.8 ± 0.7). Interestingly, most of these lines have preferential luciferase activity in the very repeatable, non-specific sites that have been previously discussed with the pGL3-Basic vector donor transgenic mice in other labs.

On the other hand, the results from the *in vitro* luciferase assays in the MC4-TKLuc heterologous lines are in rather stark contrast to the TKLuc data. The H1 Line shows a varied expression pattern from mouse to mouse, but the mean data shows that the luciferase reporter activity is clearly CNS preferential, with only one peripheral tissue yielding any reproducible positive results (Table 7.1: Hypothalamus 2.2 ± 1.8, Cortex 10.9 ± 12.9, Cerebellum 0.1 ± 0.1, Heart 0.5 ± 0.5). The H2 Line showed very low levels of *in vitro* reporter activity in the CNS and the pGL3-Basic non-specific sites of ear and paw (Table 7.1: Hypothalamus 0.4 ± 0.2, Cortex 0.3 ± 0.3, Cerebellum <0.1, Ear 0.3 ± 0.3, and Paw 0.3 ± 0.3), while all other tissues were negative.

The results from the H3 Line show the highest reproducible levels of *in vitro* luciferase activity in the CNS, but some expression was found in the non-specific pGL3-

Basic sites (Table 7.1: Hypothalamus 10.6 ± 6.1, Cortex 7.7 ± 2.1, Cerebellum 5.1 ± 2.6, Ear 1.0 ± 0.8, and Paw 0.8 ± 0.6). The line H5 founder, which did not throw any transgenic offspring, also showed a CNS preferential pattern of expression of *in vitro* luciferase activity (Table 7.1: Hypothalamus <0.1, Cortex 0.8, Cerebellum 0.1). It is not clear whether the CNS expression in the MC4-TKLuc heterologous transgenic mice was actually due to the cloned *CR-8* region or from the minimal TK promoter, itself. However, the fact that the *CR-8* heterologous promoter is sufficient to direct CNS preferential expression in three of four of these H Construct lines is very telling of this highly conserved region's possible role in endogenous MC4R expression.

Table 7.1

(G) TKLuc

Line	Tg Copy #	Transmitting	Expression: Hypothalamus	Striatum	Cortex	BrainStem	Cerebellum	Liver	Kidney	Heart	Lung	Sm Intest	SkMuscle	Ear	Paw
G3	4	Yes	1.9	1.1	1.9	1.6	3.5	<0.1	0.1	0.1	0.1	<0.1	<0.1	0.6	<0.1
G5	5	Yes	<0.1	<0.1	<0.1	<0.1	<0.1	<0.1	<0.1	0.1	0.1	<0.1	<0.1	0.1 ± 0.1	0.3 ± 0.4
G9	2	Yes	0.7 ± 0.5	1.4 ± 0.3	4.9 ± 0.6	2.0 ± 1.4	0.8 ± 0.9	<0.1	0.1 ± 0.1	14.5 ± 9.4	1.0 ± 0.1	<0.1	0.2 ± 0.1	NA	0.2 ± 0.1
G10	>>20	No	<0.1	<0.1	<0.1	<0.1	<0.1	<0.1	<0.1	<0.1	<0.1	<0.1	<0.1	0.9	0.7
G11	1	No	<0.1	<0.1	<0.1	<0.1	<0.1	<0.1	<0.1	<0.1	<0.1	<0.1	<0.1	0.2	<0.1
G13	2	Yes	10.9 ± 12.2	2.1 ± 1.6	12.7 ± 12.9	2.3 ± 1.7	6.6 ± 4.9	<0.1	<0.1	5.4 ± 5.9	<0.1	11.8 ± 3.8	<0.1	<0.1	0.3 ± 0.2

mMC4R -560bp:-496bp

(H) MC4-TKLuc

Line	Tg Copy #	Transmitting	Expression: Hypothalamus	Striatum	Cortex	BrainStem	Cerebellum	Liver	Kidney	Heart	Lung	Sm Intest	SkMuscle	Ear	Paw
H1	>>20	Yes	2.2 ± 1.8	2.1 ± 1.6	10.9 ± 12.4	2.3 ± 2.7	0.1 ± 0.1	<0.1	<0.1	0.5 ± 0.5	<0.1	<0.1	<0.1	<0.1	<0.1
H2	10-15	Yes	0.4 ± 0.2	0.2 ± 0.2	0.3 ± 0.3	0.1 ± 0.1	<0.1	<0.1	<0.1	<0.1	<0.1	<0.1	<0.1	0.3 ± 0.3	0.3 ± 0.3
H3	1	Yes	10.6 ± 6.1	4.1 ± 1.8	7.7 ± 2.1	5.0 ± 2.6	5.1 ± 2.6	<0.1	<0.1	<0.1	<0.1	<0.1	<0.1	1.0 ± 0.8	0.8 ± 0.6
H5	2	No	<0.1	0.2	0.8	0.1	0.1	<0.1	<0.1	<0.1	<0.1	<0.1	<0.1	<0.1	<0.1

<u>Discussion</u>

The absence of LacZ reporter expression in peripheral tissues in adult transgenic mice taken together with the noticeable repeated expression of the TKLuc mice in the ears, paws, tail, and snout allows me to comfortably conclude that these unexpected sites of reporter expression in the *in vivo* images of the luciferase mice are due to sequence within the luciferase vector and/or gene from pGL3-Basic and not due to expression from the MC4R promoter sequence. This conclusion is also consistent with the brain-specific/preferential expression of the tauEGFP transgene in the four independent MC4ITG transgenic lines, and it is consistent with the images and data from pGL3-Basic transgenic mice in other labs.

Furthermore, while I cannot say with confidence that the actual CNS pattern of expression in the heterologous construct mice is due to only the *CR-8* region, the data does suggest that the *CR-8* region is sufficient to direct a minimal virus promoter to CNS preferential expression.

CHAPTER VIII

EVIDENCE FOR REVERSIBLE ACUTE REGULATION OF ENDOGENOUS MC4R
EXPRESSION FOLLOWING 24 HOUR FAST

Results

Previously, others had shown that chronic (over 14 days) exposure to narcotics,

morphine (28) or cocaine (29), could regulate MC4R expression in the CNS. No

previous experiment has shown that MC4R could be regulated acutely in response to any

stimulant. In fact, a chronic diet change study in sheep showed no changes in long term

MC4R expression in the hypothalamus (21). However, MC4R deficient mice fail to

acutely respond to increases in dietary fat, while MC3R deficient mice respond similarly

to wildtype controls (78). Although these latter experiments only suggest that the

presence of MC4R will correct this physiological malady, the previous experiments

confirm that the MC4R gene promoter is amenable to regulation. In fact, one group has

recently published data that suggests MC4R itself is regulated acutely (within 24 hours)

by an increase in calories from dietary fat (55). This led me to hypothesize that acute

regulation of MC4R could be a physiological mechanism involved in the response to

changes in dietary conditions (i.e., feeding behavior).

Since the change in the level of chow consumption for MC4R deficient mice in

response to high fat diet are most likely attributed to lack of the gene rather than the

ability of the animal to regulate MC4R acutely, a more radical change in dietary

conditions would likely be needed to detect a change in the naturally weak MC4R

expression in the CNS. It is true that a goal of the project was to be able to detect and

study small changes in MC4R promoter activity in vivo, and the MC4R-luciferase transgenic mice give a readily detectable basal level of photon production, a more robust change in expression would be desirable for a pilot experiment. Thus, I first chose to test whether endogenous MC4R expression is acutely regulated by an acute fast (24 hour).

Endogenous CNS MC4R Expression in Fed and Fasted Mice

Total RNA from several CNS regions was prepared from acutely fasted and control fed non-transgenic C57Bl6 mice as previously described. Multiplex RT-real time PCR was performed on the samples for endogenous MC4R RNA and beta-actin (internal control) RNA levels. The data was normalized to the internal control and expressed relative to the average beta-actin expression in the control (fed) group. Figure 8.1 shows that endogenous MC4R expression is increased about >1 fold in response to an acute fast (Fasted 2.3 ± 0.5; Fed 1.2 ± 0.3).

Bioluminescent Imaging of 3300MC4Luc, 890MC4Luc, and TKLuc Transgenic Mice

I next wanted to test whether the luciferase activity of the MC4R promoter-luciferase fusion transgenic mice would mimic the increase seen in the endogenous gene mRNA expression. I chose to first use the long construct mice (3300MC4Luc, lines C1.1 and C4), as these have the greatest amount of MC4R promoter sequence and would be more likely to mimic physiological changes in endogenous MC4R expression in response to the acute fasting regimen. The TKLuc transgenic mouse line (Line G9) was chosen as a suitable control because it has an expression pattern of the luciferase transgene in a near ubiquitous pattern, including the CNS.
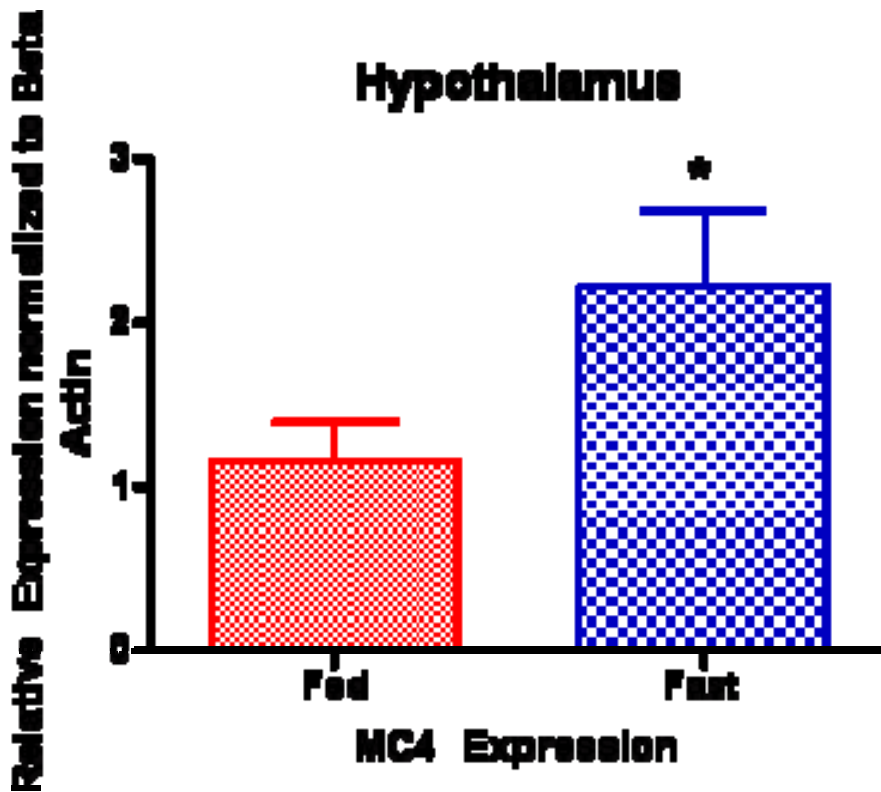
Figure 8.1

Figure 8.1: Endogenous MC4R Expression is Induced by 24 Hour Fast. Wildtype C57bl6 females were housed in cages of four animals per cage for one week prior to experiment. On the day before tissue harvesting, at 10:00AM both cages were changed; however, only one received fresh food. The second cage was then the fasted group. After a 24 hour fast, all eight female mice were sacrificed, and the hypothalamus, striatum, and cortex were harvested for RNA extraction. DNased total RNA was prepared as described above. The RNA was used to synthesis cDNA for use in Real Time Quantitative PCR. The results are an average of the four animals in each group (Fed and Fasted), and the MC4R expression was normalized to beta-actin mRNA. Error bars are S.E.M. * denotes $p<0.05$ by Two Tailed Paired t Test. Data analysis was performed using GraphPad Prism software.

The mice were depilated for bioluminescence imaging as described previously, but 72 hours prior to the first image capture, rather than the usual 24-48 hours. This alteration in protocol was deemed necessary to make sure that all experimental animals were fully recovered from the hair removal regimen. As in all other bioluminescence imaging protocols, the normal mouse chow was replaced with the high casein chow 48-

72 hours prior to the first image capture. The fed/control mice were given *ad libitum*

access to the high casein chow throughout the experimental period. The

fasted/experimental mice had their chow removed between 10:00-11:00AM (five hours

after light cycle start) immediately after the first image capture. The first image capture

was performed on Day 1 as a baseline reading for all animals. Twenty-four hours later,

Figure 8.2

Control Group

Fed	Fed	Fed
10AM Day 1 Imaged	10AM Day 2 Imaged	10AM Day 3 Imaged

Experimental Group

Fed	Fasted	Re-Fed
10AM Day 1 Imaged/ Food removed	10AM Day 2 Imaged/ Food returned	10AM Day 3 Imaged

Figure 8.2: Schematic Diagram of Fed/Fasted Protocol. Mice were prepared for imaging at least 72 hours prior to Day 1 image capture. All mice were imaged on Day 1 at approximately 10AM. During imaging, the cages for each animal were changed to fresh bedding. The experimental group animals were placed in cages that did not contain food, but were given free access to water. Twenty-four hours later, the mice were imaged on Day 2. During the imaging, food was returned to the cages of the experimental mice. The final image capture was acquired on Day 3, after 24 hours of free access to food in the experimental group.

Day 2, the second image capture was performed, and the high casein chow was returned to the fed/experimental animals immediately after this image capture. Then 24 hours later, Day 3, the final image capture was performed. See Figure 8.2 for a schematic diagram of the Fed/Fast imaging protocol.

The quantitative *in vivo* imaging results of the MC4-Luc and heterologous construct are consistent with the results from the endogenous MC4R transcripts in the hypothalamus of C57BL6 wildtype mice after a 24 hour fast (see Figure 8.3). However, the results from the TKLuc mice in this experiment taint the final results (see discussion, below). Also, it was interesting that the quantitative results from the entire body of the mice (with the quantitative data from the head subtracted) from each line imaged was slightly increased. Although the slight increase was not the ~50% increase in quantitative results seen within the head of the TKLuc line, it suggests that some of the data in these experiments is due to non-specific increase luciferase activity (see discussion, below).

Figure 8.3

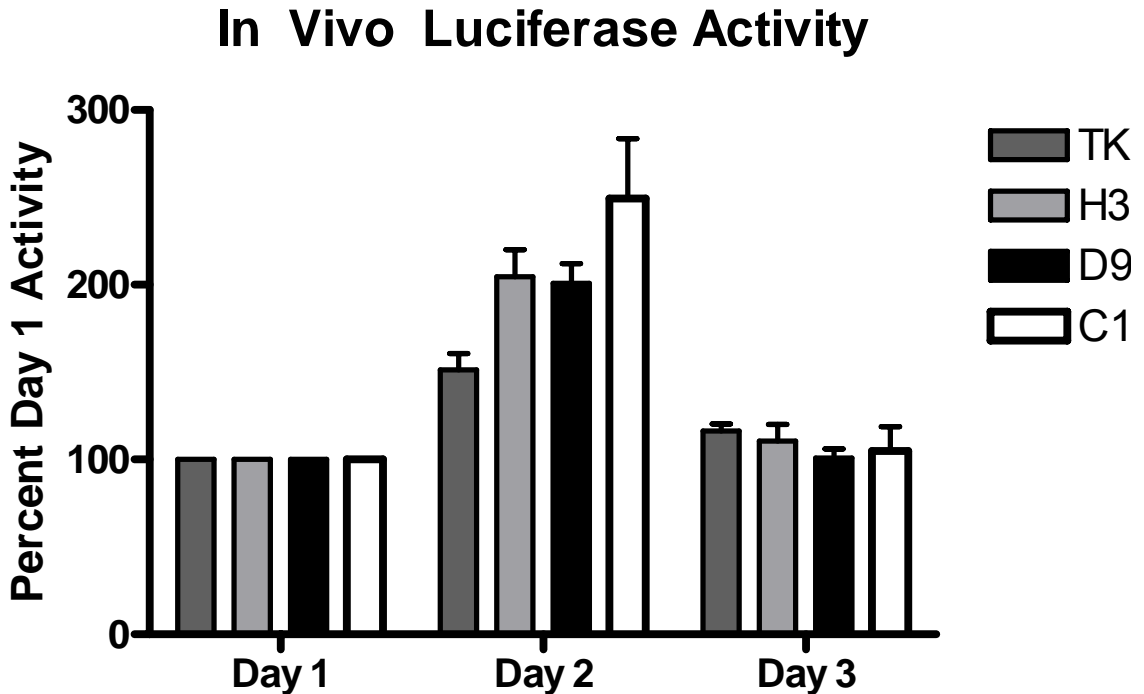## In Vivo Luciferase Activity

Figure 8.3: Luciferase Activity in Transgenic Mice is Induced by 24 Hour Fast. Following image capture on Day 3, the images were analyzed with the Living Image Software to determine the total photon capture for a given area (consistent between groups) that only included the heads of each animal. Data represents mean activity levels for the given 2-D area relative to the Day 1 activity (set to 100%). Error bars represent S.E.M.

Discussion

Given the results by Archer et al acute high fat diet experiments (52), I predicted that an acute overnight fast would decrease MC4R expression. However, the RT-Real Time PCR results for endogenous MC4R transcript expression show a clear induction of greater than one fold. Moreover, these results are more robust than those reported by Archer et al. It is possible to reconcile the data by suggesting that while MC4R expression is amenable to regulation by acute metabolic stimuli, the rapid increase in release of either alpha-MSH or AgRP will induce MC4R expression. Given the already weak expression of MC4R and its unique physiological role as a signal "input processor" for both anorectic (alpha-MSH) and orexigenic (AgRP) "output signals", it may be more

advantageous to the organism to have an increase in the number of "processors" to augment the already increased release of "signals."

A possible explanation of the results in the MC4R-luciferase fasted mice would be that the decrease in food (or water consumption) somehow increased the availability of luciferin reagent or its absorption into the CNS. Thus the results would be a false positive. However, the data from the control TKLuc mice did not suggest this result, because they did not show as robust an increase in luciferase activity *in vivo* as the 3300MC4Luc, 890C4Luc, or the heterologous H Construct mice did. Yet, the marginal increase in luciferase activity in the control TKLuc mice suggested that at least some of the increased luciferase activity in the fasted animals expressing firefly luciferase could be due to an uncontrolled variable – such as increased availability of the reagent in the CNS directly due to fasting or indirectly due to fasting by a decreased water intake while fasting. In either case, the hypothalamus is located near a point of great access to blood flow, thus reagent delivery. Therefore, the modest increase in the TKLuc mice could be due to the increased reagent delivery in general to the expression found in the head (and elsewhere), while the greater increases in luciferase activity in the various MC4R-luciferase mice could be due to a combination to the increased reagent delivery and increased reporter expression in the hypothalamus.

CHAPTER IX

GENERAL SUMMARY AND SIGNIFICANCE OF FINDINGS

While the CNS expression pattern of MC4R mRNA has been delineated, the regulatory elements of the MC4R gene that control expression in multiple brain nuclei have yet to be fully characterized. During the course of my studies, our laboratory and others have initiated several studies to identify these key regulatory elements. Using 5'-RACE (rapid amplification of cDNA ends) of mouse brain RNA, Dumont and colleagues (56) demonstrated that a major transcriptional start site lies about 430 bp upstream of the start of translation. Analysis of a series of mouse MC4R 5'-flanking region fragments fused to a luciferase reporter gene, established that fragments up to 3.3 kb would function as basal promoters when transfected into HEK293, UMR106, and GT1-7 cell lines, but not Neuro-2A neuronal cells (56).

Using a similar approach, we have further characterized the mouse MC4R promoter region; however, our preliminary studies indicate that while in general agreement with Dumont et al (56), there are several subtle differences. Using hypothalamic GT1-1 and GT1-7 cells (originally derived from tumors in the Medial Pre-optic Nucleus from mice harboring a GnRH promoter/SV40 T antigen transgene, 79), we find that MC4R promoter constructs consisting of 1600 bp of 5'-flanking sequences confer maximal basal promoter activity, whereas a 3.3kb construct is nearly as active. Shorter constructs with as little as 180bp of putative 5'-UTR of the mRNA transcript will also function as a promoter in GT1-1 cells. However, a more extensive construct

containing 7.9 kb of 5'UT region displays markedly reduced promoter activity indicating that one or more potential negative regulatory enhancer elements likely reside distally.

A comparison between mouse and human distal promoter regions indicates that several "islands" of conserved sequences indeed reside between 3.3 to 7.9 kb upstream of the putative transcriptional start site. In contrast to previous results (56), a similar profile of expression is also seen with each of the promoter fragments transfected into Neuro-2A cells, albeit at reduced overall levels of activity. This latter result does however support a previous report of MC4R expression in Neuro-2A cells (29). Overall, these results are surprising in that substantial promoter activity was not expected in any of the neuronal cells lines since detection of endogenous MC4R mRNA and protein in both tissue culture models, and *in vivo*, has been relatively difficult to date.

To overcome the limitations associated with low level of expression of MC4R in immortalized tissue culture cells, several series of transgenic mouse lines utilizing putative promoter fragments of the murine MC4R gene fused to various reporter genes (each of which have their respective strengths as noted previously) were created. Initial experiments utilizing a bicistronic tau-EGFP transgene reporter (MC4ITG construct) provided evidence that 3300 bp of upstream sequence of the MC4R gene (along with limited downstream sequences) was sufficient to drive expression exclusively in neuronal tissues since three of four independent lines all showed brain-specific expression.

However, as mentioned previously, the tau-EGFP reporter protein was not expressed in sufficient quantity to detect via fluorescent microscopy, and it could only be detected by RT-PCR. To overcome this technical hurdle, we next turned to fusion constructs containing 3300 bp of 5'-flanking sequence (and limited 3'-flanking sequence)

fused to LacZ and Firefly Luciferase reporter transgenes. The 3300MC4LacZ3 transgenic construct mice demonstrated brain-specific transgene expression in adult animals in two of two independent lines, consistent with our data from the MC4ITG transgenic mice. Unexpectedly, multiple organs in the fetuses of one line (Line A2) showed expression of the LacZ reporter. At the of these experiments, no one had studied the expression of endogenous MC4R in non-CNS tissue in developing embryonic or fetal organs, but shortly after our findings, Mountjoy and colleagues published an *in situ* study of endogenous MC4R mRNA expression in the developing rat fetus (66). Interestingly, our observed reporter expression pattern in peripheral tissues in Line A2 fetal mice closely parallels the data presented in this paper (66), including expression in the developing heart and skeletal muscles. Even more interesting is the fact that this widespread fetal expression pattern is entirely lost in the adult Line A2 mice. This result is consistent with the adult CNS-specific expression of the endogenous MC4R gene *in vivo* in rodents.

Some species of animals, chicken (61) and fish (62), do not express MC4R exclusively in the CNS, though it is believed to be involved in feeding behavior, at least in fish (80, 81). Our data taken together with the data from Mountjoy et al (66) suggests that promoter elements in the proximal 3.3 kb could have evolved in mammals to restrict expression of MC4R in the CNS in adult tissues. Given the increased use in teleost (*Danio rerio*) and the bioinformatics tools now available for cross examination of conserved genomic DNA sequences, this remains an interesting hypothesis that will likely be addressed in the near future by MC4R investigators.

The next set of transgenic animals utilized the Firefly Luciferase reporter gene. This reporter gene is commonly used for *in vitro* studies because of its low background and highly sensitive linear results, but recent technological advances, mainly by Xenogen, Inc., have allowed investigators to take advantage of luciferase *in vivo*. Our results from the panel of MC4R flanking sequence-luciferase fusion constructs (3300MC4Luc3, 3300MC4Luc, 890MC4Luc, and 430MC4Luc) are largely consistent with the tau-EGFP and LacZ reporter transgenic mice. Of the four representative 3300MC4Luc3 (Construct B) lines chosen to characterize, three of four showed CNS preferential expression of the reporter by *in vitro* assays. Of the three lines that showed CNS preferential expression, the relative ratio of *in vitro* luciferase activity was similar, suggesting that the MC4R flanking sequences were acting reproducibly in these lines. The highest peripheral expression in these CNS-preferential lines was in the ears, paws, and tails. As previously noted, these sites (along with the snout) are non-specific expression in transgenic mice using the Promega pGL3-Basic vector for the Firefly luciferase reporter transgene (72-74).

Our results from the 3300MC4Luc (Construct C) transgenic mice were similar to that of the 3300MC4Luc3 mice in respect of the ratio of *in vitro* luciferase activity in the CNS. However, of the three representative lines chosen for characterization (one of which had at least three independently segregating genomic integration sites) all showed CNS-preferential expression, if the non-specific ear, paws, and tail results are properly discounted. Surprisingly, three of four independent 890MC4Luc (Construct D) lines showed exclusive CNS expression in *in vitro* assays (note: the expression seen in the dorsal midline of Lines D5 and D9 are presumed to be spinal cord expression). This was

an unexpected result because only about 500 bp of putative promoter sequence with the 5'-UTR is all the MC4R sequence in this construct. However, the data from the *in vitro* studies showed that this sequence had a very strong positive promoter activity. Also, this sequence contains seven of the twelve highly conserved regions in the proximal 5'-flanking sequence, including the 100% conserved *CR-8* region.

The results from the 430MC4Luc (Construct E) transgenic mice were also surprising. This construct contained only the putative 5'-UTR of the murine MC4R transcript, yet all three lines expressed the transgene in the CNS, and two of the three lines showed CNS-preferential patterns of expression – and one of those was CNS-specific. This result makes sense, given the *in silico* sequence conservation results, which show that on average the 5'-UTR is the most highly conserved sequence in the gene outside of the coding sequence. Overall, the luciferase data as a whole is consistent with the CNS-preferential results from the other two reporter transgenics. Also, the results suggest that elements within the 5'-UTR at a minimum, and the first 500 bp of putative promoter sequence is sufficient for CNS preferential expression of MC4R in adult mice.

Moreover, our transgenic data is consistent with a recent report by Mountjoy and colleagues (57), in which they show that 1.5 kb of 5'-flanking sequence is sufficient to replicate endogenous MC4R expression in one transgenic mouse line. These results agree with our initial findings, especially with the data from the 890MC4Luc construct being sufficient to direct brain-specific expression. However, our heterologous promoter studies indicate that as little as 65 bp including the highly conserved *CR-8* region are capable of conferring CNS-specific expression in the context of a minimal TK promoter.

Furthermore, this region has also been the focus of other studies including those by our collaborators in screening obese patient populations for single nucleotide polymorphisms. We predicted that mutations found in the *CR-8* region could interfere with basal and possibly induced expression of MC4R, thus reducing the total functional activity of MC4R in feeding behavior neurons and result in obesity or a heightened risk thereof. The severity of obesity or weight aberrations will depend on the severity of expression loss. Other contributors to the overall severity of weight aberrations include environmental, life style, and epistatic effects of other genes, which make the study of small changes in promoter activity in this region difficult to fully characterize. Age could also affect the severity of the phenotype presented in adult sample populations; however, the early onset cohort of our collaborators would likely exclude any such weak promoter mutation. These studies are currently on-going.

Another study that concerning this region of the MC4R promoter was recently presented by Naville and colleagues (82). This study focused on the Sp1 sites in and around the *CR-8* region of the human MC4R promoter. Their findings show that a complete loss of the Sp1 site in the *CR-8* region of the human MC4R gene by mutagenesis results in a loss of 80% or more of basal promoter activity *in vitro*. Our results with site-directed mutagenesis of the human G-502A SNP, though not as great a loss in promoter activity, showed a 13% loss in the human sequence context. These results are consistent with the *CR-8* region being important for at least basal promoter activity of the MC4R gene, and gives further credence to the SNP discovery efforts in this region pursued by our colleagues.

In summary, although the study of the MC4R promoter has been technically

challenging, these experiments indicate that a key regulatory elements likely reside in the *CR-8* region and in the 5'-flanking untranslated region of the MC4R transcript. Confirmation of these findings may have to wait for additional technological developments either with the identification of a tissue culture cell line expressing MC4R at more substantial levels, or in the field of transgenics, with the development of a system to eliminate position-dependent expression effects due to transgene insertion sites.

BIBLIOGRAPHY

1. Various authors. Insight: Obesity Reviews. *Nature*. 2000; 404:631-77. Review.

2. Vaisse C, Clement K, Guy-Grand B, and Froguel P. A frameshift mutation in human MC4R is associated with a dominant form of obesity. *Nature Genetics*. 1998; 20:113-14.

3. Yeo GS, Farooqi IS, Aminian S, Halsall DJ, Stanhope RG, and O'Rahilly S. A frameshift mutation in MC4R associated with dominantly inherited human obesity. *Nature Genetics*. 1998; 20:111-12.

4. Zhang Y, Proenca R, Maffei M, Barone M, Leopold L, and Friedman JM. Positional cloning of the mouse obese gene and its human homologue. *Nature*. 1994; 372(6505):425-32.

5. Grönke S, Mildner A, Fellert S, Tennagels N, Petry S, Müller G, Jäckle H, and Kühnlein RP. Brummer lipase is an evolutionary conserved fat storage regulator in Drosophila. *Cell Metab*. 2005; 1(5):323-30.

6. Williams G, Harrold JA, and Cutler DJ. The hypothalamus and the regulation of energy homeostasis: lifting the lid on a black box. *Proc Nutrition Society*. 2000; 59(3):385-96. Review.

7. Bray GA, Inoue S, and Nishizawa Y. Hypothalamic obesity: The autonomic hypothesis and the lateral hypothalamus. *Diabetologia*. 1981; 20(Supplement):366-77.

8. Eberle AN. The Melanocortin Receptors. Chapter 1, p 3-4 (Roger D. Cone ed., Humana Press 2000).

9. Nakanishi S, Inoue A, Kita T, Nakamura M, Chang ACY, Cohen SN, and Numa S. Nucleotide sequence of cloned cDNA for bovine corticotropin-β-lipotropin precursor. *Nature*. 1979; 278:423–27.

10. Fan W, Boston BA, Kesterson RA, Hruby VJ, and Cone RD. Role of melanocortinergic neurons in feeding and the *agouti* obesity syndrome. *Nature*. 1997; 385:165-68.

11. Bagnol D, Lu X, Kaelin CB, Day HE, Ollmann M, Gantz I, Akil H, Barsh G, and Watson SJ. Anatomy of an Endogenous Antagonist: Relationship between Agouti-Related Protein and Proopiomelanocortin in Brain. *J Neuroscience*. 1999; 19:RC26:1-7.

12. Chai B, Neubig RR, Millhauser GL, Thompson DA, Jackson PJ, Barsh GS, Dickinson CJ, Li J, Lai Y, and Gantz I. Inverse agonist activity of agouti and agouti-related protein. *Peptides*. 2003; 24(4):603-09.

13. Robbins LS, Nadeau JH, Johnson KR, Kelly MA, Roselli-Rehfuss L, Baack E, Mountjoy KG, and Cone RD. Pigmentation phenotypes of variant extension locus alleles result from point mutations that alter MSH receptor function. *Cell*. 1993; 72:827-34.

14. Hustad CM, Perry WL, Siracusa LD, Rasberry C, Cobb L, Cattanach BM, Kovatch R, Copeland NG, and Jenkins NA. Molecular Genetic Characterization of Six Recessive Viable Alleles of the Mouse Agouti Locus. *Genetics*. 1995; 140(1): 255–65.

15. Mountjoy KG, Robbins LS, Mortrud MT, and Cone RD. The cloning of a family of genes that encode the melanocortin receptors. *Science*. 1992; 257(5074):1248-51.

16. Magenis RE, Smith L, Nadeau JH, Johnson KR, Mountjoy KG, and Cone RD. Mapping of the ACTH, MSH, and neural (MC3 and MC4) melanocortin receptors in the mouse and human. *Mamm Genome*. 1994; 5(8):503-08.

17. Labbe O, Desarnaud F, Eggerickx D, Vassart G, and Parmentier M. Molecular cloning of a mouse melanocortin 5 receptor gene widely expressed in peripheral tissues. *Biochemistry*. 1994; 33(15):4543-49.

18. Griffon N, Mignon V, Facchinetti P, Diaz J, Schwartz JC, and Sokoloff P. Molecular cloning and characterization of the rat fifth melanocortin receptor. *Biochem Biophys Res Commun*. 1994; 200(2):1007-14.

19. Gantz I, Shimoto Y, Konda Y, Miwa H, Dickinson CJ, and Yamada T. Molecular cloning, expression, and characterization of a fifth melanocortin receptor. *Biochem Biophys Res Commun*. 1994; 200(3):1214-20.

20. Kishi T, Aschkenasi CJ, Lee CE, Mountjoy KG, Saper CB, and Elmquist JK. Expression of melanocortin 4 receptor mRNA in the central nervous system of the rat. *J Comp Neurol.* 2003; 457, 213-35.

21. Iqbal J, Pompolo S, Dumont LM, Wu CS, Mountjoy KG, Henry BA, and Clarke IJ. Long-term alterations in body weight do not affect the expression of melanocortin receptor-3 and -4 mRNA in the ovine hypothalamus. *Neuroscience*. 2001; 105(4):931-40.

22. Smolnik R, Perras B, Molle M, Fehm HL, and Born J. Event-related brain potentials and working memory function in healthy humans after single-dose and prolonged intranasal administration of adrenocorticotropin 4-10 and desacetyl-alpha-melanocyte stimulating hormone. *J Clin Psychopharmacol*. 2000; 20(4):445-54.

23. Huszar D, Lynch CA, Fairchild-Huntress V, Dunmore JH, Fang Q, Berkemeier LR, Gu W, Kesterson RA, Boston BA, Cone RD, Smith FJ, Campfield LA, Burn P, and Lee F. Targeted disruption of the melanocortin-4 receptor results in obesity in mice. *Cell*. 1997; 88:131-41.

24. Butler AA, Kesterson RA, Khong K, Cullen MJ, Pelleymounter MA, Dekoning J, Baetscher M, and Cone RD. A unique metabolic syndrome causes obesity in the melanocortin-3 receptor-deficient mouse. *Endocrinology*. 2000; 141:3518-21.

25. Ni XP, Pearce D, Butler AA, Cone RD, and Humphreys MH. Genetic disruption of gamma-melanocyte-stimulating hormone signaling leads to salt-sensitive hypertension in the mouse. *J Clin Invest*. 2003; 111:1251-58.

26. Van der Ploeg LH, Martin WJ, Howard AD, Nargund RP, Austin CP, Guan X, Drisko J, Cashen D, Sebhat I, Patchett AA, Figueroa DJ, DiLella AG, Connolly BM, Weinberg DH, Tan CP, Palyha OC, Pong SS, MacNeil T, Rosenblum C, Vongs A, Tang R, Yu H, Sailer AW, Fong TM, Huang C, Tota MR, Chang RS, Stearns R, Tamvakopoulos C, Christ G, Drazen DL, Spar BD, Nelson RJ, and MacIntyre DE. A role for the melanocortin 4 receptor in sexual function. *Proc Natl Acad Sci USA*. 2002; 99:11381-86.

27. Alvaro JD, Tatro JB, Quillan JM, Fogliano M, Eisenhard M, Lerner MR, Nestler EJ, and Duman RS. Morphine down-regulates melanocortin-4 receptor expression in brain regions that mediate opiate addiction. *Mol Pharmacol*. 1996; 50:583-91.

28. Alvaro JD, Taylor JR, and Duman RS. Molecular and behavioral interactions between central melanocortins and cocaine. *J Pharmacol Exp Ther*. 2003; 304:391-99.

29. Adan RA, van der Kraan M, Doornbos RP, Bar PR, Burbach JP, and Gispen WH. Melanocortin receptors mediate alpha-MSH-induced stimulation of neurite outgrowth in neuro 2A cells. *Brain Res Mol Brain Res*. 1996; 36:37-44.

30. Böhm M, Eickelmann M, Li Z, Schneider SW, Oji V, Diederichs S, Barsh GS, Vogt A, Stieler K, Blume-Peytavi U, and Luger TA. Detection of functionally active melanocortin receptors and evidence for an immunoregulatory activity of alpha-melanocyte-stimulating hormone in human dermal papilla cells. *Endocrinology*. 2005; 146(11):4635-46.

31. Morgane PJ and Kosman AJ. A rhinencephalic feeding center in the cat. *Am J Physiol*. 1959; 197(1):158-62.

32. Spiegelman BM and Flier JS. Obesity and the regulation of energy balance. *Cell*. 2001; 104:531-43. Review.

33. Douglass J, McKinzie AA, and Couceyro P. PCR differential display identifies a rat brain mRNA that is transcriptionally regulated by cocaine and amphetamine. *J Neurosci.* 1995; 15:2471–81.

34. Cowley MA, Smart JL, Rubinstein M, Cerdan MG, Diano S, Horvath TL, Cone RD, and Low MJ. Leptin activates anorexigenic POMC neurons through a neural network in the arcuate nucleus. *Nature*. 2001; 411:480-84.

35. Bouret SG, Draper SJ, and Simerly RB. Trophic action of leptin on hypothalamic neurons that regulate feeding. *Science*. 2004; 304:108-10.

36. Shutter JR, Graham M, Kinsey AC, Scully S, Luthy R, and Stark K. Hypothalamic expression of ART, a novel gene related to agouti, is up-regulated in obese and diabetic mutant mice. *Genes Dev*. 1997; 11:593-602.

37. Ollmann MM, Wilson BD, Yang YK, Kerns JA, Chen Y, Gantz I, and Barsh GS. Antagonism of central melanocortin receptors in vitro and in vivo by agouti-related protein. *Science*. 1997; 278:135-38.

38. Rosenfeld RD, Zeni L, Welcher AA, Narhi LO, Hale C, Marasco J, Delaney J, Gleason T, Philo JS, Katta V, Hui J, Baumgartner J, Graham M, Stark KL, and Karbon W. Biochemical, biophysical, and pharmacological characterization of bacterially expressed human agouti-related protein. *Biochemistry*. 1998; 37:16041-52.

39. Fong TM, Mao C, MacNeil T, Kalyani R, Smith T, Weinberg D, Tota MR, and Van der Ploeg LHT. ART (protein product of agouti-related transcript) as an antagonist of MC-3 and MC-4 receptors. *Biochem Biophys Res Commun*. 1997; 237:629-31.

40. Yang YK, Thompson DA, Dickinson CJ, Wilken J, Barsh GS, Kent SBH, and Gantz I. Characterization of Agouti-related protein binding to melanocortin receptors. *Mol Endocrinol*. 1999; 13(1):148-55.

41. Hahn TM, Breininger JF, Baskin DG, and Schwartz MW. Coexpression of Agrp and NPY in fasting-activated hypothalamic neurons. *Nature Neuroscience*. 1998; 1(4):271-72.

42. Stanley BG and Leibowitz SF. Neuropeptide Y injected in the paraventricular hypothalamus: a powerful stimulant of feeding behavior. *Proc Natl Acad Sci USA*. 1985; 82:3940-43.

43. Erickson JC, Clegg KE, and Palmiter RD. Sensitivity to leptin and susceptibility to seizures of mice lacking neuropeptide Y. *Nature*. 1996; 381:415–21.

44. Cowley MA, Smith RG, Diano S, Tschöp M, Pronchuk N, Grove KL, Strasburger CJ, Bidlingmaier M, Esterman M, Heiman ML, Garcia-Segura LM, Nillni EA, Mendez P, Low MJ, Sotonyi P, Friedman JM, Liu H, Pinto S, Colmers WF, Cone RD, and

Horvath TL. The distribution and mechanism of action of ghrelin in the CNS demonstrates a novel hypothalamic circuit regulating energy homeostasis. *Neuron*. 2003; 37(4):649-61.

45. Ellacott KL, Halatchev IG, and Cone RD. Characterization of leptin-responsive neurons in the caudal brainstem. *Endocrinology*. 2006; 147(7):3190-95.

46. Oliveira KJ, Ortiga-Carvalho TM, Cabanelas A, Veiga MA, Aoki K, Ohki-Hamazaki H, Wada K, Wada E, and Pazos-Moura CC. Disruption of neuromedin B receptor gene results in dysregulation of the pituitary-thyroid axis. *J Mol Endocrinol*. 2006; 36(1):73-80.

47. Könner AC, Janoschek R, Plum L, Jordan SD, Rother E, Ma X, Xu C, Enriori P, Hampel B, Barsh GS, Kahn CR, Cowley MA, Ashcroft FM, and Brüning JC. Insulin Action in AgRP-Expressing Neurons Is Required for Suppression of Hepatic Glucose Production. *Cell Metab*. 2007; 5(6):438-49.

48. Marty N, Dallaporta M, and Thorens B. Brain glucose sensing, counterregulation, and energy homeostasis. *Physiology*. 2007; 22:241-51.

49. Yamada T and Katagiri H. Avenues of Communication between the Brain and Tissues/Organs Involved in Energy Homeostasis. *Endocr J*. 2007 May 18 [E-Pub ahead of print].

50. Vaisse C, Clement K, Durand E, Hercberg S, Guy-Grand B, and Froguel P. Melanocortin-4 receptor mutations are a frequent and heterogeneous cause of morbid obesity. *J Clin Invest*. 2000; 106:253–62.

51. Farooqi IS, Keogh JM, Yeo GS, Lank EJ, Cheetham T, and O'Rahilly S. Clinical spectrum of obesity and mutations in the melanocortin 4 receptor gene. *N Engl J Med*. 2003; 348(12):1085-95.

52. Ho G and MacKenzie RG. Functional characterization of mutations in melanocortin-4 receptor associated with human obesity. *J Biol Chem*. 1999; 274:35816-22.

53. Kublaoui BM and Zinn AR. *MC4R* Mutations—Weight before Screening! *J Clin Endocrin & Metab*. 2006; 91(5):1671-72. Editorial.

54. Kobayashi H, Ogawa Y, Shintani M, Ebihara K, Shimodahira M, Iwakura T, Hino M, Ishihara T, Ikekubo K, Kurahachi H, and Nakao K. A Novel homozygous missense mutation of melanocortin-4 receptor (MC4R) in a Japanese woman with severe obesity. *Diabetes*. 2002; 51:243-46.

55. Archer ZA, Rayner DV, Duncan JS, Bell LM, and Mercer JG. Introduction of a High-Energy Diet Acutely Up-Regulates Hypothalamic Cocaine and Amphetamine-

Regulated Transcript, MC4R and Brown Adipose Tissue Uncoupling Protein-1 Gene Expression in Male Sprague-Dawley Rats. *J Neuroendocrinology*. 2005; 17:10–17.

56. Dumont LM, Wu CS, Aschkenasi CJ, Elmquist JK, Lowell BB, and Mountjoy KG. Mouse melanocortin-4 receptor gene 5'-flanking region imparts cell specific expression in vitro. *Mol Cell Endocrinol*. 2001; 184(1-2):173-85.

57. Daniel PB, Fernando C, Wu CS, Marnane R, Broadhurst R, and Mountjoy KG. 1 kb of 5' flanking sequence from mouse MC4R gene is sufficient for tissue specific expression in a transgenic mouse. *Mol Cell Endocrinol*. 2005; 239(1-2):63-71.

58. Lubrano-Berthelier C, Cavazos M, Le Stunff C, Haas K, Shapiro A, Zhang S, Bougneres P, and Vaisse C. The human MC4R promoter: characterization and role in obesity. *Diabetes*. 2003; 52(12):2996-3000.

59. Mercer EH, Hoyle GW, Kapur RP, Brinster RL, and Palmiter RD. The dopamine beta-hydroxylase gene promoter directs expression of E. coli lacZ to sympathetic and other neurons in adult transgenic mice. *Neuron*. 1991; 7(5):703-16.

60. Zinn KR, Chaudhuri TR, Szafran AA, O'Quinn D, Weaver C, Dugger K, Lamar CR, Kesterson RA, Wang X, and Frank SJ. Noninvasive bioluminescent imaging in small animals. In Press

61. Takeuchi S and Takahashi S. Melanocortin Receptor Genes in the Chicken—Tissue Distributions. *General & Comparative Endocrinology*. 1998; 112**:**220–31.

62. Klovins J, Haitina T, Fridmanis D, Kilianova Z, Kapa I, Fredriksson R, Gallo-Payet N, and Schiöth HB. The melanocortin system in Fugu: determination of POMC/AGRP/MCR gene repertoire and synteny, as well as pharmacology and anatomical distribution of the MCRs. *Mol Biol Evol*. 2004; 21(3):563-79.

63. Khong K, Kurtz SE, Sykes RL, and Cone RD. Expression of functional melanocortin-4 receptor in the hypothalamic GT1-1 cell line. *Neuroendocrinology*. 2001; 74(3):193-201.

64. Kistler-Heer V, Lauber ME, and Lichtensteiger W. Different developmental patterns of melanocortin MC3 and MC4 receptor mRNA: predominance of Mc4 in fetal rat nervous system. *J Neuroendocrinol*. 1998; 10(2):133-46.

65. Mountjoy KG and Wild JM. Melanocortin-4 receptor mRNA expression in the developing autonomic and central nervous systems. *Brain Res Dev Brain Res*. 1998; 107(2):309-14.

66. Mountjoy KG, Wu CS, Dumont LM, and Wild JM. Melanocortin-4 receptor messenger ribonucleic acid expression in rat cardiorespiratory, musculoskeletal, and integumentary systems. *Endocrinology*. 2003; 144(12):5488-96.

67. Uvarov P, Pruunsild P, Timmusk T, and Airaksinen MS. Neuronal K+/Cl- co-transporter (KCC2) transgenes lacking neurone restrictive silencer element recapitulate CNS neurone-specific expression and developmental up-regulation of endogenous KCC2 gene. *J Neurochem.* 2005; 95(4):1144-55.

68. Desai A, Turetsky D, Vasudevan K, and Buonanno A. Analysis of transcriptional regulatory sequences of the N-methyl-D-aspartate receptor 2A subunit gene in cultured cortical neurons and transgenic mice. *J Biol Chem.* 2002; 277(48):46374-84.

69. Wilson T and Hastings JW. Bioluminescence. *Annu Rev Cell Dev Biol.* 1998; 14:197–230. Review.

70. Rice BW, Cable MD, and Nelson MB. In vivo imaging of light-emitting probes. *J Biomed Opt.* 2001; 6:432–440.

71. Sadikot RT and Blackwell TS. Bioluminescence imaging. *Proc Am Thorac Soc.* 2005; 2(6):537-40.

72. Ciana P, Biserni A, Tatangelo L, Tiveron C, Sciarroni AF, Ottobrini L, and Maggi A. A novel peroxisome proliferator-activated receptor responsive element-luciferase reporter mouse reveals gender specificity of peroxisome proliferator-activated receptor activity in liver. *Mol Endocrinol.* 2007; 21(2):388-400.

73. Klopstock N, Levy C, Olam D, Galun E, and Goldenberg D. Testing transgenic regulatory elements through live mouse imaging. *FEBS Lett.* 2007; 581(21):3986-90.

74. Lyons SK, Lim E, Clermont AO, Dusich J, Zhu L, Campbell KD, Coffee RJ, Grass DS, Hunter J, Purchio T, and Jenkins D. Noninvasive bioluminescence imaging of normal and spontaneously transformed prostate tissue in mice. *Cancer Res.* 2006; 66(9):4701-07.

75. Lowe WL, Fu R, and Banko M. Growth factor-induced transcription via the serum response element is inhibited by cyclic adenosine 3',5'-monophosphate in MCF-7 breast cancer cells. *Endocrinology.* 1997; 138(6):2219-26.

76. Cunningham AL, Diefenbach RJ, Miranda-Saksena M, Bosnjak L, Kim M, Jones C, and Douglas MW. The cycle of human herpes simplex virus infection: virus transport and immune control. *J Infect Dis.* 2006; 194 Supp't 1:S11-18. Review.

77. Ellison AR and Bishop JO. Herpesvirus thymidine kinase transgenes that do not cause male sterility are aberrantly transcribed and translated in the testis. *Biochim Biophys Acta.* 1998; 1442(1):28-38.

78. Butler AA, Marks DL, Fan W, Kuhn CM, Bartolome M, and Cone RD. Melanocortin-4 receptor is required for acute homeostatic responses to increased dietary fat. *Nat Neurosci*. 2001; 4(6):605-11.

79. Mellon PL, Windle JJ, Goldsmith PC, Padula CA, Roberts JL, and Weiner RI. Immortalization of hypothalamic GnRH neurons by genetically targeted tumorigenesis. *Neuron*. 1990; 5(1):1-10.

80. Song Y, Golling G, Thacker TL, and Cone RD. Agouti-related protein (AGRP) is conserved and regulated by metabolic state in the zebrafish, Danio rerio. *Endocrine*. 2003; 22(3):257-65.

81. Song Y and Cone RD. Creation of a genetic model of obesity in a teleost. *FASEB J*. 2007; 21(9):2042-49.

82. Blondet A, Gout J, Durand P, Bégeot M, and Naville D. Expression of the human melanocortin-4 receptor gene is controlled by several members of the Sp transcription factor family. *J Mol Endocrinol*. 2005; 34(2):317-29.